Conference Program

First International PEEK Meeting
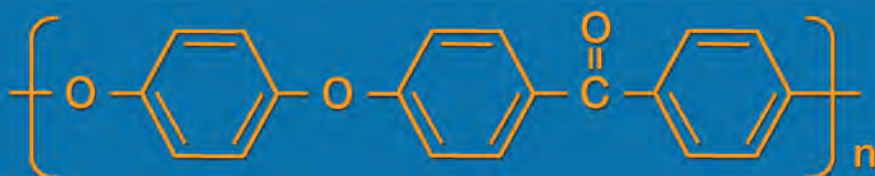
The Union League
Philadelphia, PA
April 25 - 26

2013

Organized by:

IRC
IMPLANT RESEARCH CENTER

E^{x}ponent®

Steven M. Kurtz, Ph.D.
Research Associate Professor, Drexel University
Corporate Vice President and Director, Exponent

Sponsored by:

Invibio®
BIOMATERIAL SOLUTIONS

First International PEEK Meeting

Dear Participant,

The purpose of the meeting is to bring together engineers, scientists and clinicians from academia and industry and present leading edge research on advancements in medical grade PEEK technology and clinical applications. The focus of the first meeting is on:

- Bioactive PEEK composites

- Advances in motion preservation PEEK applications for spine

- Tribological performance of orthopaedic bearings incorporating PEEK

- Retrieval studies of PEEK implants

- Advances in PEEK formulations for implants

- Structural composites and woven fiber applications of medical PEEK

- Advances in biologic aspects of PEEK wear debris

Abstracts were evaluated by the Scientific Committee for inclusion in the program, either as a podium presentation or a poster.

Scientific Committee

Steven Kurtz, Ph.D.
Conference Organizer
Exponent, Inc. & Drexel University

Craig Valentine, Ph.D.
Invibio, Ltd.

Scott Herbert
Rapidwerks

Prof. Bill Walsh
University of New South Wales
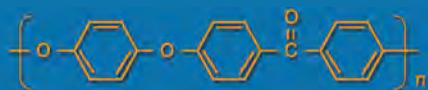
Prof. Jeffrey Tipper
University of Leeds

Prof. John Fisher
University of Leeds

Anand Agarwal, M.D.
University of Toledo

Richard Field
Epsom & St Helier University Hospitals NHS Trust

Jim Nevelos, Ph.D.
Stryker Orthopaedics

Todd Lanman, M.D.
UCLA School of Medicine

Sponsored by:

Invibio®
BIOMATERIAL SOLUTIONS

First International PEEK Meeting Agenda
Day One - Thursday, April 25, 2013

Welcome

8:00 am	On-site registration opens	
9:00 am	Welcome, Opening remarks	*Steven Kurtz*

Session I: Properties, Test Methods, and Processing
Moderator: Steven Kurtz

9:15 am	Properties and Testing of PEEK Composites	*Craig Valentine*
9:45 am	Macromolecular and Morphological Characterization of Medical Grade PEEK Polymers *(p. 9)*	*Anuj Bellare*
10:00 am	Cryogenic Machining of PEEK *(p.11)*	*Jeffery Knopf*
10:15 am	Measurements of Free Radicals in UV- and X-Irradiated PEEK *(p.13)*	*Shah Jahan*

10:30   Morning coffee break

Session II: Biocompatibility of PEEK
Moderators: Bill Walsh & Ryan Roeder

11:00 am	PEEK Biocompatibility	*Jeff Toth*
11:20 am	Investigation into the Osseointegration of Oxygen Plasma Modified and Unmodified PEEK in a Sheep Model *(p.15)*	*Sasha Poulsson*
11:35 am	PEEK Wear Particles	*Joanne Tipper*
11:50 am	Fibroblasts and osteoblasts cultivated on surface modified PEEK compounds *(p.17)*	*Tobias Spintig*

12:05 pm   Lunch break

Session III: Changing the Cellular Reactions to PEEK Biomaterials
Moderators: Jeff Toth and Joanne Tipper

1:40 pm	Hydroxyapatite – PEEK: Preclinical *in vivo* and *in vitro* Characterization	*Bill Walsh*
2:00 pm	Osteointegrative Coating Solutions for PEEK-based Implants *(p.18)*	*Gianlucca Zappini*
2:15 pm	Plasma immersion in implantation treatment of poly-ether ether ketone for surface biofunctionalization *(p.20)*	*William Lu*
2:30 pm	Bioactive PEEK Composites and Scaffolds	*Ryan Roeder*
2:50 pm	Novel method for making homogeneous bioactive PEEK compounds using an ultrasonic co-feeding and on-line mixing system *(p.21)*	*Zhongqi Li*
3:05 pm	Porous PEEK and Surface Modified PEEK for Muscoskeletal Applications *(p.23)*	*Robert Poggie*

3:20 pm   Afternoon coffee break

Session IV: Wear Properties in Biomedical Applications
Moderator: Louise Jennings and Jim Nevelos

3:45 pm	CFR PEEK Tribology	*Dr. Louise Jennings*
4:00 pm	PEEK on PEEK Articulations in Spinal Disc Arthroplasty *(p.24)*	*Dr. Tim Brown*
4:15 pm	Smart modifications of PEEK by self-initiated surface graft polymerization for orthopaedic bearings *(p.26)*	*Dr. Masayuki Kyomoto*
4:30 pm	Frictional Heating of PEEK-UHMWPE Bearing Couple on Pin-on-disk Tester *(p.28)*	*Doruk Baykal*
4:45 pm	The wear of CFR-PEEK and PEEK OPTIMA articulating against HXLPE *(p.29)*	*Tony Unsworth*

5:00 pm   **Day 1 Meeting Adjourns**
Drexel transportation to The Academy of Natural Sciences

6:00 pm   **Dinner Reception at The Academy of Natural Sciences**
Following dinner, Drexel transportation will provide bussing to Center City

Day Two - Friday, April 26, 2013

8:00 am   **On-site registration opens**

Session V: Biomechanical Performance of Medical Devices
Moderator: Steven Kurtz

8:30 am	PEEK Rod Biomechanics	*Anand Agarwal*
8:50 am	Investigation of Carbon Fiber reinforced PEEK Self-Tapping Suture Anchors *(p.31)*	*E. Feerick*
9:05 am	Particulate and gravimetric Wear Rate Analysis and Flexural Fatigue Testing of a PEEK Medial Knee Interpositional Arthroplasty Implant *(p.32)*	*S. Crosbie*
9:20 am	Characterization of a Novel Polyetheretherketone Implant for Total Knee Replacement *(p.34)*	*Kathy Rankin*
9:40 am	Preclinical Testing of the MITCH Cup	*Jim Nevelos*

10:00 am   **Morning coffee break**

Session VI: Clinical Performance and Retrieval Studies of PEEK Medical Devices
Moderators: Anand Agarwal, M.D. and Jim Nevelos

10:20 am	Clinical Trials of the MITCH Cup	*Richard Field*
10:40 am	PEEK Patient Specific Implants *(p.36)*	*John Disegi*
10:55 am	A Novel, Flexible PEEK Implant for Treatment of Vertebral Compression Fractures: From Concept to Clinic *(p.37)*	*Jeff Emery*
11:10 am	Development and Clinical Experience with PEEK Rods	*Steve Kurtz*
11:30 am	Revision and Retrieval Analysis of PEEK Rod Systems for Fusion and Posterior Dynamic Stabilization *(p.39)*	*Steve Kurtz*
11:45 am	Characterization of In Vivo Changes and Histological Responses of Retrieved PEEK Rod Systems *(p.41)*	*Genymphas Higgs*

12:00 pm   **Meeting adjourn**

Podium Abstracts

First International PEEK Meeting

**The Union League
Philadelphia, PA
April 25 - 26**

2013

Posters

Macromolecular and Morphological Characterization of Medical Grade PEEK Polymers

Bellare, A[1], Le, K-P[2], Yau, S-S[2] and Spiegelberg, S[3]

[1]Brigham & Women's Hospital, Harvard Medical School, Boston, MA; [2]Stryker Orthopaedics, Mahwah, NJ;

[3]Cambridge Polymer Group, Boston, MA

anuj@alum.mit.edu

Introduction: In recent years, poly (ether ether ketone), PEEK), has received considerable attention as a biomaterial since it is a high performance thermoplastic and has been shown to be biocompatible [1, 2]. PEEK has a glass transition temperature (Tg) of approximately 143°C and a commonly observed melting temperature (Tm) of 335-345°C, making it a rigid polymer with high tensile strength and modulus [3, 4]. It is finding increasing use in trauma, orthopedic and spine implants due to its high mechanical properties, especially when reinforced with carbon fibers, which imparts a modulus comparable to that of cortical bone [3]. As a thermoplastic with a high Tg, it is possible to manipulate the macroscopic mechanical properties by controlling its semi-crystalline morphology. For example, rapid quenching from the melt state to a temperature lower than Tg induces a low crystallinity while isothermal crystallization and slow cooling induce a higher degree of crystallinity in PEEK [4]. The molecular weight of the polymer also has a strong influence on the maximum achievable crystallinity of the polymer due to entanglement effects [5]. In this study, we examined the morphology of four medical grade PEEK polymers using a variety of characterization techniques to determine whether there were significant differences between their molecular and nanostructures.

Materials and Methods: Four different medical grades of PEEK resins were compression molded into 2 mm thick sheets and slow cooled from the melt state under identical conditions (referred to as PEEK-1, PEEK-2, PEEK-3 and PEEK-4). Gel permeation chromatography (GPC) was performed using a Polymer Laboratories GPC 120 equipped with PL GPC-AS MT heated autosampler and PLgel Guard plus mixed bed-B 30cmx10mm columns. 30 mg of PEEK polymer was dissolved in 15 ml of 50:50 (w/w) 1, 2, 4-trichorobenzene:phenol containing antioxidant, gently boiled for 60 minutes, transferred to a heating block at 115°C for 30 minutes, filtered through a 1 mm glass fiber pad into the autosampler vials and then injected into the column at a flow rate of 0.8 mL/min. The molecular weights were measured using a refractive index detector against polystyrene (EasiCal PS-1) standards. The data was analyzed using Polymer Laboratories "Cirrus" software and provided the number average (Mn), weight average (Mw) and z-average (Mz) molecular weights for the PEEK resins. Density measurement was conducted following ASTM D792. The percent crystallinity was calculated by linear regression method (% Crystallinity = 730.35 x Density – 922.43) using the correlation between density and crystallinity established by Jonas et al [6]. Additional crystallinity measurements were conducted using a Diamond Perkin Elmer differential scanning calorimeter (DSC) to measure the degree of crystallinity following ASTM F2026 using a 20 °C/min heating/cooling rate with first and second heats. A heat of fusion of 130 J/g of the pure PEEK crystal was used to calculate crystallinity. Infrared (IR) crystallinity was measured according to ASTM D2778-09. The surfaces of the molded PEEK samples were imaged in reflectance mode with an Agilent 640IR equipped with a 610 microscope. The background was collected against a gold slide. The resulting spectra were subjected to a Kramers-Kronig transformation, baseline corrected, and then the peak heights at 1305 and 1280 1/cm were calculated. The IR crystallinity was calculated using the equation in ASTM F2778-09 that relates the peak height ratio back to crystallinity of PEEK samples measured by wide angle X-ray experiments. Three locations per sample were analyzed. Small angle x-ray scattering (SAXS) data was collected from each 2mm thick PEEK sheet using a conventional laboratory CuKα rotating anode SAXS instrument (Rigaku S-Max3000). The collimated beam had a diameter of approximately 0.4 mm. The SAXS scattering intensity was collected by a two-dimensional gas-filled wire array detector with an angular scattering range of $q_{min}=0.05$ [1/nm] and $q_{max}=1.0$ [1/nm], where the scattering vector, q, is defined as: $q = (4\pi/\lambda)\sin\theta$ where λ is the wavelength of the x-ray used (=0.154 nm) and θ is one-half the scattering angle. The sampling volume associated with each x-ray measurement was estimated to be 0.25 mm³.

Results: Molecular characterization by GPC revealed a Mn in a range of 42-30K g/mole (see Table 1). PEEK-4 had the lowest polydispersity index (=ratio of Mw to Mn) compared to the other grades of PEEK. Mn, Mw and Mz were all significantly different from one grade of PEEK to another (ANOVA, p<0.05).

Table 1. Number average (Mn), weight average (Mw) and z-average (Mz) molecular weight for PEEK.

ID	Mn [g/mol]	Mw [g/mol]	Mz g/mol]
PEEK-1	35726±181	114026±121	209294±808
PEEK-2	34314±194	108352±470	227540±958
PEEK-3	42074±1448	115913±86	210317±1654
PEEK-4	30278±683	74426±432	124297±1617

There were significant differences in the value of the degree of crystallinity (X) observed using IR, density and DSC. The lowest crystallinity was observed using IR followed by density while DSC provided the highest values of crystallinity (see Figure 1). For the IR and density methods, there was no statistically significant difference in the crystallinity of PEEK-2 and PEEK-3 while the crystallinity of all other pairs of PEEKs was significantly different from each other. In the case of DSC, except for PEEK-1 whose crystallinity was not significantly different (ANOVA, p>0.05) compared to

PEEK-3, all other pairs showed a significant difference in crystallinity measured from the 1st and 2nd heats. The degree of crystallinity of PEEK-3 and PEEK-4 observed during the 2nd heat was 2-3% lower than the crystallinity observed during the 1st heat (ANOVA, p,0.05) while there was no statistically significant decrease in crystallinity for PEEK-1 and PEEK-2 despite the lower average value observed during the 2nd heat (ANOVA, p.0.05).
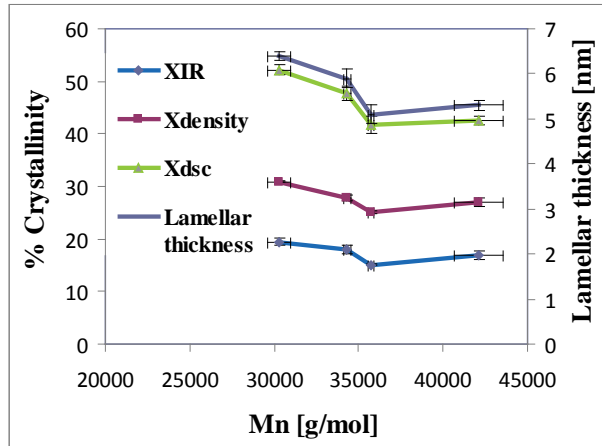

Figure 1. Summary of crystallinity and lamellar thickness trends with Mn.

Radially averaged scattering functions showed very little difference in the scattering behavior between various samples with all samples exhibiting a broad peak at a scattering vector of ~0.4 [1/nm] (see Figure 2).
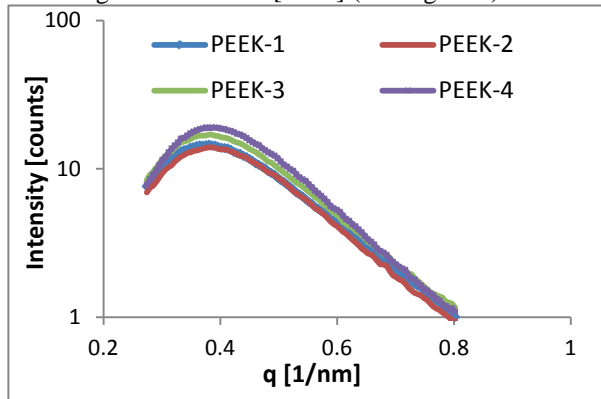

Figure 2. Scattering curves for PEEK polymers.

Inverse Fourier transformation of the scattering function provided the one-dimensional correlation function, which is related to the scattering function as follows:

$$p(r) = (1/2\pi^2 A)\int_0^\infty q^2 I(q)\cos(qr)dq$$

where p(r) is the one dimensional correlation function, A is the area of the lamella, I(q) is the scattering function, q is the scattering vector, r is the radial distance perpendicular to the lamellar surfaces. The inter-lamellar spacing (sum of the lamellar and amorphous layer thickness) was obtained from the first maximum of the scattering function (See Figure 3). The lamellar thickness, D, was calculated by multiplying the inter-lamellar spacing by the crystallinity obtained from DSC (See Table 2). The highest lamellar thickness was observed in

PEEK-4 while there was no statistically significant difference in the lamellar thickness of PEEK-1 and PEEK-3, both of which were significantly lower than those of PEEK-2 and PEEK-4.
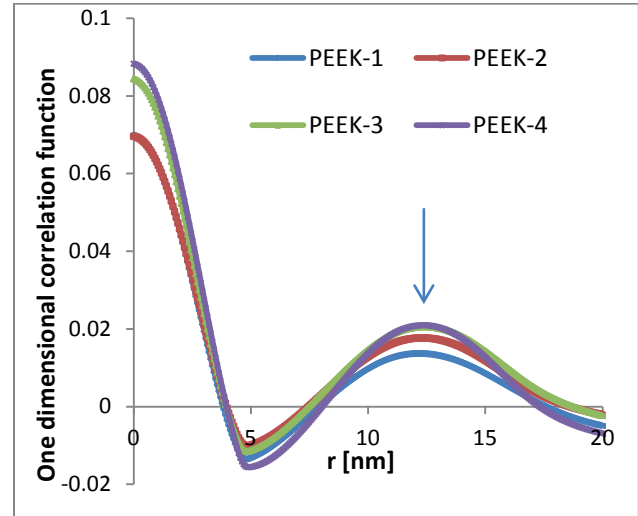
Figure 3. One dimensional correlation functions versus radial distance for PEEK polymers (arrow points to inter-lamellar spacing "L").

Table 2. SAXS inter-lamellar spacing (L), DSC crystallinity and lamellar thickness (D)

ID	L [nm]	X_{DSC} [%]	D [nm]
PEEK-1	12.2	41.8±1.7	5.1±0.2
PEEK-2	12.3	47.8±1.3	5.9±0.2
PEEK-3	12.4	42.5±0.8	5.3±0.1
PEEK-4	12.3	52.2±0.9	6.4±0.1

Discussion: The four PEEK polymers characterized in these studies showed only small differences in their lamellar nanostructure. The primary reason is that they were subjected to identical thermal histories. Thus any differences may be attributed to the difference in their molecular weight distributions. Among the four grades, PEEK-4 had the most narrow molecular weight distribution and lowest Mn, and consequently had the highest crystallinity and lamellar thickness. A low molecular weight is known to lead to a higher rate of crystallization as well as a high overall crystallinity due to a low viscosity, enabling the macromolecules to be incorporated into the crystalline lamella more easily than a higher molecular weight resin, which is less likely to be easily disentangled. Future studies are required to determine whether such morphological differences result in significant differences in macroscopic mechanical properties relevant to the use of PEEK polymers in orthopedic implants.

References: [1] Williams DF et al, *J Mat Sci Lett*, 6:188, 1987, [2] Hallab, NJ et al, *J Biomed Mater Res*, 100B:480-92, 2012   [3] Kurtz S, Devine JN, *Biomat*, 28:4845-69, 2007 [4]Lee Y, Porter R, *Macromol*, 21:2770-6, 1988 [5] Chivers RA, Moore DR, *Polymer*, 35(1):110-6, 1994 [6] Jonas A, et al, *Polymer* 32(18):3364-70, 1991

Cryogenic Machining of PEEK

Knopf, Jeffrey A.[1], Ghosh, Ranajit [1]
[1]Air Products and Chemicals, Inc., Allentown, PA
Knopfja@airproducts.com; Ghoshr@airproducts.com

Introduction: Rate of deformation and temperature management are fundamental considerations in the processing of thermoplastic polymers, especially materials used in the fabrication of medical devices such as PEEK. With respect to injection molding, mechanical work imparted to the material, residence time, the condition the screw and barrel process, and melt and mold temperature all have a substantial influence on the mechanical properties and surface features of the molded part and are typically monitored and carefully controlled. With respect to polymer machining, deformation is controlled by careful selection of "time dependent" machining conditions including cutting speed and feed rate and other application dependent parameters such as cutting edge radius, tool angles and tool surface tribological properties. The machinability of polymeric materials also depends on "temperature dependent" material characteristics including glass transition temperature (Tg), melt temperature (Tm), and viscosity. The accepted notion is that the best machining performance and optimum surface finish for polymer machining occurs within a small temperature window "Cold flow Region" around this glass transition region identified in the Figure 1 schematic below. As polymers are cooled through and below their Tg, their stiffness increases dramatically, typically several orders of magnitude.
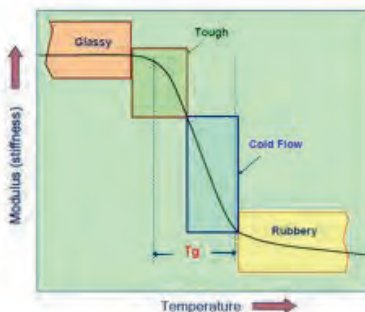
Figure 1: Typical stiffness curve for polymers with machinability regions

2

The Cold Flow Region exhibits more elastic deformation characteristics, compared to higher temperature ranges, where the material stiffness is significantly lower and the material exhibits rubber-like behavior.

Machining in the rubbery range is characterized by significant tearing and waviness in thermoplastic polymers. At a temperature range lower than the Cold Flow Region, thermoplastics are characterized by transitional brittle/ductile behavior, material smearing and unacceptable surface finish (tough region) following machining. At lower temperatures, extremely brittle and glassy behavior is exhibited by thermoplastic polymers and machining is characterized by micro-chipping and possible fracturing of the part surface.

For PEEK, with a Tg of nominally 143°C, the material stiffness at room temperature is sufficient to enable machining; however, research has shown that localized frictional heating during the machining process can cause non-homogeneous plastic deformation leading to burr formation and surface variability. However, since the stress field set up around the cutting edge of a tool leading to plastic deformation is highly dependent on temperature, an opportunity exists to positively influence surface characteristics by carefully controlling temperature during the machining operation.

To date, despite the important role temperature plays in the machining of thermoplastic polymers, precise control of heat removal from the machining operation has not been possible since coolants traditionally used in machining metal parts are: (i) not suitable for medical polymers, and (ii) do not offer temperature control capability for optimized performance. Cryogenic liquids and gases have been applied to cool polymeric materials; however, previous academic and industrial attempts at cryogenic machining have been hampered by issues related to heat leaks, pulsed flow and brittle fracture due to overcooling.

Therefore, the following objectives are critical in designing an effective, economical cooling system for machining thermoplastic polymers: (i) provide a residue-free coolant, (ii) provide fast startup and cooldown, (iii) prevent overcooling/undercooling, and (iv) allow machining of various polymers with different Tg's.

Methods and Materials: In order to provide temperature control during the machining of thermoplastics, Air Products and Chemicals introduced a temperature feature to its Icefly® Cryogenic Machining Technology, a technology successfully applied to metals machining since 2000. The ICEFLY® Cryogenic Machining Technology for machining thermoplastics was developed based on the above-mentioned objectives and offers the following features:

- Uses a controlled mixture of atomized liquid and gaseous nitrogen to impart cooling
- Sources cooling from liquid nitrogen (LIN), an environmentally-friendly coolant that immediately vaporizes and disperses on impact without leaving a residue on the finished part
- Eliminates the problems associated with heat leaks and pulsed flow by using a patented temperature-controlled cryogen delivery technology
- Uses feedback control to balance cooling intensity and heat generation

An experimental design was established to evaluate surface characteristics of milled PEEK samples using conventional CNC machining equipment and cutting tools. Samples of PEEK were milled according to machining parameters customary to PEEK machining under dry conditions with no external source of cooling and under temperature controlled conditions, with temperature control provided by ICEFLY® Cryogenic Machining Technology. The cryogenic gas sourced from ICEFLY® Cryogenic Machining Technology was applied to the PEEK work piece surface through a proprietary nozzle as the work piece was milled to a specification typical of a spinal implant. The surface of the work piece milled under temperature controlled conditions was also "brushed" under temperature controlled conditions with a proprietary brush insert enabled through the CNC interface. The work piece sample milled with no external cooling was analyzed for burr formation and compared to the work piece sample milled and brushed under temperature controlled conditions. A series of tests were also conducted with PEEK to assess variation in work piece dimensions following a turning operation conducted under dry conditions with no external source of cooling and under temperature controlled conditions.

Results: The combination of cryogenic gas cooling and cryo-brush deburring was shown to virtually eradicate the presence of burrs in a surface pattern characteristic of spinal implants compared to the control where no external cooling was applied. Temperature control during machining also provided more consistent and predictable work piece dimensions consistent with improved tolerance control compared to work pieces machined with no temperature control.

Discussion: The initial experimental work demonstrated the feasibility of minimizing the formation of burrs by applying a temperature controlled cryogenic gas to the surface a PEEK work piece during the milling operation and the ability to remove any residual burrs with a temperature controlled brushing operation. Improvements in work piece dimensional control also appear to be a benefit of temperature controlled machining. Future work will focus on further optimization of machining variables under temperature controlled conditions and quantitative and qualitative analysis of microstructure artifacts for filled and unfilled PEEK samples machined under temperature controlled conditions.

Measurements of Free Radicals in UV- and X-Irradiated PEEK

M. S. Jahan, T. Riahinasab and B. M. Walters

Department of Physics, The University of Memphis, 216 Manning Hall, Memphis TN. 38152, USA

mjahan@memphis.edu

Introduction: PEEK is a biocompatible semicrystalline thermoplastic that is mechanically strong and thermally stable; it is also known to be radiation resistant [1]. However, in a recent study, Awaja et al. detected free radicals in plasma-treated PEEK at room temperature [2]. The lifetimes of the radicals were found to be approximately 24 hours. In another study, Li et al. observed radicals at liquid nitrogen-temperature (77 K) in UV-, gamma- and e-beam-irradiated PEEK [3]. At room temperature, the gamma- and e-beam-induced radicals decayed in less than 20 min, and the UV-induced radicals decayed in about 24 hours. While no structural information about the radicals was provided, these authors suggested that the residual (present in as-received PEEK before irradiation) and the UV-induced radicals were similar or identical. Awaja et al., however, noted that the residual radical could be produced during the manufacturing process.

In this report, we characterize the residual free radicals (which we will call "R1") in as-received, unirradiated, neat (unfilled) PEEK, as well as an additional radical type (which we will call "R2") that is observed after UV- and X-irradiation in air at 23°C. Microwave power-saturation and spectral subtraction methods were used to isolate R2 from R1. R2 was then further characterized and monitored in air at room temperature for much longer times (three weeks) than previously reported.

Methods and Materials: 10 mil. (0.254 mm) neat (unfilled) Victrex® PEEK film and PEEK pellets (provided by Orthoplastics Ltd, UK) were used for this study. UV-irradiation was performed with a broad-band ultra-violet-visible (UV-Vis) lamp (250 Watt, Oriel® 688 10 Arc Lamp). For X-irradiation, an X-ray source (Scientific America) operating at 50 kV and 45 mA was used. Free radicals were detected at 23°C using an X-band electron spin resonance (ESR) spectrometer (EMX300, Bruker). The spectrometer, fitted with a mixed mode resonance cavity, operating at 9.8 GHz microwave frequency, and 100 KHz modulation and detection frequencies. For calibration of the spectral splitting factor, g-value, an organic free radical DPPH (2,2-diphenyl-1-picrylhydrazyl) with g factor value of 2.0036±0.0002 was used; for free radical concentration, a ruby standard by NIST was employed.

Results: It is clear that an additional radical type is created upon UV- and X-irraditaion, as seen by the additional features in Figure 1, such as that around 3500 Gauss (arrow (a)). UV and X-Ray appear to produce the same type of additional (R2) radicals in PEEK upon irradiation.
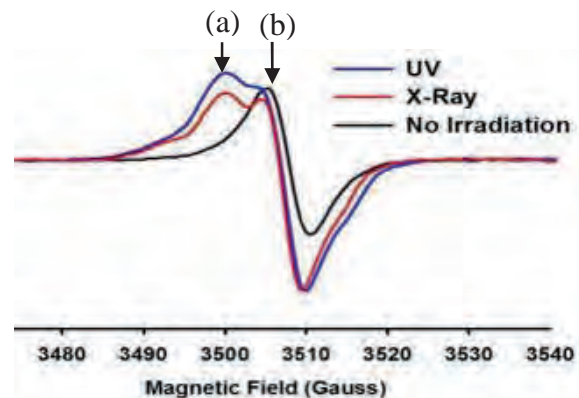
Figure 1. First derivative ESR spectra of PEEK. Black Line: PEEK (as received, non-irradiated) with a g-value of 2.0034. Blue and red lines: PEEK after UV- and X-irradiation, respectively. The peak at (a) identifies a feature of the "R2" radical. The arrow from (b) identifies a peak of the "R1" radical.

The R1 radical of non-irradiated PEEK has a g-value of approximately 2.0034 and line width (max. peak to min. peak distance) of about 5.2 Gauss. The calculated g-values were g = 2.0034±0.0002 for R1 and g = 2.0057±0.0004 for R2; a spectrum representing only the R2 radical is shown in Figure 2 (below).
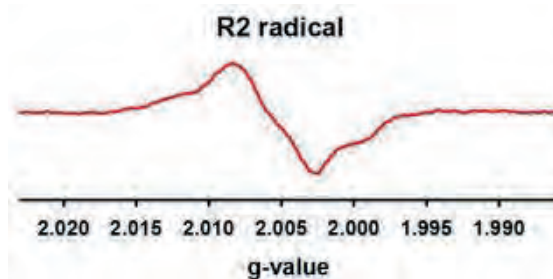
Figure 2. An extracted ESR spectrum of R2, obtained by subtracting data of non-irradiated PEEK (containing R1) from irradiated PEEK (containing R1 and R2), leaving us with only R2. In order to account for small differences in operating frequencies between measurements, g-values were used (as opposed to magnetic field in Gauss) in the x-axis.

The R1 radical (e.g. (b) of Figure1) appears to be unaffected by heat up to the PEEK melting temperature of 343°C. However, the quantity of radicals appear to increase when additional heat is applied beyond melting (see Figure 3); this is likely due to thermal breakdown or hemolysis of PEEK molecules. The free radical concentrations in the as-received PEEK that we tested were about 1.3×10^{15} spins/gram. With heat beyond melting, this concentration increased to about 1.8×10^{15} spins per gram.
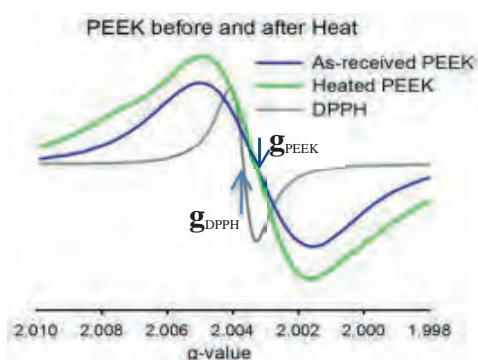
Figure 3. As received PEEK (blue line) that was then heated over a gas flame beyond melting (green line). For g-value reference positioning, a spectrum of DPPH is shown, which we measured to be about 2.0037 at the time of our testing of PEEK (2.0034 for R1; 2.0057 for R2).

Radical R2 concentration was found to increase with UV-exposure, as shown in Figure 4 (below); we have observed similar increases with X-irradiation as well. While we did quantify radicals in one sample for each time period (Figure 4 (b)) to get some idea of the growth trend, additional data will be required for statistically significant results and to better determine the effects of varying radiation types.
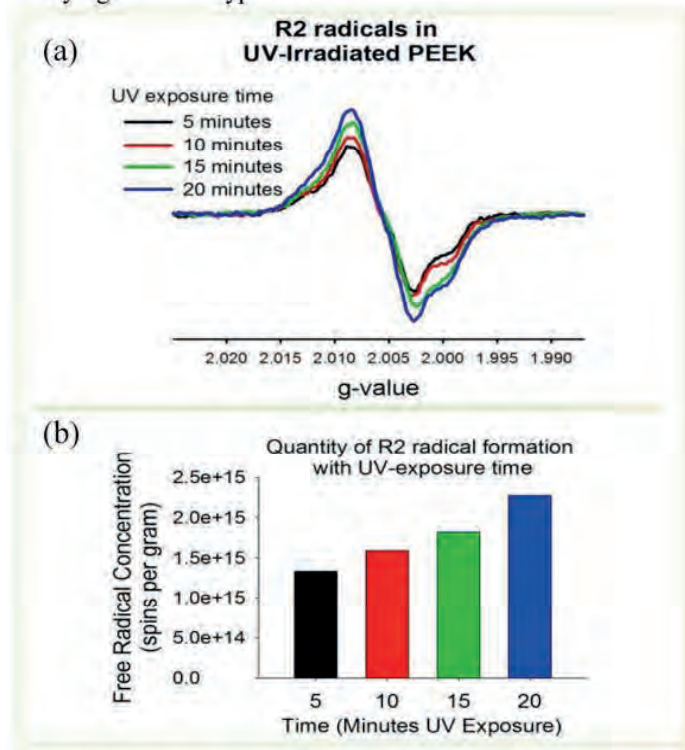
Figure 4. R2 formation with UV-irradiation time. Shown are (a) ESR spectra obtained via data subtraction like in Figure 2, and (b) corresponding radical concentration for one of the samples.

While the new R2 radical, formed in PEEK via irradiation, does decay with time in air at room temperature, we were able to still observe UV-induced radicals after more than three weeks (Figure 5).
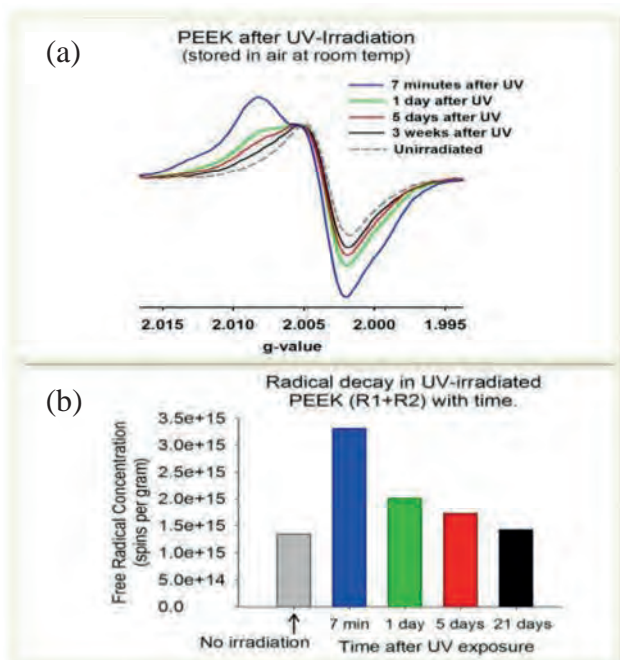
Figure 5. (a) ESR experimental spectra of PEEK after UV-irradiation and (b) corresponding radical concentrations. The grey line/bar represents the R1-only radical of PEEK before irradiation.

Summary: PEEK radical (R2) was detected in UV- and X-ray irradiated PEEK at 23°C. Additional work is needed to gain knowledge about the decay behavior and the molecular structure of the radical R2. The residual radical R1 (present in as-received PEEK) was found to be very stable. It could not be quenched or annealed by heating at or above melting temperature, rather its concentration increased.

References: [1] Kurtz SM. The PEEK Biomaterials Handbook, 1st Edition, Elsevier, 2012. [2] Awaja et al., Free Radicals Generated by Ion Bombardment of a Semi-Crystalline PEEK Surface, Plasma Process. Polym. 2012, 9, 174-9. [3] HM Li et al., The Effects on Polyether-etherketone and Polyethersulfonate of Electron and γ Irradiation, IEEE Trans. Dielectr. Electr. Insul., 1999, 6, 295-303.

Investigation into the Osseointegration of Oxygen Plasma Modified and Unmodified PEEK in a Sheep Model

AHC Poulsson[1], D Eglin[1], C Kamenisch[1], C Sprecher[1], Y Agrawal[1], D Nehrbass[1], S Zeiter[1], RG Richards[1]

[1]AO Research Institute, AO Foundation, Davos, CH.

spoulsson@gmail.com

Introduction: Polyetheretherketone (PEEK) has come into the spotlight as a replacement for metals in devices such as spine cages and patient specific CMF implants due to its radiolucency, good strength and wear properties[1]. PEEK is generally described in literature as bioinert, whereby it does not illicit a response from the body, whether that be positive or negative[2,3]. Many polymers such as PEEK have an intrinsic low surface energy. Surfaces with higher energy are known to promote rapid cellular adhesion and spreading, compared to surfaces with lower energy[4,5]. This can in turn lead to implant loosening as a result of fibrous encapsulation. To improve cellular adhesion and thereby influence the tissue interaction, the surface energy of PEEK can be increased by plasma surface modification. The effect of increasing the surface energy of PEEK has been studied *in vitro* and has been found to statistically significantly increase levels of human primary osteoblast cell adhesion to the surface of modified PEEK in comparison to unmodified PEEK. Higher levels of mineralization have also been found on the modified PEEK surfaces and more characteristic phenotypic expression for human primary osteoblast cells. The study presented here aims to investigate the effect of oxygen plasma modification of PEEK on the direct bone contact in the cancellous bone of the distal femur and proximal tibia and cortical bone of the tibia in a sheep model. The goal of this study was therefore to evaluate the interaction of modified PEEK compared to unmodified PEEK within cancellous and cortical bone and to evaluate the histological and mechanical stability of this interaction.

Methods and Materials: PEEK-OPTIMA® implants (Invibio Biomaterial Solutions, UK), were injection moulded (PO) or machined (PA) and then implanted with or without oxygen plasma surface modification. The plasma surface modification was performed with a Pico Plasma System (Diener Electronics, DE) for 2400sec. Surface chemical compositions were characterized by X-ray photoelectron spectroscopy (XPS), wettability by water contact angles and changes in topography by atomic force microscopy (AFM) and SEM. These implants were used in a total of 24 female Swiss Alpine Sheep, which were euthanized at 4 weeks, 12 weeks, and 26 weeks. Each sheep had 4 cortical bone defects per tibia, 2 cancellous bone defects per distal femur and 2 cancellous bone defects per proximal tibia. For the distal femur and proximal tibia, defects were created using a 4 mm drill bit, and the implants inserted according to a random scheme. Unicortical defects were then made on the tibia for the implants by stepwise increasing the diameter using a 2mm, 3mm and 4mm drill bit, and the 4 implants placed. In this bilateral model, the tibial implants had a length of 12 mm long, while the distal femur and proximal tibia had a length of 15 mm, both with a diameter of 4mm. Postoperatively, the sheep were housed in individual pens for the first 3 to 5 weeks and consequently group housed for the duration of the study. New bone formation was marked with two fluorochromes, calcein green and xylenol orange. At euthanasia samples were harvested in order to perform histological analysis, histomorphometry and biomechanical testing. The distal femur and left tibia were utilised for the mechanical tests, while the proximal tibia and right tibia were taken for histology and histomorphometry. The implants were mechanically pushed out of the femur/tibia with a cylindrical plunger of 3.8 mm diameter attached to the cross-head of an Instron 5866 (Universal Test Instrument, Norwood, MA, USA) test apparatus. Load was applied to the implant at a cross-head speed of 0.5 mm/min until the bone-implant interface ruptured as defined from the peak on the load-deformation curve. The histological samples were fixed in 70% ethanol for 2-3 weeks, and then dehydrated in an ascending series of alcohol before being transferred to xylene, and finally infiltrated with and embedded into methylmethacrylate (MMA). The polymerized blocks of MMA were cut into serial cross sections (150-250 µm thick) containing both bone and implant, which were glued onto opaque plexiglass slides, ground and polished to a final thickness of 80-180 µm using a microgrinding system (Exact®, Germany) and stained with Giemsa Eosin (GE) or left unstained for fluorochrome labeling analysis. The GE-stained slides were imaged using light microscopy (Axioplan, Zeiss®) and flurochromes by confocal microscopy (LSM Axiovert 200M, Zeiss®). The stained sections were evaluated by quantitative histomorphometric assessment for the amount of bone and for the amount of direct bone contact to the PEEK implant surface (bone-implant contact ratio).

Results: The analysis of the surface chemistry by XPS correlated with our previous findings for our *in vitro* study showing that unmodified PEEK had ~12 atom% surface oxygen[6]. The modified PEEK had ~17 atom% after 2400s exposure. High resolution C1s spectra showed the oxygen incorporation to primarily be a result of increasing C=O and O-C=O functional groups. Examination of the surface topography by AFM showed no significant change in the surface topography of the modified PEEK. However, the modified surfaces did appear to be etched and some pitting was observed.
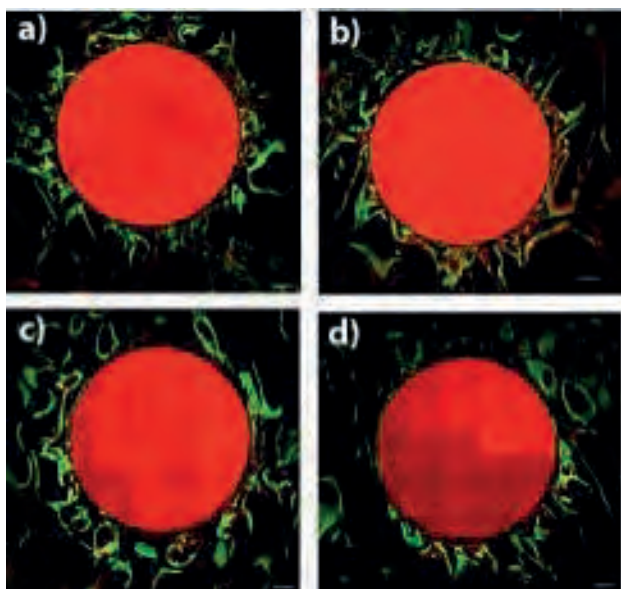
Fig 1: Fluorochrome labeling with calcein green 1 week post-implantation and xylenol orange 3 weeks post-implantation in the 4 week cancellous bone samples from the proximal tibia showing the new bone formation after the implantation of a) PO, b) POm, c) PA, d) PAm (red circle are the PEEK implants).

The interaction of the injection moulded modified (POm) and unmodified (PO) PEEK and machined modified (PAm) and unmodified (PA) PEEK implants was evaluated histologically and biomechanically after 4, 12 and 26 weeks in cortical and cancellous bone. The push-out tests indicate that there was a difference between the machined and injection moulded surfaces, however whether there was an effect from the surface modification has yet to be identified. The new bone formation, (Fig. 1) evaluated by the fluorochrome labeling showed that there was a large amount of remodeling between week 1 and 3 in the cancellous bone. There is an indication that there was more activity at 3 weeks, with more xylenol orange present directly surrounding the implants, and that the remodeling was occurring in the surroundings at 1 week with a strong signal from the calcein green. For the cortical bone, there was less activity, but ongoing remodeling was apparent. At the later time point of 12 weeks, there was less bone remodeling, however there was more in the cortical bone than in the cancellous, which is expected as the cortex remodels more slowly. By 26 weeks there was very little remodeling visible in both the cortical and cancellous bone, indicating that the implants had integrated well by this time-point. The GE staining from the 4 week time-point as shown in Fig. 2 for cancellous bone, showed very minimal inflammation and higher bone density surrounding the implant than in the surrounding tissue, confirming the remodeling observed with the fluorochrome labeling. In the cortical bone after 4 weeks, there was good implant contact to the surrounding bone and very little soft tissue was observed close to the implant. By 12 weeks the bone-implant contact was well established in both the cortical and the cancellous bone was higher with no visible inflammation from any of the implant surfaces. By 26 weeks, the majority of implants had integrated nicely though some patches of soft tissue could be observed. The differences between the modified and unmodified injection moulded and machined implants are currently being objectively analyzed using histomorphometry.
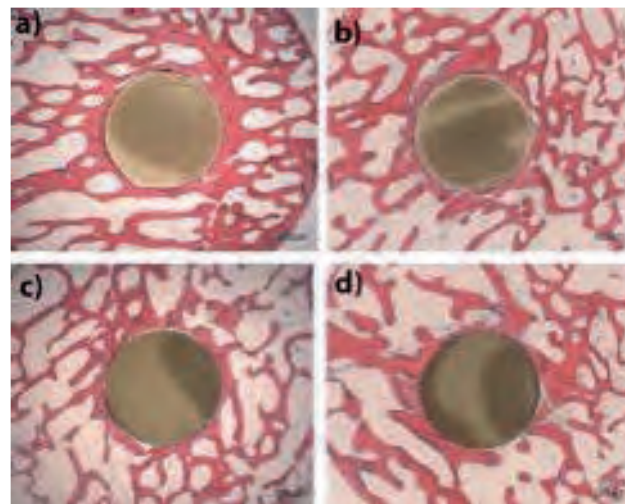
Fig 2: GE staining of the cancellous bone after 4 weeks implantation of a) PO, b) POm, c) PA, d) PAm PEEK implants (pink-bone, blue-soft tissue, white-bone marrow).

Discussion: The scale-up of the plasma surface modification from laboratory samples to modification of 3D implants has been successful, producing near identical levels of oxygen incorporation as observed in the *in vitro* studies. The histological evaluation of the PEEK samples showed that they have integrated well, showing early bone formation and very little inflammatory response. The histomorphometry is expected to identify if there are any differences between the integration of the injection moulded and machined PEEK and their modified versions.

References: 1. Kurtz, S. M.; Devine, J. N. Biomaterials 2007, 28 (32), 4845-4869. 2. Noiset, O; Schneider, Y-J; Marchand-Brynaert J. Journal of Polymer Science Part A: Polymer Chemistry 1997, 35 (17), 3779-3790. 3. Boccaccini, A. R.; Peters, C.; Roether, J. A.; Eifler, D.; Misra S.K.; Minay, E. J. Journal of Materials Science 2006, 41 (24), 8152-8159. 4. Lopez, G. P.; Ratner, B. D.; Tidwell, C. D.; Haycox, C. L.; Rapoza, R. J.; Horbett, T. A. Journal of Biomedical Materials Research 1992, 26, 415-439. 5. Kasemo, B. Biological Surface Science. Surface Science 2002, 500, 656-677. 6. Poulsson, A. H. C.; Richards, R. G. Surface Modification Techniques of PEEK; Including Plasma Surface Treatment . In PEEK Handbook, Kurtz, S. M., Ed.; Elsevier: 2011.

Fibroblasts and osteoblasts culivated on surface modified Polyetheretherketon (PEEK) compounds

Spintig, T[1]; Weinhold, H[1]; Müller, W-D[1]; A.Schwitalla[1]

[1]Universitätsmedizin Charité Berlin, Departement of Dental Research and Oral Biology, Berlin, Germany;

tobias.spintig@charite.de

Introduction: Polyetheretherketon (PEEK) is a very promising material in medical and dental research. Compounding PEEK with different contens (carbon-, glassfiber) increased the variety of application [1,2]. It could be shown [3,4] that the proliferation of fibro- and osteoblasts is not negatively influenced by such PEEK compounds. The verificaton of PEEK as a biomaterial for dental implants should be investigated.

Aim of this study is a surface modification of different PEEK compounds to improve the interaction with fibroblast and osteoblast cells without changing or affecting the main bulk properties.

As prearrangement PEEK material parameters [5], the effect of SBF cultivation [6] and the influence of fetal calf serum (FCS) [7] on cell proliferation were investigated.

Methods and Materials: 252 PEEK discs (diameter 10mm) have been manufactured from three different PEEK compounds and were polished with siliciumcarbid (up to 4000 grain size). Afterwards 126 of the specimens were blasted (4 bar pressure) with two different bioceramics: 63 specimens with TCP (tricalciumphosphate) with an average grain size of 7µm and 63 specimens with GB14 (resorbable bioglass ceramic) with a grain size from 100µm to 250µm – 126 specimens remained untreated (polished).

Fig.1: number of specimens

Compound	polished	TCP-blasted	GB14-blasted
PEEK BC1WH	42	21	21
PEEK BC1CA30	42	21	21
PEEK 450GL30	42	21	21

SEM Pictures were taken followed by an EDX-Analysis.
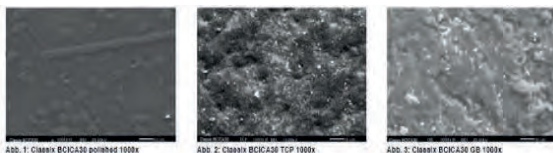
Pic1.: PEEK Classix BCICA30 (SEM 1000x) polished, TCP-, GB14-treated

Different concentrations of FCS and cell-numbers were incubated in well-plates for 21 days followed by a statistical analysis to determinate a reasonable FCS/cell-number combination.

Afterwards the specimens were cleaned, sterilized and placed in well-plates. A solution of 25.000 fibroblasts per ml (without any FCS) was added on 63 polished specimens (21 of each compound). In a similar way a solution of 25.000 human osteoblasts (HOB) per ml was added on 189 surface modified PEEK compounds. Medium was changed every three days.

Proliferation (IFM (Alicona©), fluorescence microscopy, Alamar-Blue®) and cell morphology were detected for 21 days (days of detection: 1, 3, 5, 7, 10, 14, 21) followed by a statistical analysis.

Results: A concentration of 25.000 cells per ml without FCS was choosed for testing the cell cultivation on PEEK specimens because the proliferation primary depends on the FCS concentration. Proliferation (after 21 days) is indepent from cell number at the beginning.

The number of fibroblasts on polished specimens increased from 105 cells/mm to 310 cells/mm over 21 days whereas the single cell viability was constantly over that period. Glassfibre reinforced PEEK showed highest cell number – followed by carbonfibre reinforced and PEEK Classix. There is no difference in cell morphology shown.

Alamar-Blue® of HOB showed an increase of cell metabolism during the period of detection. The Extinction differs between the PEEK-compounds and between the surface modifications. Polished specimens show comparable results whereas TCP and GB14 treated surfaces decreases in comparision to polished specimens. The number of cells per specimen increased (from day 1 to day 21) for all compounds. Cell morphology depends on surface modification (Pic.2).
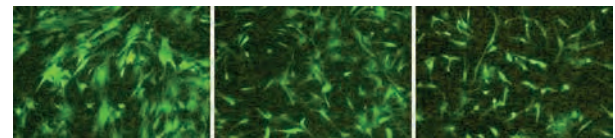
Pic2.: PEEK Classix BCICA30 Day 5 (fluorescence 10x) polished, TCP-, GB14-treated

Discussion: Single cell viability is comparable for all PEEK compounds. Different treatments of PEEK surfaces do have an influence on proliferation and morphology of human osteoblast cells in vitro. Polished surfaces showed comparable results for all compounds. The Proliferation of HOB on TCP and GB14 treated surfaces decreases for PEEK BCIWH and 450GL30. How reliable it is, should be investigated more in detail in the future.

References: [1] S.W. Ha et al. (1997) - Surface activation of PEEK and formation of calcium phosphate coatings by precipitation; [2] S. Strametz et al. (2005) - Response of primary fibroblasts and osteoblasts to plasma treated PEEK surfaces; [3] T. Lin et al. (1997) - Glass PEEK promotes proliferation and osteocalcin production of human osteoblastic cells; [4] L. Petrovic et al. (2006) - Effect of ßTCP filled polyetherether-ketone on osteoblast cell proliferation in vitro; [5] T. Spintig et al. (2008) - PEEK - a potential dental material; [6] T. Spintig et al. (2009) – Modified Polyetheretherketon (PEEK) cultivated in SBF; [7] T. Spintig et al. (2012) – Fibroblasts culivated on different Polyetheretherketon (PEEK) compounds;

Osteointegrative Coating Solutions for PEEK-based Implants

Zappini G[1], Mallardo A[1], Robotti P[1], George B[2], Stübinger S[3], Preve E[1]

[1]Eurocoating SpA, Trento, Italy
[2]Surface Dynamics, Cincinnati, OH, USA
[3]MSRU, Vetsuisse Faculty, University Zurich, CH
gianlucazappini@eurocoating.it

Introduction:

The use of PEEK is notably increasing in the biomedical field, especially in spine applications, due to its biocompatibility, radiolucency and favorable stiffness values. However, the material itself offers limited possibility for direct bone anchorage. In order to improve the stability of the bone-implant interface, PEEK implants can be coated with Titanium (Ti) or Hydroxyapatite (HA) via Plasma Spray (PS) processes. This approach is challenging because PEEK is a material susceptible to degradation when exposed to high temperatures as those typically developed during PS, yet in the past years low thickness coatings could be successfully developed.[1,2]

Nevertheless, the porosity and roughness of these coatings are relatively low when compared with the state of the art represented by the highly porous coatings found on metallic substrates. Aim of this work is to show a further development step allowing highly porous Ti coatings application also on PEEK.

Materials and Methods:

Samples made of unfilled PEEK (Optima® LT1) and carbon-fiber reinforced (CFR) PEEK (Optima® LT1CA30 and Motis®, Invibio Ltd, UK) were coated by Eurocoating SpA and Surface Dynamics.

Different PS technologies (Air Plasma Spray and Vacuum Plasma Spray) were used along with HA and Ti raw materials powders of different grain sizes in order to obtain coatings with different properties.

Physical analyses were performed on coatings for assessing thickness and porosity (ASTM F1854), roughness (ISO 4287, 4288), and adhesion (ASTM F1147). Chemical analyses were carried out on the coated substrates by FT-IR techniques (ASTM F2778).

Biocompatibility, osteointegration and fixation capability of four selected coatings were assessed trough an in-vivo study in sheep. Three groups of differently Ti-coated implants, one group of Ti/HA-double-coated implants were compared to two uncoated groups of implants (Optima® LT1 and Motis®, used as reference). Overall, n=108 cylindrical samples were implanted into the pelvis shaft of n=6 sheep. After 2 and 12 weeks samples were retrieved and analyzed via histomorphometry and pull-out mechanical testing. The animal study was performed at the Vetsuisse Faculty, University of Zurich (CH).

Results and Discussion:

Newly developed porous Ti-coating showed very good adhesion values on both unfilled and CFR PEEK samples (data shown in Table).
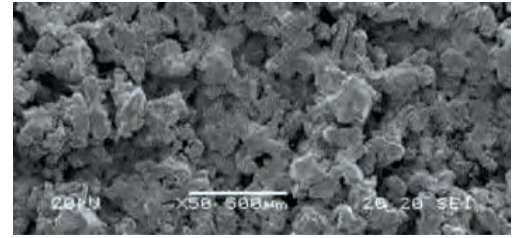
Fig. 1- Porous Ti-coating on PEEK; top view, SEM observation

Compared to previously developed Ti and HA coatings higher thickness layers are also achieved. The open-porous structure is evident in figures 1 and 2.

Fig. 2- Porous Ti-coating; micrographic cross-section

Main coatings properties are summarized in the following Table:

Coating	Typical nominal thickness (µm)	Average roughness (Ra, µm)	Adhesion values on unfilled PEEK (MPa)	Adhesion values on CFR-PEEK (MPa)
Ti, low roughness	80±20	8±1	28±4	32±6
Ti, high roughness	250±50	19±2	--	30±5
Ti, porous	400±50	40±3	38±5	44±4
HA	65±20	6±2	19±3	22±5

For all coatings FT-IR analyses did not indicate changes in the chemical structure of the coated substrates.

All in-vivo tested implants could be placed without complications and with good primary stability. Pull-out values at 2 weeks, unexpectedly for such a short time, already revealed an increase in stability for the coated implants compared to the two uncoated groups of implants (highly significant for 3 of the 4 groups). In all coated groups a significant increase of retention could be observed from 2 to 12 weeks. At the end of the investigation period, all coated groups showed a significantly improved pull-out strength versus the uncoated implants.

The following Table summarizes the mean values of pull-out strength at 2 and 12 weeks, calculated dividing the maximum pull-out force by the coated area of the implant:

Bulk material and coating	Pull-out strength (MPa)	
	After 2 weeks	After 12 weeks
LT1, uncoated	0.2±0.1	0.2±0.1
Motis, uncoated	0.3±0.2	0.2±0.1
LT1 coated with Ti, low roughness	1.3±0.4	4.7±1.2
Motis coated with Ti, high roughness	1.9±0.6	6.7±1.9
Motis coated with Ti, porous	0.8±0.7	5.6±1.4
Motis double-coated Ti/HA	2.2±0.5	7.5±1.7

Preliminary histomorphometrical and fluorescent microscopic analyses are available. Further data collection is in progress.

Conclusion:
Recent optimizations in Plasma Spray process control and technology are allowing application of titanium coatings on PEEK characterized by high porosity and wider pores size. These features, recognized to be suitable for fixed osteointegration in clinical application, were experienced before on metallic orthopedic components only.
Evidences of the biocompatibility and high osteointegrative potential of different coating solutions have been shown using an in vivo animal study.

Bibliography:
1. Robotti P. and Zappini G., in PEEK Biomaterials Handbook, 2012 Elsevier; Chapter 9, pp 119-143.
2. T. Friesem et al. NuNec™: A PEEK-on-PEEK Cervical Arthroplasty System: In Clinical Perspective. Spinal Surgery News, Winter 2009.

Plasma immersion ion implantation treatment of poly-ether ether ketone for surface biofunctionalization

Lu, WY[1,2], McKenzie, DR[2], Dunstan, CR[1], Bilek, MMM[2]

[1] Biomedical Engineering, The University of Sydney. [2] Applied Plasma Physics, The University of Sydney, Australia.

william.lu@sydney.edu.au

Introduction: Poly-ether ether ketone (PEEK) has emerged as a leading biomaterial for replacing metal implant components due to its stability in biological systems as well as outstanding mechanical properties. However, due to the inertness of the material, cell attachment and growth remains suboptimal which limits the types of applications it can be utilized. Therefore, interest has been focused on modifying the surface of PEEK materials in order to improve its bioactivity. Recently, Plasma Immersion Ion Implantation (PIII) was shown to produce favorable surfaces when used to treat a range of polymeric biomaterials. It was demonstrated that the convenient PIII treatment not only improves the bioactivity and blood compatibility of many surfaces, but also provides a one-step method to covalently immobilize cellular proteins such as ECM and growth factors onto the treated surfaces. The aim of this project is to study the effects of the PIII treatment on PEEK and explore methods of achieving improved bone cell responses by changing surface properties with PIII as well as using PIII to bio-functionalize PEEK surfaces with bone matrix proteins.

Methods and Materials: Semi-crystalline PEEK as a 250 µm thick film (APTIV 1000 series) was purchased from Victrex UK. The ethanol cleaned samples were immersed in nitrogen plasma at 100W and then PIII treated by applying 20 kV pulses lasting for 20 µs with a repetition rate of 50 Hz for a duration of 40 to 1600 seconds. The characterization of the treated surfaces had been evaluated by contact angle measurements, XPS and ATR-FTIR. The covalent immobilization of proteins was performed simply by incubating the treated samples in buffer containing various ECM proteins for an adequate amount of time. The coated surfaces were then evaluated by ELISA, microBCA and ATR-FTIR detection coupled with SDS washing. Cell culture studies had also been performed with MG-63 and MC-3T3 E1 cell lines as well as human primary osteoblasts to assess the biological performances of the created surfaces. In particular, cell attachment, cell spreading, cell proliferation and gene expression were evaluated.

Results: Contact angle studies have shown that the hydrophobic recovery after longer PIII treatments occurs at a much higher rate due to a large decrease in the polar component of the surface energy. Interestingly, this result seems unique to PEEK and polystyrene (PS) with the opposite trend observed in polymers such as polyethylene (PE) and Polyethylene terephthalate (PET).

Protein immobilization studies had demonstrated that proteins remain detectable on the surfaces even after harsh washing and boiling conditions only for the PIII treated samples. This confirms that proteins are covalently linked to the modified surfaces and ageing tests also demonstrate that this ability remains present even at one year after treatment.

ELISA detection of tropoelastin bound to PEEK
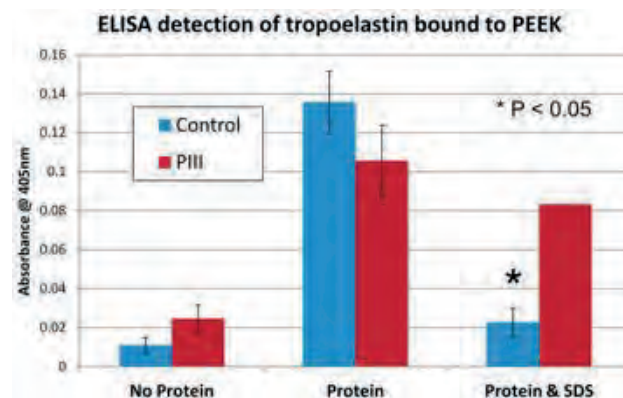
Cell attachment results have shown that the PIII treatment of PEEK surfaces alone increases the bone cell attachment rate by over 80% for both MG-63 cell lines as well as human primary osteoblasts. Cell spreading and proliferation were also observed to be significantly improved. Cell culture studies performed on the protein coated surfaces revealed that the covalently linked ECM proteins on the treated surfaces was able to perform equally well compared to the controls. This demonstrates that the covalent linked ECM proteins still remain to be highly biologically active.

Discussion: Overall, the current results had shown that cell attachment to PEEK can be largely improved by using PIII alone to modify the surface properties. Protein immobilization studies coupled with SDS washing confirms a covalent linkage between the surface and the proteins. The immobilized proteins remain biologically active thus confirming the possibility of using PIII to further bio-functionalize PEEK surfaces with bone matrix proteins that may help in further improving the bioactivity of PEEK. These findings will help us further understand the effects of the PIII treatment process on PEEK in which the outcomes may help us improve its bioactivity for bone related applications.

Novel Method for making homogeneous Bioactive PEEK compounds using an ultrasonic Co-feeding and On-line Mixing System

Zongqi Li,[1] Jordan Chant,[2] Mohammad Vaezi[1], Marcus Jarman-Smith[3], Jo Wilson[3], Shoufeng Yang[1]*

[1] School of Engineering Sciences, University of Southampton, Southampton, UK, SO17 1BJ
[2] School of Chemistry, University of Southampton, Southampton, UK, SO17 1BJ
[3] Invibio Biomaterial Solutions, Hillhouse International, Thornton Cleveleys, UK.
s.yang@soton.ac.uk

Introduction: PEEK-OPTIMA® is an implant grade polyetheretherketone polymer, and has been used clinically since 1999. The properties of PEEK are already considered useful to produce flexible implants, and the introduction of porosity may provide a transitional zone between the bone and biomaterial, further reducing stress shielding in load-bearing applications. Porous PEEK biomaterial with uniform pore distribution can allow the opportunity for the material to better integrate or interact with surrounding tissue. Interest has grown in enhancing the osseointegration of PEEK through mixing with bioactive materials such as 45S5 Bioglass to manufacture porous PEEK production.

Granular segregation, sometimes described as the Brazil nut effect, is a common phenomenon in granular materials mixing in which particles of different sizes are used. The larger and/or low density particles end up to the top when these particulate mixtures are stirred, shaken or jostled [1,2]. This effect is fatal in many industrial processes where an ordered mixture is strictly required.

In this work, the feasibility of an ultrasonic co-feeding system was demonstrated by preparing homogeneous mixtures from two materials with different physical properties. Meanwhile, a homogenous mixing of commercially used implant grade polyetheretherketone polymer (PEEK) and bioglass which are prone to segregate during traditional stir mixing was proved for further bioactive compound fabrication.

Materials and Methods: Two or more ultrasonic micro-feeders originally designed by Yang and coworkers [3, 4] were employed to complete the online mixing task. To verify the real time flow rate of the two different material powders, the nozzles with different size were designed for micro-feeders. Before mixture preparation, a programmed processing control platform has been built in which a seven places micro-balance is used to verify the flow rate of individual powder. Different mixing proportions of two materials are achieved by adjusting the ratio of flow rates.

Glass beads and sands with narrow particle size distribution (around 140 μm and 200 μm, respectively) were also used to demonstrate the capability of co-feeding system on homogenous mixing different materials with different physical properties, such as particle size, particle shape and density.
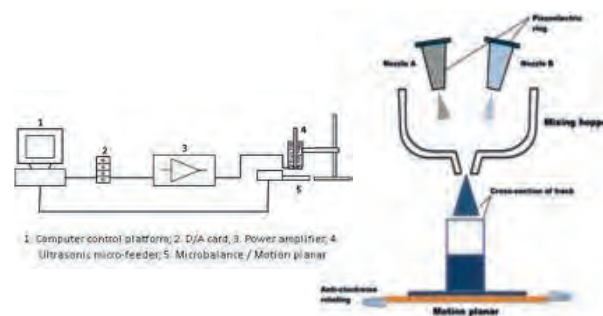
Figure 1 Schematic diagram of ultrasonic co-feeding System

Poloxamer, a low density polymer with good spherical shape and sieved to 200 μm, was also used to demonstrate the mixing uniformity of materials with different density.

Sub-millimeter rod-shaped PEEK-OPTIMA® granule (Invibio Biomaterial Solutions Ltd., UK) and bioglass were fed simultaneously into a mould with co-feeding system in a ratio of 50/50 (wt/wt) for further heat treatment to prepare a homogeneous bioactive compound. The blend could then be heated at 400 ℃ for 45 minutes to melt the PEEK and bond to the filler to create a PEEK Bioactive compound suitable for machining into test samples.

X-Ray Computed Tomography (X-ray CT) imaging technology has been used to evaluate the mixing uniformity through 3-dimensional image of the mixture.

Results: A scalable, reproducible method for the production of homogenous mixture from materials with different physical properties is developed. The system contains two or more micro-feeders through which particles from several microns to a few millimeters could be co-fed accurately. For each pair of materials, various

Figure 2 X-ray computed tomography image of cross-section of mixtures: glass beads and sands (left); poloxamer and glass beads (right)
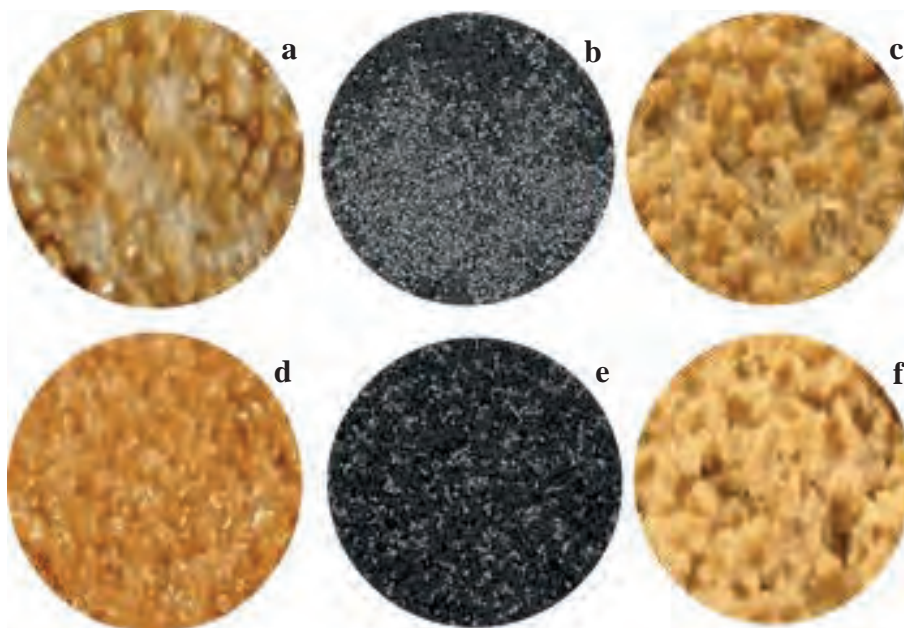
Figure 3 Samples of bioactive production of PEEK: a. Dry powder PEEK and Bioglass mixture from stir mixing; b. 2D CT image of sample (a); c. Sintered sample (a); d. Dry powder PEEK and Bioglass mixture from ultrasonic co-feeding system; e. 2D CT image of sample (d); f. Sintered sample (d)

mixing ratios were also achieved by controlling the flow rate of particles from the feeders.

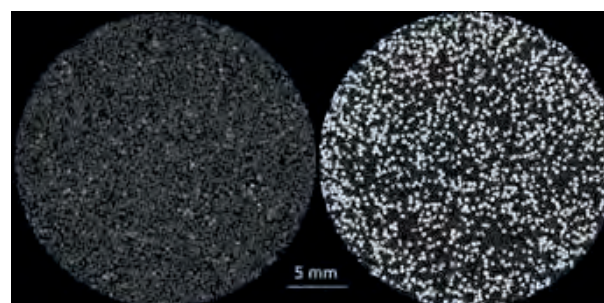The use of ultrasonic vibrations aids in breaking arches of particles in the nozzle by applying a continuous force. As a result, these vibrations when switched on, can initiate the flow of powder; when switched off, particle-particle and particle-wall frictions lead to formation of arches causing powder flow arrest immediately without using any mechanical stopper.

Top-view images derived from X-ray CT data are assessed for homogeneous and inhomogeneous distributions of mixed samples with different size, shape and/or density of particles at different layers exhibiting a reasonable homogenous distribution.

Discussion: The flow rate was appropriately set up to a few grams per second to balance the uniformity and filling efficiency in small scale vessels. However, relative high flow rate can be achieved as well by adjusting nozzle size if necessary.

The porous PEEK sample with narrow pore size distribution was fabricated by this ultrasonic co-feeding method which has made a significantly improvement comparing with traditional stir mixing.

References:

1. A. Rosato, K. J. Strandburg, F. Prinz and R. H. Swendsen, Physical Review Letters, 1987, 58, 1038-1040.
2. M. E. Möbius, B. E. Lauderdale, S. R. Nagel and H. M. Jaeger, Nature, 2001, 414, 270
3. S. Yang, J.R.G. Evans, Materials Science and Engineering A, 2004, 379, 351–359.
4. Zongqi Li and Shoufeng Yang, Nano Life, 2012, 2

Porous PEEK and Surface Modified PEEK for Musculoskeletal Applications

[1]Robert Poggie, [2]Simon Carrier, [2]Phillip Rouseau, [2]Daniel Morrissette, [3]Helmut Thissen, [3]Paul Pasic, [3]Graham Johnson, [3]Penny Bean, [3]Keith McLean, and [4]William Walsh

[1]BioVera, Montreal, QC, Canada, [2]PPD Group, Waterville, QC, Canada, [3]CSIRO Materials Science and Engineering, Clayton VIC, Australia, [4]Surgical Orthopaedic Research Laboratory, University of New South Wales, Sydney NSW, Australia
orthobob@videotron.ca

Introduction: Polyetheretherketone is the thermoplastic of choice for orthopaedic devices due to biocompatibility and strength. Despite PEEK's widespread clinical use, two limitations include lack of a commercially viable scaffold for osteointegration and relative poor affinity to bone. The purpose of this work was to develop a reliable means to manufacture porous PEEK and to covalently bond a polymer coating for improved bone cell response for porous and solid devices.

Methods and Materials: The porous PEEK is fabricated with a proprietary lost porogen process with 600 micron diameter salt. Coatings were deposited on solid and porous PEEK by covalent immobilisation of a macro-initiator carrying carboxylic acid functional groups and Reversible Addition Fragmentation Chain Transfer (RAFT) radical polymerisation chain transfer agent moieties following reductive amination of the polymer substrate. Controlled free radical graft polymerisation of homo- and copolymers representing different ratios of butyl methacrylate, phosphate methacrylate, acrylic acid, aminoethyl methacrylate and N-isopropyl- acrylamide was performed. Surface analysis was done with X-ray photoelectron spectroscopy (XPS) and static contact angle measurements for wettability. Chemical stability of the coating was determined with respect to gamma radiation (15, 25 kGy). *In vitro* cell culture experiments were performed with human Saos-2 bone-derived cells on solid PEEK. Cell attachment was quantified after 1, 3 and 7 days. Cell cultures were carried out for 21 days to evaluate mineralisation. In-vivo evaluation of bone ingrowth into porous PEEK cylinders (80% porous, 20 mm long, 6 mm diameter, Figure 1 below) was evaluated by histology after implantation for 12 weeks in 4-5 year old skeletally mature sheep (Merino Ewes).
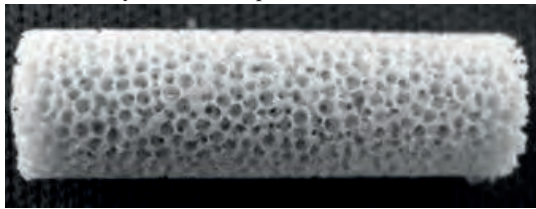

Figure 1: 80% porous PEEK cylinder (6mm x 20mm)

Results: Typical properties for the porous PEEK materials as a function of porosity, 72-80%, are shown below in Table 1.

Table 1: Compressive strength, stiffness, permeability

	72%	74%	76%	78%	80%
Strength (MPa)	8.67	6.88	5.62	4.16	3.17
Stiffness (MPa)	273.8	226.7	180.2	145.5	125.0
Perm, $k(m^2)x10^{-10}$)	0.18	0.26	0.36	0.47	0.66

The results of coating experiments indicated that copolymers representing 33 mol% phosphate methacrylate and 67 mol% butyl methacrylate (PB) had the largest effect on cell attachment and growth. Results for 1, 3, and 7 day cell growth on solid PEEK are shown in Table 1 and Figure 2. Notably, the results of 21-day Saos-2 cell cultures indicated a four-fold increase in mineralisation for PB coated PEEK as compared to uncoated PEEK based on Alizarin Red S absorbance measurements (565 nm).

Table 2. Saos-2 cell on solid PEEK with and w/o PB coating. (Results shown as a % of TCPS at Day 7).

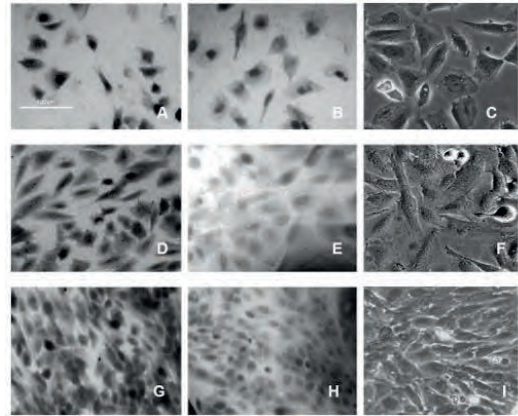|	% Cell Growth		
	Day 1	Day 3	Day 7
Virgin PEEK	25.4 ± 2.3	47.9 ± 4.1	92.0 ± 4.4
PEEK+PB	16.1 ± 4.2	92.9 ± 3.1	146.2 ± 3.9

Figure 1: Saos-2 cells after 7 days with A, D, G for solid PEEK, B, E, H for PB coated porous PEEK, and C, F, I for TCPS. Time points are 1 day A, B, C; 3 days D, E, F; 7 days G, H, I.

XPS showed the covalent immobilization of the PB coating on PEEK substrates and porous PEEK cylinders. XPS of PB coated porous PEEK structures before and after gamma radiation (15 and 25 kGy doses) indicated unchanged elemental values, except for a small increase in oxygen. The major constituents of the PB coating were 23% oxygen, 1% nitrogen, 0.6% phosphorous, 1% sulfur, and the balance carbon. The thickness of the PB coating was estimated at 10 nm. Wettability of PEEK (n=10, std dev 0.02, 0.03) obtained from virgin PEEK and subsequent to the three steps of surface processes are below.

Table 3: Wettability of PEEK and modified PEEK

SAMPLE	Contact Angle
Virgin PEEK	95.4
PEEK-Amine	72.8
PEEK-Amine-RAFT	60.6
PEEK-Amine-RAFT-PB	68.9

Early results from the ovine study indicate bone ingrowth for virgin, PB-coated, and BMA-soaked 80% porous PEEK.

Discussion: Pore size and porosity of porous PEEK are similar to porous metals currently used in orthopaedics. The range of strength of porous PEEK is sufficient for bone reconstruction, with ancillary fixation or other structural means of support for higher load applications. The compressive modulus (270 MPa) is similar to cancellous bone and permeability similar to human cancellous bone. A RAFT-based graft copolymer coating was shown to be uniformly applied to porous PEEK and to substantially increase Saos-2 cell attachment, proliferation and mineralisation on solid PEEK. XPS confirmed the presence of the coating within porous PEEK. XPS showed chemical stability of the coating in the range of 15 to 25 kGy. Bone ingrowth was confirmed for coated 80% porous PEEK with and without BMA.

PEEK on PEEK Articulations in Spinal Disc Arthroplasty

Brown, TB[1]
[1]Pioneer Surgical, Marquette, MI, USA
timbrown@pioneersurgical.com

Introduction: Over the past several years, total disc arthroplasty and nucleus replacement for the lumbar and cervical spine has been developed as an alternative to arthrodesis as a treatment option for degenerative disc disease. In many ways the development of this technology has paralleled that of total joint arthroplasty, with a central element in the design of these devices being an articulating component as the premise for their motion preserving characteristics. As a consequence, they bear the same risks of device wear and durability. In order to ensure a reasonable assurance of safety and performance of these devices, *in vitro* wear simulations are performed. However, unlike total joint replacements, there is no substantial clinical retrieval history, and knowledge about their clinical wear behaviour remains limited. ASTM and ISO have developed testing methodologies for evaluating the wear properties of these devices; however, they have not been clinically validated. To this end, when evaluating candidate materials for assessment of the various potential influences on a respective devices' wear properties, multiple rather than relying on one set of parameters, is essential. PEEK-OPTIMA (PEEK) is widely used in long term implantable medical devices due to its excellent material properties. However, self-mating PEEK (PEEK/PEEK) represents a unique and novel articulating material for use in the spine. Consequently, the wear properties are largely unknown for this application. Therefore, how deviation from a single set of testing parameters translates to differences in the amount of wear is clinically important.

Methods and Materials: For lumbar spine applications, five groups (n = 6) of nucleus replacement devices manufactured from PEEK with a ball/socket articulation were tested on a spine wear simulator. The implants were submersed in newborn calf serum (20g/l) at 37°±2°C. Group 1 consisted of ±7.5° flexion/extension to 10 million cycles (Mc) followed by ±7.5° lateral-bending to 10 Mc. This sequence was alternated to 40 Mc. Groups 2-5 were tested according to ISO 18192-1 to 10 Mc (**Figure 1**), except that group 3 incorporated frequency shifting to insure a non-repetitive load and motion profile (**Figure 2**). Frequency shifting consisted of 2.84 Hz compressive load, 2.0 Hz flexion/extension, 1.9 Hz lateral bending, and 2.11 Hz axial rotation to maximize cross shear effects. Groups 1-3 and 5 were exposed to 30 kGy gamma sterilization in air. Group 4 was exposed to the combined effects of 200 kGy followed by simulated aging. The simulated aging process was similar to ASTM F2003-02, which was developed to measure accelerated aging in UHMWPE packaged in air, except that the aging time was extended from 14 days to 40 days. Groups 1-4 incorporated a cyclic load magnitude of 225-1024 N consistent with the load sharing of a nucleus replacement

device. For group 5, the compressive load was 600-2000 N, consistent with the total lumbar disc load established in ISO 18192.
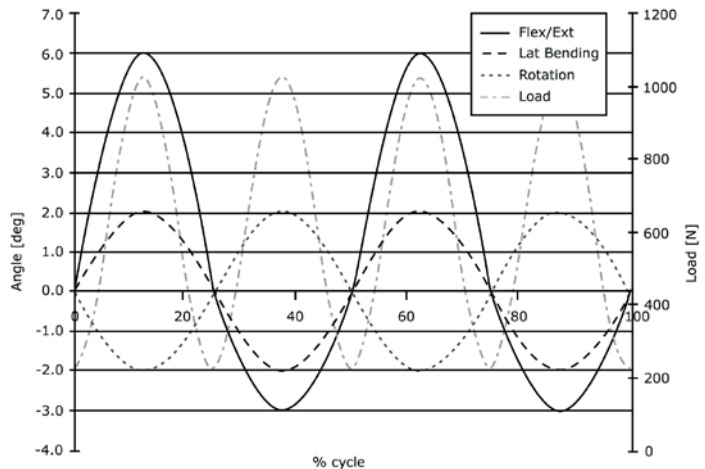
Figure 1: Load and motion profile for groups 2, 4, 5.
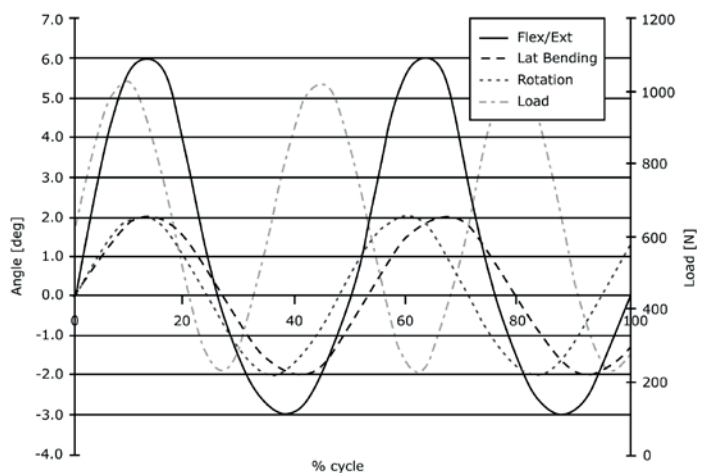
Figure 2: Load and motion profile for group 3.

For cervical spine applications, four groups (n = 6) of cervical arthroplasty devices manufactured from PEEK with a ball/socket articulation were tested on a spine wear simulator. **Table 1** summarizes the testing methodology. In addition, a comparative study was performed against a UHMWPE/CoCr device with established clinical use to further validate the use of PEEK/PEEK as an articulating combination. **Table 2** summarizes the testing methodology. The load and motion profiles are shown in **Figure 3**. Average wear rates for all tests were determined using linear regression analysis with significant differences ($p < 0.05$) determined using either a one-way ANOVA or Wald test.

Results: All implants in each group tested maintained full

Table 1: Testing methodology for the cervical arthroplasty device

Group	Load/Motion	Frequency	Test Fluid*	Duration
1a-TDR	ASTM	2 Hz	20g/L serum	0-10 Mc
1b-TDR	ISO	2 Hz	20g/L serum	10-20 Mc
2a-TDR	ASTM	1 Hz	20g/L serum	0-4 Mc
2b-TDR	ISO	1 Hz	20g/L serum	4-7 Mc
3-TDR	ISO	1 Hz	5g/L serum	3 Mc
4-TDR	ISO	2 Hz	Saline	10 Mc

*All testing fluid was maintained at 37° C with the exception of Group 3, which was maintained at 23° C to minimize protein degradation.

Table 2: Testing methodology for the cervical arthroplasty device

Group	Load/Motion	Frequency	Test Fluid*	Duration
PEEK	ISO	1 Hz	5g/L serum	15 Mc
UHMWPE/CoCr	ISO	1 Hz	5g/L serum	5 Mc

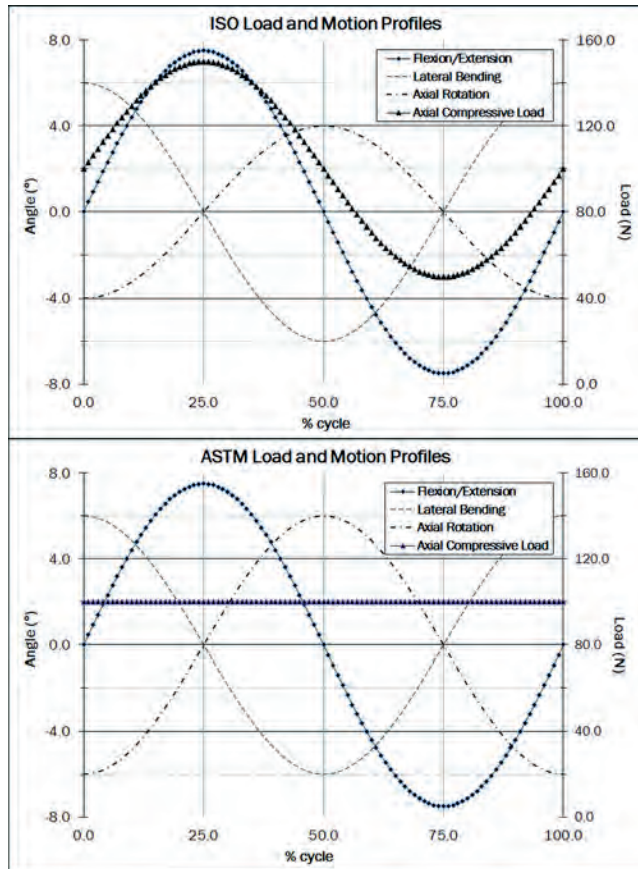*All testing fluid was maintained at 23° C to minimize protein degradation.

Figure 3: Load and motion profiles for the cervical arthroplasty device (ISO top, ASTM bottom)

functionality throughout each test duration. Visual and light microscopy revealed no evidence of gross deformation, delamination or fatigue cracks in the implants after testing. Closer examination under light microscopy revealed an abrasive wear mechanism occurring, with scratches and highly polished surfaces for all groups. **Tables 3** and **4** summarize the wear rates for the nucleus replacement and cervical arthroplasty device.

Table 3: Wear rates for the nucleus replacement device

Group	Wear rate (mm³/Mc)			p
	1-10 Mc	10-20 Mc	0-40 Mc	
1-NR	0.23 ± 0.02	0.21 ±0.01	0.22 ± 0.01	<0.05*
2-NR	0.41 ± 0.04	-	-	<0.05**
3-NR	0.42 ± 0.05	-	-	<0.05**
4-NR	0.52 ± 0.09	-	-	<0.05**
5-NR	0.92 ± 0.04	-	-	<0.05#

*vs. all groups, **vs. 5, # vs. all groups

Table 4: Wear rates for the cervical arthroplasty device

Group	Wear rate (mm³/Mc)	p
1a-TDR	0.26 ± 0.01	<0.05*
1b-TDR	0.32 ± 0.02	<0.05**
2a-TDR	0.58 ± 0.07	<0.05#
2b-TDR	0.57 ± 0.03	<0.05^
3-TDR	0.67 ± 0.10	<0.05Δ
4-TDR	0.89 ± 0.08	<0.05¥
PEEK/PEEK	0.53 ± 0.03	<0.05
UHMWPE/CoCr	0.96 ± 0.01	

*vs. all groups, **vs. all except 1a, # vs. 4, ^vs. 3 and 4, Δvs. 4, ¥vs. all groups

Discussion: These series of tests have provided the first comprehensive assessment of the wear characteristics of PEEK as a self-mating bearing material for disc arthroplasty applications. The results of these tests show that the simulated wear behavior of self-mating PEEK is highly dependent on the testing methodology, and that a single set of parameters cannot fully predict the performance of these devices. For the nucleus replacement device, there were significant increases in the wear rate when multi-directional vs. unidirectional motion was employed, and when the compressive load was increased. Exaggerated cross shear motion was not shown to have an impact, similar to excessive sterilization; which was to be expected given the resistance of PEEK to radiation/oxidation degradation. For the cervical device, a high dependency was shown on the testing environment. Although there was a small but significant increase in the wear rates comparing ASTM to ISO methods, there was more dependency on the protein content (3x increase in the wear rate) and the cyclic test frequency (2x increase in the wear rate). A comparison study against a clinically established bearing couple (UHMWPE/CoCr) revealed a significantly less wear rate for the self-mating PEEK device. From a clinical perspective, the ramifications of these results are not known at this time. Long term clinical data and ongoing retrievals are needed for validation of these outcomes.

Smart modification of PEEK by self-initiated surface graft polymerization for orthopedic bearings

Kyomoto, M[1,2], Moro, T[1], Yamane, S[1,2], Takatori, Y[1], Ishihara, K[1]
[1]The University of Tokyo, Tokyo, Japan, [2]KYOCERA Medical Corporation, Osaka, Japan
kyomoto@mpc.t.u-tokyo.ac.jp

Introduction: Poly(ether-ether-ketone) (PEEK) is considered a promising novel biomaterial for orthopedic applications because it exhibits excellent mechanical properties, chemical stability, and non-magnetic nature as compared to polyethylene or metallic materials. However, conventional PEEK cannot satisfy these requirements, e.g., wear resistance and biocompatibility for use in the fabrication of an artificial joint. Therefore, the use of PEEK as implants, either as a reinforcing agent or as a surface modifier, has been studied with focus on the wear resistance and biocompatibility of the polymer. We propose here, a new and safer method for constructing a nanometer-scale modified surface on the PEEK and carbon-fiber-reinforced PEEK (CFR-PEEK) substrates by self-initiated photoinduced graft polymerization to form smart PEEK biomaterials. In this study, we have demonstrated the fabrication of a highly hydrophilic and biocompatible nanometer-scale modified surface by the photoinduced graft polymerization of 2-methacryloyloxyethyl phosphorylcholine (MPC). The new and safer polymerization system is called "self-initiated surface graft polymerization." We hypothesize that the cartilage-like surface obtained by the surface modification of biocompatible poly(MPC) (PMPC) exhibits excellent biocompatibility and hydrophilicity under physiological conditions.

Methods and Materials: PEEK (450G; Victrex PLC, Thornton-Cleveleys, UK) and polyacrylonitrile (PAN)-based CFR-PEEK (Sumiploy CK4600; Sumitomo Chemical Co., Ltd., Tokyo, Japan) specimens were machined from extruded bar stocks, which were fabricated without the use of stabilizers. PEEK and CFR-PEEK specimens were immersed in a 0.5-mol/L MPC (NOF Corp., Tokyo, Japan) aqueous solution. Photo-induced graft polymerization was carried out at 60°C for 90 min on the PEEK and CFR-PEEK surfaces under UV irradiation at the intensity of 5 mW/cm^2. The surface chemical properties of the PMPC-grafted PEEK and CFR-PEEK were examined using Fourier transform infrared spectroscopy (FT-IR) and X-ray photoelectron spectroscopy (XPS). The fabricated PMPC layers on the PEEK and CFR-PEEK surfaces were observed using an atomic force microscope (AFM) and a transmission electron microscope (TEM). The static water-contact angle of PMPC-grafted PEEK and CFR-PEEK was measured by a sessile drop method using an optical bench-type goniometer. The wear test of the PMPC-grafted PEEK liner against the Co–Cr alloy femoral ball component (size: 26 mm) was performed using a 12-station hip joint simulator (MTS Systems Corp., Eden Prairie, MN) according to ISO14242-3. The mechanical properties of untreated and PMPC-grafted PEEK were evaluated using tensile, flexural, small punch, and creep deformation tests according to ISO527, ISO178, ASTM F2183, and ASTM D621, respectively.

Results: After grafting, the peaks ascribed to the MPC unit were clearly observed in both FT-IR and XPS spectra. Smooth 100-nm-thick PMPC layers were clearly observed on the surface of the PEEK substrate (Fig. 1).
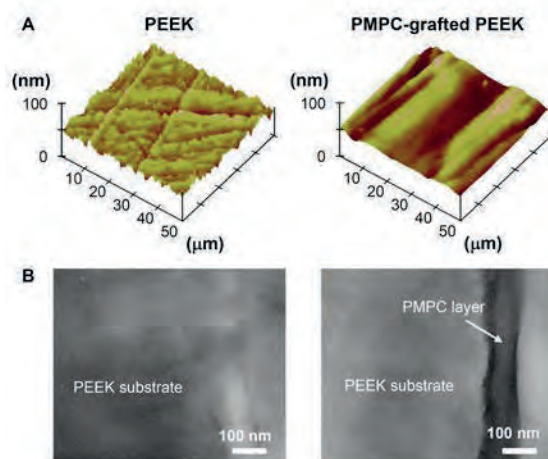

Figure 1. (A) Surface AFM and (B) cross-sectional TEM images of untreated and PMPC-grafted PEEK.

The contact angle of both untreated PEEK and CFR-PEEK was 90°, and it decreased markedly to 7° after PMPC grafting (Fig. 2A). The coefficient of dynamic friction of PMPC-grafted PEEK was considerably decreased to 0.010; these values imply a reduction of more than 90% as compared to those for untreated PEEK (Fig. 2B). It was observed that the gravimetric wear in the PMPC-grafted PEEK cups was significantly lower than that in the untreated PEEK cups (Fig. 3). Flexural properties and creep deformation did not differ significantly between untreated PEEK and PMPC-grafted PEEK and CFR-PEEK. In contrast, there was a small but significant difference in the flexural strength and strain, and the failure of untreated PEEK and PMPC-grafted PEEK was examined in this study. However, all PEEK materials met the ASTM F2026 requirements.

Discussion: We successfully demonstrated the fabrication of a highly hydrophilic and biocompatible nanometer-scale modified surface by PMPC grafting onto the surface of self-initiated PEEK and CFR-PEEK. The self-initiated surface graft polymerization was brought about by the generation of semi-benzopinacol-containing radicals of the benzophenone units in PEEK, which acted as a photoinitiator during the grafting polymerization. This polymerization system was realized in the absence of a photoactive low molecular compound and in an aqueous

Table 1 Mechanical properties of untreated and PMPC-grafted PEEK and CFR-PEEK

Test methods	Standards	Properties	PEEK		t-Test	CFR-PEEK		t-Test
			Untreated	PMPC-grafted		Untreated	PMPC-grafted	
Tensile test	ISO527	Yield strength (MPa)	109.4 (0.4)*	109.9 (0.6)	N.S.	N.A.	N.A.	–
		Ultimate strength (MPa)	71.5 (1.5)	71.7 (1.7)	N.S.	91.7 (4.6)	90.7 (5.0)	N.S.
		Elongation (%)	24.0 (9.5)	24.4 (9.0)	N.S.	2.9 (0.6)	2.3 (0.3)	N.S.
Flexural test	ISO178	Ultimate strength (MPa)	168.9 (0.6)	173.7 (1.8)	< 0.05	147.3 (6.9)	149.1 (5.3)	N.S.
		Ultimate strain (%)	6.4 (0.1)	6.7 (0.2)	< 0.05	2.8 (0.2)	2.8 (0.1)	N.S.
		Modulus (GPa)	3.9 (0.0)	3.9 (0.0)	N.S.	5.8 (0.1)	5.8 (0.0)	N.S.
Small punch test	(ASTM F2183)	Work to failure (MPa)	573.9 (16.1)	660.9 (13.7)	< 0.05	95.7 (8.9)	101.2 (7.1)	N.S.
Creep test	ASTM D621	Creep defromation (%)	0.0 (0.0)	0.0 (0.0)	N.S.	0.0 (0.0)	0.0 (0.0)	N.S.

*: The standard deviations are shown in parentheses.

medium; this is human-friendly and exhibits excellent biocompatibility. The wettability of PMPC-grafted PEEK was considerably greater than that of untreated PEEK because of the presence of a PMPC layer; MPC is a highly hydrophilic compound. The coefficient of dynamic friction was dependent on the wettability. A significant reduction in the static water-contact angle of PMPC-grafted PEEK resulted in a substantial improvement in the friction property.
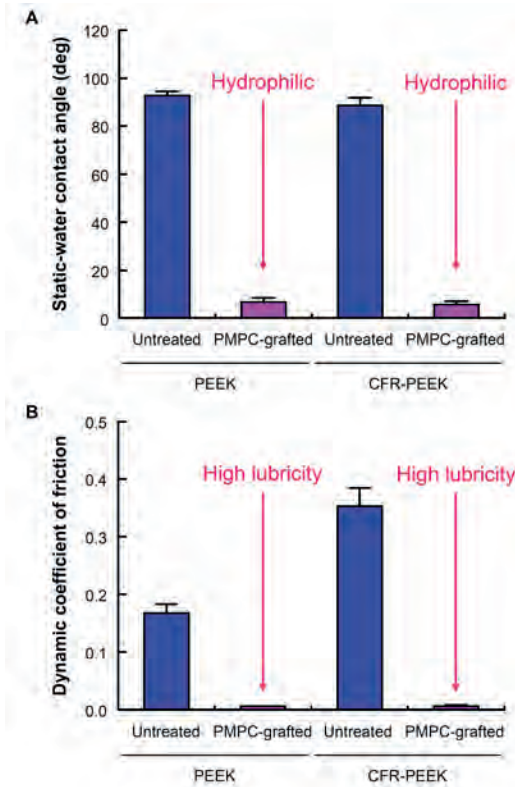

Figure 2. (A) Static contact angle and (B) dynamic coefficient of friction of untreated and PMPC-grafted PEEK and CFR-PEEK.

Further, the wear of the PMPC-grafted PEEK was considerably lower than that of the untreated PEEK. Fluid-film lubrication (or hydration lubrication) of the PMPC-grafted surface was achieved by the intermediate hydrated layer. When the PEEK surface was modified by PMPC grafting, the grafted PMPC caused a significant reduction in the sliding friction between the graft surfaces because the thin water films that were formed acted as extremely efficient lubricants. The water-lubrication systems using PMPC suppressed the direct contact of the counter-bearing face with the PEEK substrate to reduce the frictional force. Thus, the PMPC-graft layer was expected to significantly increase the durability of the bearing biomaterials.
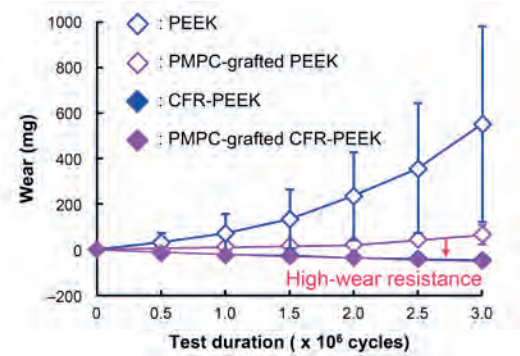
Figure 3. Time course of gravimetric wear of PMPC-grafted PEEK and CFR-PEEK cups during the hip simulator test.

As shown in Table 1, the mechanical properties of PEEK and CFR-PEEK remained unchanged even after PMPC grafting. This indicated that the self-initiated photoinduced graft polymerization proceeded only on the surface of the PEEK substrate, whereas the properties of the substrate remained unchanged. The retention of the properties of the substrate was very important for clinical use because the biomaterials used in the implants acted not only as surface-functional materials but also as structural materials *in vivo*. The smart modification of PEEK using the self-initiated surface graft polymerization of PMPC, exhibiting unique properties such as lubricity and high wear resistance, will bring a novel bearing material in the field of orthopedic surgery.

Frictional Heating of PEEK-UHMWPE Bearing Couple on Pin-on-disk Tester

Baykal, D[1]; Rau, AC[2]; Underwood, RJ[2]; Siskey, RS[1,2]; Kurtz, SM[1,2]

[1]School of Biomedical Engineering, Health and Science Systems, Drexel University, USA [2]Exponent Inc., USA

skurtz@exponent.com

Introduction: Poly(aryl-ether-ether-ketone) (PEEK), which has been successfully employed in spinal implants and femoral stems, is also considered for use as a bearing material in other types of orthopedic bearings (e.g., THA or TKA).[1] Although earlier studies focused on carbon fiber-reinforced PEEK articulating against ceramic and CoCr counterfaces, all-polymer bearings involving PEEK are also being considered.[2,3] Since PEEK has a low coefficient of conductivity, heat generated during articulation may not easily dissipate leading to elevated temperature at the bearing surfaces possibly resulting in protein precipitation in the lubricant.[4] These precipitates may produce transfer film on articulating surfaces and result in misleading wear test results in vitro.[4]

Heat generated during elliptical Pin-on-disk articulation of UHMWPE-PEEK and UHMWPE-CoCr bearing couples, lubricated by either bovine serum or water on a Pin-on-disk, was characterized using an approach previously investigated for TKA by Lu and McKellop.[4] We hypothesized that, at steady state, heat generated by articulation would not differ between UHMWPE-PEEK and UHMWPE-CoCr bearing couples. We also hypothesized that the coefficient of friction at steady state would be similar for both bearing couples when lubricated by either bovine serum or water.
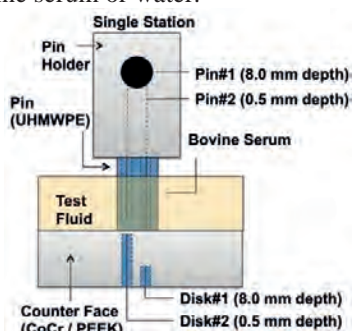

Figure 1-Thermocouples were inserted into specimens at known depths from surfaces

Methods and Materials: The pin was fabricated from compression molded GUR 1020 stock material that was gamma irradiated (100 kGy) and annealed for 24 hours at 120 °C. The cylindrical pin had a height of 25.4 mm and diameter of 9 mm. The counter face disks of 44 mm diameter were wrought CoCr alloy (n=1) with an average roughness (R_a) of <14 nm and PEEK-OPTIMA (Invibio Limited, UK) (n=1) with an average roughness (R_a) of <17 nm. For the pin and each of the disks, two thermocouples (type K, PFA insulated, Omega Eng., CT, USA) with a radius of 0.003 inches were placed 0.5 mm and 8 mm away from the articulating surface through holes drilled from the back of the specimens. Another thermocouple was submerged in the lubricant (Fig. 1).

Multidirectional wear testing of UHMWPE-CoCr and UHMWPE- PEEK bearing couples was conducted on an OrthoPOD Pin-on-Disk machine (AMTI, Watertown, MA). The lubricant used was Wear Testing Fluid (HyClone, Logan, UT) with a protein concentration of 20 g/L. Each pin had its own chamber filled with approximately 25 mL of lubricant. The water bath surrounding the chambers was maintained at 37±1 ^{0}C. An elliptical wear pattern (major axis 10 mm and minor axis 5 mm) was employed to facilitate multidirectional wear at 1 Hz. Static loading was applied to give a 2 MPa of contact pressure on the articulating surfaces of the pins. Each test lasted 25200 cycles (7 hours). Data from thermocouples was acquired at 0.03 Hz. Steady state temperature was sampled from 157 measurements during the last 5200 cycles of testing. At the end of each test, coefficient of friction was measured using a linear track.

Results: The steady state temperatures for both bearing couples with bovine serum as lubricant are shown in table 1. Steady state temperatures with water as lubricant were similar and not shown here. The coefficient of friction at steady state for UHMWPE-PEEK couple in serum and water were 0.17 ± 0.02 and 0.14 ± 0.02, respectively whereas, for UHMWPE-CoCr couple, they were 0.08 ± 0.02 and 0.07 ± 0.02 in serum and water respectively. All groups were different in terms of friction (p<0.01; Kruskal-Wallis test).

Table 1 - Steady State Temperature - Average ± St. Dev. (ºC)

Location	UHMWPE on CoCr	UHMWPE on PEEK
Disk #2 (0.5 mm depth)	39.2 ± 0.1	48.2 ± 0.2
Disk #1 (8 mm depth)	38.5 ± 0.1	40.1 ± 0.2
Pin #2 (0.5 mm depth)	38.9 ± 0.1	49.0 ± 0.1
Pin #1 (8 mm depth)	38.3 ± 0.1	42.1 ± 0.1
Lubricant	38.5 ± 0.1	41.9 ± 0.1

Discussion: The steady state temperatures suggest that UHMWPE-PEEK couple generated more frictional heat during articulation. Coefficient of friction was also higher for the UHMWPE-PEEK couple. Higher frictional heating and low heat conductivity of UHMWPE-PEEK couple resulted in higher temperatures compared to UHMWPE-CoCr. A limitation of this study was that temperatures at the surfaces were not directly measured and heat partition between sliding surfaces, lubricant, water bath and surrounding is unknown. In the future, it may be useful to repeat the study with the testing chamber insulated to contain the heat generated by articulation. Finite element analysis may also be used to predict surface temperatures and compare with 66$^°$C, which is the critical temperature for lubricant protein precipitation.[4]

References: [1] S.M. Kurtz, J.N. Devine. Biomaterials 28 (2007) 4845–4869 [2] A. Wang et al. Wear 225–229 (1999) 724–727 [3] G. Langohr et al. Proc. IMechE., Part J 225 (2011), 499-513 [4] Z. Lu, H. McKellop. Proc. IMechE., Part H 211 (1997) 101-108

The wear of CFR-PEEK and PEEK OPTIMA articulating against HXLPE

East R, Briscoe A*, Jarman-Smith M*, Simpson D**, Collins S**, Unsworth A.
School of Engineering and Computing Sciences, Durham University, * Invibio Ltd, ** Corin Ltd.
tony.unsworth@durham.ac.uk

Introduction

The articulating surfaces of most artificial joints use material combinations which involve at least one hard surface such as metals, particularly CoCrMo or ceramics (alumina or ZTA). These may articulate against a polymer or similar hard materials but from time to time the idea of using an all polymer combination is suggested [1]. This would avoid problems of stress shielding due to the polymer's modulus being closer to that of bone but also would reduce the weight and the body's reaction to the wear particles produced.

This paper investigates the use of PEEK, both reinforced and unreinforced, sliding against highly-cross-linked polyethylene (HXLPE)

Materials and Methods

A pin-on-plate machine with reciprocation and rotation was used. Pins were made from PEEK with and without carbon-fibre reinforcement, which rotated about their long axes while the reciprocating plates were all made of HXLPE. The load applied was 40N onto a pin of 5 mm diameter giving a nominal stress of 2MPa. Pins and plates were controlled for fluid uptake. The lubricant was new-born calf-serum diluted in deionised water to give a protein content of 18 g/l. It also contained 0.2% sodium-azide to retard bacterial growth and 20mM EDTA to prevent calcium deposition.

Three sets of pins were used; CFR-PEEK orientated with the fibres (8µm diameter, 25µm long) running predominantly axially along the pin, CFR-PEEK with fibres running predominantly at right angles to the axis of rotation and PEEK OPTIMA which had no fibres.

Results and Discussion

Table 1 shows the wear factors for the three tests and Figure 1 illustrates these. The axially-orientated carbon-fibre filled pins wore the greatest (wear-factor 0.138×10^{-6} mm^3/Nm) and the HXLPE plates also had a very high wear-factor in this combination (97.5×10^{-6} mm^3/Nm): So much so that the experiments had to be terminated due to the penetration of the pins into the plates.

The tangentially orientated carbon-fibre-filled pins showed improved performance both for the pins (0.052×10^{-6} mm^3/Nm) and the plates (49.3×10^{-6} mm^3/Nm). Thus not only did the pins themselves wear less, they were less abrasive to the plates. The lowest wear was that associated with PEEK-OPTIMA articulating against HXLPE plates. Here the wear-factors were 0.038×10^{-6} mm^3/Nm for the pins and -0.025×10^{-6} mm^3/Nm for the plates. The minus indicates a gain in weight which, when examined under FTIR, was seen to be due to a transfer film of PEEK on the surface of the HXLPE. To put this into context this wear is much lower than HXLPE against CoCrMo alloy.

Conclusion

An all plastic joint seems feasible using PEEK OPTIMA and HXLPE but further tests at higher stresses would reassure that possible adverse conditions could be accommodated.

Reference

1. Sibly TF and Unsworth A, Wear of cross-linked polyethylene against itself: J.Biomedical Engineering, 1991,**13**.217-220

Acknowledgements

Experiment	Pin wear factor $(\mathrm{mm}^3/\mathrm{Nm})$	Plate wear factor $(\mathrm{mm}^3/\mathrm{Nm})$
1	$1.38 \pm 0.893 \times 10^{-7}$	$9.75 \pm 4.47 \times 10^{-5}$
2	$3.84 \pm 1.94 \times 10^{-8}$	$-2.50 \pm 5.12 \times 10^{-8}$
3	$5.20 \pm 6.25 \times 10^{-8}$	$4.93 \pm 4.36 \times 10^{-5}$

Table 1: Wear-factors 1; CFR-PEEK axial fibres, 2, PEEK OPTIMA, 3, CFR-PEEK tangential fibres.
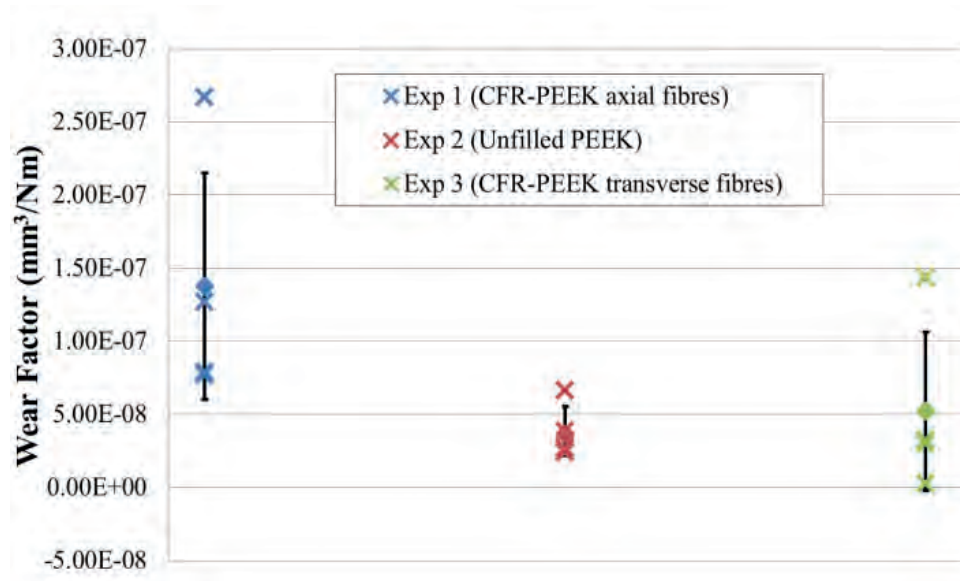

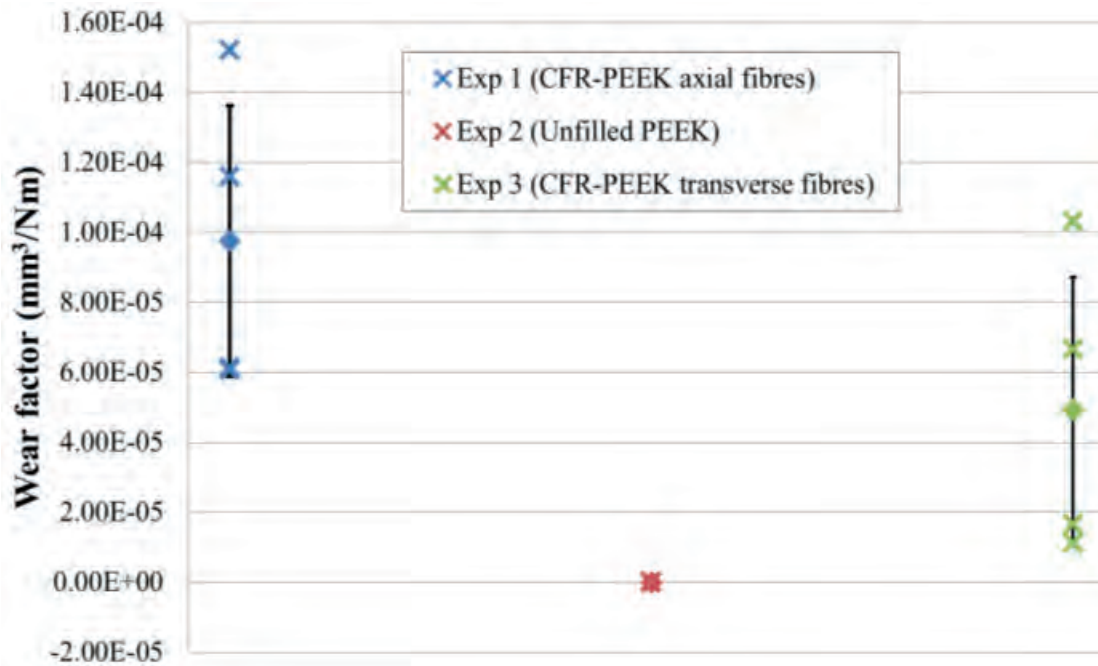Figure 1(a) Wear-factors for pins against HXLPE Plates

Figure 1(b) Wear-factors for plates against different pins

Investigation of Carbon Fiber reinforced PEEK Self Tapping Suture Anchors

Feerick, E.M.[1], Wilson, J.[2], O'Bradaigh, C.M.,[1] McGarry, P.[1]

[1]Dept of Mechanical & Biomedical Engineering, National University of Ireland Galway, Ireland

[2]Invibio Biomaterial Solutions Ltd., Thornton-Cleveleys, UK

jwilson@invibio.com

Introduction: The number of rotator cuff repairs is growing annually due to an aging population[1]. In the USA per patient costs typically associated with a rotator cuff repair are $17,427[2]. Therefore the development of next generation suture anchors that can perform as required while also offering efficient and economical surgery times is paramount in meeting the expected future demand for rotator cuff repair. PEEK-OPTIMA CFR is a radiolucent, non-degradable biomaterial with a Young's modulus close to that of bone and offering excellent wear and fatigue properties. The objective of this study is to investigate the self tapping ability of PEEK-OPTIMA CFR suture anchors for rotator cuff repair.

Methods and Materials: Experimental suture anchor insertion tests were conducted to investigate the torque and axial forces required to insert a self tapping PEEK-OPTIMA CFR suture anchor. Specifically the performance of the suture anchor material and thread design was considered. A standard laminated composite test block (Sawbones, Malmo, Sweden) was used to represent the cortical and cancellous layers that must be penetrated by a self tapping suture anchor as it is inserted. The block consisted of a 2 mm top layer of 40 pcf polyurethane to represent the cortical shell and the bottom layer consisted of 15 pcf polyurethane foam to represent cancellous bone. Five insertion tests (n=5) were conducted using a Zwicki-Line biaxial test machine. The experimental set up is shown in Figure 1(A-B). In addition to experimental testing, finite element simulations were conducted to determine the stress distribution in the suture anchor and in the surrounding foam when subjected to a torque force. The 3D model generated is shown in Figure 1(C). All simulations were conducted using the finite element solver Abaqus 6.11. Simulations were also conducted to compare the difference in stress state between a PEEK-OPTIMA CFR anchor and a titanium equivalent.
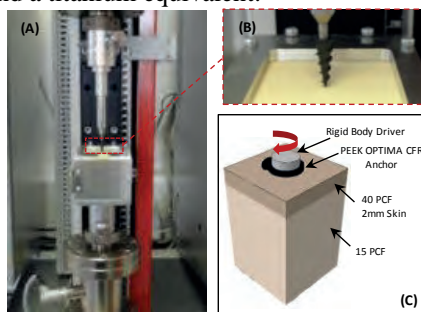

Figure 1: (A-B) Experimental test set up; **(C)** Computational 3D Model for 5 deg rotation of anchor

Results: The average axial and torsion forces required to insert a PEEK-OPTIMA CFR suture anchor are shown in Figure 2(A). The initial critical force is the axial force applied to drive the tip of the anchor into the material.

Once the threads of the anchor come into contact with the foam the torque rises and a drop in axial force is also observed as highlighted on the graph of Figure 2(A). This is the point at which self tapping commences. If at any point the anchor becomes wedged an increase in axial force is observed until the threads of the anchor again begin to self tap. This study is the first to report the self tapping performance of a PEEK-OPTIMA CFR suture anchor. The results of the finite element simulations are summarized in Figure 2(B). As the peak experimental forces occurred at full insertion all simulations were conducted with the anchor heads 0.5 mm above the surface of the foam. A section view of the anchor embedded in the Sawbone foam at 5 degrees of rotation illustrates the peak stresses occurring in the driver head. The peak shear stress in a PEEK-OPTIMA CFR suture anchor (Figure 2(C)) is half that in a titanium suture anchor (Figure 2(B)).
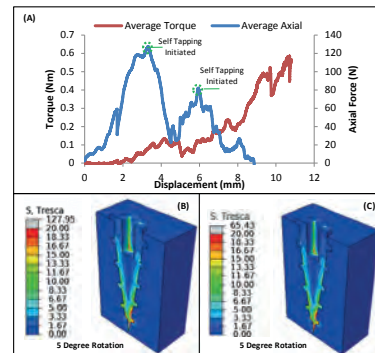

Figure 2: (A) Experimental test results of axial and torque forces versus insertion depth; **(B)** Shear stress distribution for titanium anchor **(C)** Shear stress distribution for PEEK-OPTIMA CFR anchor

Discussion: The results of the present study are the first reported for a self tapping PEEK-OPTIMA CFR suture anchor. The experimental curve of Figure 2(A) requires a maximum of 0.65 Nm for insertion which is below the typical limiting torque of 1.5 Nm for self taping cortical bone screws[4]. The thread design of the present study required two instances of self tapping initiation; therefore further study of design optimization of the screw threads is necessary to reduce this to one instance. The comparison of a PEEK-OPTIMA CFR and a titanium equivalent suture anchor highlights the lower shear stress required in the anchor head for a 5 degree anchor rotation. The development of an optimized thread design would offer faster surgery times while also taking advantage of the fatigue, radiolucent and bone like modulus of PEEK-OPTIMA CFR.

References: 1. Tempelhof S, Rupp S, Seil R. (1999) Journal of Shoulder and Elbow Surgery 8(4):296-299 **3.** American Academy of Orthopaedic Surgeons, Research Statistics on Rotator Cuff Repairs, National Inpatient Sample, 1998-2004. Data obtained from: The Agency for Healthcare Research and Quality **4.** Feerick, E. M. and McGarry, J. P., 2012. J. Biomech 45, 1666-1672.

Particulate and Gravimetric Wear Rate Analysis and Flexural Fatigue Testing of a PEEK Medial Knee Interpositional Arthroplasty Implant

Stephen H. Crosbie[1], Jeffrey C. Felt, John P. Mehawej, David A. Markman, Mark A. Rydell
ABS Corporation, Minnetonka, MN, USA
[1]*scrosbie@advbiosurf.com*

Introduction:

ABS Corp. was granted FDA 510(k) clearance and CE Mark approval in February of 2006 for the Cobalt Chrome (CoCr) OrthoGlide medial interpositional arthroplasty implant. This implant is positioned between the femoral condyle and the tibial plateau of the medial knee compartment and provides a low friction glide path for the femoral condyle. The implant attains stabilization through geometrical conformance to the tibial plateau, needing no screws or bone cement. While very stable, patient feedback indicates some received inadequate initial pain relief during the first year of implantation. At one year patients were experiencing significant improvement in pain similar to those who have received a Unicompartmental or Total Knee Arthroplasty.

To address the delayed pain relief of some patients ABS looked at replacing CoCr with a different material. PEEK was chosen as an alternative low friction bearing material because it is more compliant to the femoral condyle, which would reduce early pain levels. PEEK has been used widely as a biomaterial in spinal implants with excellent biocompatibility, mechanical properties, and wear resistance. PEEK has a compressive modulus similar to subchondral bone, in contrast to CoCr which has a flexural modulus 2 orders of magnitude greater than that of subchondral bone. The PEEK Mobility implant is made from medical grade Invibio PEEK Optima LT1, and has identical geometry to the CoCr OrthoGlide. The PEEK Mobility received CE Mark approval on Sept. 17, 2010.

This Study is a summary of the PEEK Mobility wear particulate, gravimetric wear rate, and flexural fatigue testing used in preparation for the CE Mark Technical File submission for the PEEK Mobility implant.

Methods and Materials:

Gravimetric Wear Rate

All wear testing was performed using PEEK Optima LT1 implants tested on ABS Knee Motion Machines (KMM). The KMM utilizes four degrees of freedom during articulation: femoral flexion/extension (applied), tibial translation (applied), axial load through femur (applied), and external rotation. The KMM was programmed to simulate a kinematic walking cycle with 7 mm anterior tibial translation with 5° of external rotation during flexion/extension at 1 Hz with a cyclic input load of 40-400 lbf. The loads represent 4 times average body weight of 167 lbf., with 60% of body weight on the medial tibial plateau. All testing was done in a 50% bovine serum solution (BSS).

A 10 million cycle (MC) wear test was conducted to determine long-term gravimetric wear rates for the PEEK Mobility implant using Delrin femurs that were roughened every 100,000 cycles (daily). Nine implants were tested. Another gravimetric wear test was performed using the KMM at 40-300 lbf. cyclic loading by sequentially using 15 human cadaver femurs which articulated against a single PEEK Mobility implant for 300,000 cycles. All femoral condyles were denuded with a femoral rasp to remove enough cartilage to expose an area of subchondral bone with a minimum diameter of 10 mm (in any direction). The partially denuded donor femurs were tested at different intervals since each femur was run until it eventually collapsed from a subsidence fracture.

To objectively demonstrate the aggressive nature of the KMM test, ABS performed a study to examine the wear rates of GVF ultra high molecular weight polyethylene (UHMWPE) machined to PEEK Mobility dimensional specifications. Six implants were tested on the KMM to 1 million cycles using the same kinematic loading cycles and roughed Delrin femurs used to test the PEEK Mobility implants.

Particulate Analysis

After conducting wear-generating gait simulations on the KMM using both roughened Delrin femurs and denuded human cadaveric femurs, a collected representative sample of the 50% BSS solution was analyzed using SEM. The cadaveric femur composite sample group was made from BSS solution samples from all 15 tests, while the Delrin femur test consisted of 3 representative samples from the 0-1 MC, 4.5-5.5 MC, and 9-10 MC groups.

Cyclic Flexural Fatigue Testing

All cyclic flexural fatigue testing was performed on an Endura-Tec load/displacement machine. All tests utilized a Delrin tibial plateau test fixture where the PEEK Mobility implant is supported at the anterior, posterior and lateral edges but not in the center or medial edge. The central unsupported anterior-posterior (AP) span of the fixture is 42.9 mm. The center of the implant is compressed with vertical cyclic load using an anatomically modeled Delrin femur. Testing was performed on the 58-3 configuration implants, which is the longest AP length (58mm) and the thinnest (3mm) implant produced.

Cyclic Flexural Fatigue testing was performed under cyclic vertical compression load varying sinusoidally from 40 to 400 lbf. to 10 MC at 4 Hz.

Axial flex fatigue limit testing was performed under compression loads of 575 lbs, 750 lbs, 1000lbs, and 1250

lbs to determine the material's axial compressive endurance limit to at least 10 MC without failure.

Compressive Failure testing was performed to determine the yield point and Load/Deflection characteristics of the implant under a ramp profile from no load to 2000 lbf. at a rate of 25 lbf. /sec.

Results:

Gravimetric Wear Rate
The average wear for 9 PEEK Mobility implants tested to 10 MC using the roughened Delrin femur was 5.8 ± 3.1 mg/MC. This data includes several severe single day wear rates caused by unplanned fluid loss. Removal of these deviations yields an effective wear rate of 2.3 ± 0.9 mg/MC for the implants tested to 10 million cycles.

The control-corrected wear rate of the PEEK Mobility implant using the 15 cadaveric femurs was 5.45 mg/ 307,000 cycles which extrapolated using a linear regression (worst case for predicting long term wear) to 17.86 mg/1 MC. The sharp edges created from the fracturing of the femoral condyle (all femurs were tested to subsidence fracture or collapse) plus third body wear caused by large amounts of pulverized bone chips contributed to wear rates much higher than what would be expected for this implant in a live, intact knee capsule.

The average wear rate for UHMWPE OrthoGlide implants tested on the KMM was 384.5 mg/MC. This test could only be run to 1 million cycles since many of the implants were almost worn through by 1 MC.

Particulate Analysis
The resulting analysis was able to detect particles as small as 0.05 µm. The average observed equivalent circle diameter (ECD) of the analyzed particles ranged from 0.21 to 0.74 µm. The cadaver femur testing produced an average ECD of 0.21 µm, while the Delrin femur testing produced an average ECD of 0.74 µm, 0.36 µm, and 0.38 µm for the 0-2.5, 4.5-5.5, and 8-9 MC samples respectively. Mean particle aspect ratios ranged from 1.68 to 2.05.

A published study of UHMWPE wear particles found in synovial fluid collected 1 year after total knee arthroplasty procedures reported a similar particulate geometry. The average ECD particle size ranged from 0.67 to 0.78 µm and the aspect ratio ranged from 1.90 to 2.30 for medial pivot and posterior-stabilized prostheses respectively.

Cyclic Flexural Fatigue Testing
Six implants were cyclically flexural fatigue tested from 40-400 lbf. at 4 Hz for 10 MC. All implants met the acceptance criteria: no cracking, and no deformation causing visible roughness to the glide path on the superior surface of the implant. All implants retained functionality.

One implant was cyclically tested from 75-750 lbf. at 4 Hz for 10 MC. The test was performed to determine the

implant's ability to withstand loads well above those experienced inside the human body. The implant survived the test retaining full functionality, without cracking and without deformation causing visible roughness to the glide path on the superior surface of the implant.

Five PEEK implants were crush tested from 0-2000 lbf. at a rate of 25 lbf. /second. All tested implants were plastically deformed without cracking. Similarly, CoCr OrthoGlide implants were crush tested under the same regime and showed permanent deformation without cracking or breaking.

Discussion:
The KMM wear testing protocol produced a wear rate that was approximately two orders of magnitude higher for UHMWPE than for PEEK Optima implants. This robust testing regime produced a 10 MC effective wear rate for PEEK implants of 2.3 mg/MC. This compares to the UHMWPE implant wear rate of 384.5 mg/MC.

Studies from 11 peer-reviewed journal articles of gravimetric wear rate statistics for ultra-high-molecular-weight polyethylene (UHMWPE) total knee replacement implants tested in knee motion simulators, where an UHMWPE bearing is articulated on a polished metal surface, were collected for comparison. The average wear rate of 8 *in-vitro* studies that tested cross-linked UHMWPE in a bovine serum test solution was 7.2 mg/MC. This wear rate is greater than the average *in-vitro* wear rate observed for the PEEK Mobility implant using roughed Delrin femurs.

The average observed equivalent circle diameter (ECD) of the analyzed PEEK particles ranged from 0.21 to 0.74 µm. This corresponds to wear particles generated *in-vitro* in a survey of journal articles of FDA-approved total knee replacement implant testing (0.5 to 1.2 µm). The most biologically active size range for wear particles is 0.1-1.0 µm. Since the size of generated wear particles cannot be controlled, the most effective way to prevent adverse reactions to these biologically reactive particles is to minimize the volume of wear debris produced.

PEEK Optima was chosen as an alternative material for the CoCr OrthoGlide so that the implant could flex or conform to the tibial plateau and femoral condyle without breaking, and maintain a reduced frictional glide surface in early onset Osteoarthritic patients. PEEK Optima has shown excellent resilience to heavy loads under cyclic flexural loading without cracking or any distortions to the superior surface glide path while demonstrating very low wear rates in *in-vitro* testing using cadaveric and Delrin femurs.

Characterisation of the Fixation of a Novel Polyetheretherketone Implant for Total Knee Replacement

K. Rankin[1], M. T. Bah[1], A. S. Dickinson[1], I. Sinclair[2], A. Briscoe[3], M. Browne[1]

[1] Bioengineering Science Research Group [2] Materials Research Group, University of Southampton, SO17 1BJ, UK
[3] Invibio Ltd, Technology Centre, Hillhouse International, Thornton Cleveleys, Lancashire, FY5 4QD, UK

K.Rankin@soton.ac.uk

Introduction: Total knee replacement (TKR) is becoming an increasingly prevalent procedure for the treatment of degenerated articular joint surfaces. However, prosthesis wear and interfacial fixation failure leading to osteolysis, loosening of components and revision surgery, remains a predominant cause of component failure [1]. A traditional high modulus metallic implant (~220GPa) can cause stress shielding of the surrounding tissues *in-vivo*, which may lead to loss of bone mass, leaving it weak and porotic, necessitating revision surgery [2]. A lower modulus implant has the potential to reduce these effects.

Poly-ether-ether-ketone (PEEK) is a thermoplastic with proven bioinertness, good wear resistance, excellent mechanical properties and an elastic modulus of 4GPa, similar to that of bone (1-20GPa) [3]. PEEK is currently under consideration as a candidate for the femoral component of TKRs. The fixation of such an implant system would be a critical factor in determining the success of the prosthesis *in-vivo* since the lower modulus PEEK material may induce higher interfacial shear stresses and micromotions. Bone cement (polymethylmethacrylate) promotes good initial implant stability and is more forgiving of surgical technique when positioning the implant compared to cementless implant systems. Cementation has been chosen as the most realistic option for the fixation of a PEEK femoral component [4].

The bone at the distal end of the femur and the proximal end of the tibia is predominantly loaded in compression and shear as the joint contact areas roll, slide and rotate over one another during gait [5]. The mechanical integrity of the construct governs the long term stability of the implant, but may be compromised by interfacial defects and cement mantle fatigue, leading to crack propagation and implant loosening [6]. The most vulnerable areas of the construct are the implant-cement and cement-bone interfaces. The roughness achievable on PEEK surfaces, and therefore the degree of mechanical interlock, is limited by the material itself. While highly roughened surfaces can be manufactured on metallic implants through grit blasting and moulding of features, these processes are not so applicable to polymer based materials. Therefore, in the present study, the PEEK-cement interfacial shear strength was investigated using both standard roughening procedures and Finite Element (FE) simulations to assess the feasibility of achieving appropriate primary fixation using contemporary roughening techniques.

Methods and Materials: To determine the shear strength of the PEEK-cement interface, a single lap joint shear test method was chosen as described in ASTM F1044-05. 60x25x6mm injection moulded test plates of PEEK-OPTIMA (unfilled PEEK) and MOTIS (30% milled carbon fibre PEEK) were tested with two surface finishes: (I) smooth injection moulded finish with a surface roughness R_a value of ~0.5μm and (II) rough grit blasted finish with a surface roughness R_a value of ~5μm. Palamed medium viscosity cement (Heraeus Medical GmbH) was applied by hand to the PEEK

samples in a mould which facilitated a 25x25mm^2 overlap. Two cementing mixing times were selected to determine whether increased wetting of the PEEK surface resulted in increased interfacial strength: (I) working phase cementing (waiting time 1 min 30s) and (II) premature cementing (after 30s mixing). Test samples were arranged in the jaws of an Instron 5569 electromechanical test machine with aluminium alignment plates. The load applied at failure was recorded and the interfacial shear strength was then calculated from equation 1.

$$Interfacial\ Shear\ Strength\ (MPa) = \frac{Applied\ Load\ (N)}{Interfacial\ Area\ (mm^2)} \qquad (1)$$

An FE model was developed to assess the shear stresses at the TKR femoral PEEK implant-cement interface for comparison with the experimental results to determine if the stresses generated *in-vivo* may exceed the PEEK-cement interfacial shear strength. To this end, Computer Tomography (CT) data of a male angiograph patient were segmented to generate a model of the left distal femur, which was then implanted with a left, cruciate retaining TKR femoral component with a 4GPa Young's modulus and a Poisson's ratio of 0.36 (Figure 1a).
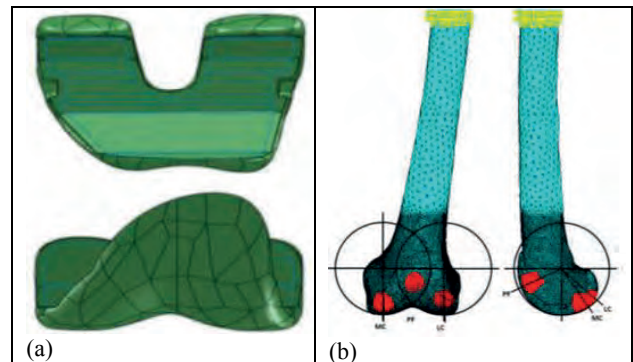

Figure 1: TKR Implant Geometry (left) and boundary conditions for Heel Strike (right) showing Medial Condyle (MC), Patellofemoral (PF), Lateral Condyle (LC) loading and diaphyseal constraint.

The femoral component was positioned according to typical operative techniques and attached to the bone using either a bonded or frictional contact (coefficient of friction = 0.3). The femur was cut approximately two thirds of its length above the knee, as the proximal part was outside the region of interest. The implanted femur was meshed using dense linear tetrahedral elements, with 1.5-2mm side length in the implant, distal bone and cut bone, and 5-6mm in the diaphyseal bone outside the region of interest (Figure 1b). Heterogeneous isotropic material properties were applied to the bone elements from the grayscale values of the CT-scan voxels using Bonemat, and a bone density (ρ) vs. Young's Modulus (E) relationship of: $E = 6950\rho^{1.49}$. The density was linearly correlated to the CT scan Hounsfield Unit (HU): 1.73g/cc for a dense cortical diaphyseal location (1.73g/cc) vs. 0g/cc for a non-mineralised location in the medullary cavity Shell elements of constant Young's modulus 10GPa and thickness 0.5mm were applied to the external surface of the bone to reproduce

thin cortical bone lost during CT scan segmentation or arising from partial volume effects. The thickness of the interdigitated cement layer was varied between 2mm and 4mm [8]. For each specific thickness, all FE elements of the distal femur part (cancellous bone alone) associated with nodes within 2mm of the implant surface were modelled as cement with a Young's modulus fixed at 2500 MPa [9]. Boundary conditions were applied to the model representing Heel Strike (HS). Forces were applied directly to nodes on the implant or subchondral bone bearing surface. Three joint contact forces were applied to the FE model, at the medial and lateral condyles (MC and LC), and at the patellofemoral contact (PF), see Table 1 [2]. Forces were applied across 10mm radius contact patches (Figure 1b). The diaphyseal cut surface was constrained against displacement in all directions.

Load Case	Force Location	Resultant Force, N	Flexion, deg	Adduction, deg
Heel Strike	MC	1651.8	34.4	0.97
	LC	990.5	47.9	0.94
	PF	1753.2	-64.3	-24.2

Table 1: FE model loading conditions

Results: The smooth injection moulded PEEK-cement samples separated when removed from the mould, hence no shear strength data was recorded. The rough grit blast finish PEEK-cement results are shown in Table 2 for both cementing techniques together with reported steel-cement shear strength values [7].

Sample Type	Cementing Technique	Average Shear Strength, MPa	Standard Deviation, MPa
OPTIMA	WP	1.53	0.35
OPTIMA	Premature	1.38	0.26
MOTIS	WP	2.14	0.40
MOTIS	Premature	2.50	0.50
STEEL [7]	Premature	9.90	0.96

Table 2: Average PEEK-cement interfacial shear strengths for working phase (WP) and premature cemented samples compared with steel-cement shear strength ($R_a \sim 3$ μm) [7]

The FE simulations revealed that during heel-strike, implant interface maximum shear stresses occurred anteriorly near the left flange in both the bonded (2.9MPa) and frictional contact (4.3MPa) cases. Figure 2 displays the shear stress distribution when the cement layer is 2mm thick. Frictional contact was found to increase shear stresses during heel-strike. As the cement thickness increased from 2mm to 4mm, the magnitude of the highest stresses remained approximately the same, as was the stress distribution around the implant surface. As for the cement layer itself, an increase in the cement thickness did not result in a major change in the magnitude of cement highest tensile/compressive stresses which remained comparable. In fact, during heel-strike for example, a slight decrease (2.7 to 2.5MPa) was predicted when the cement thickness was greater than 2mm.

Discussion: There was no significant difference between the shear strength of PEEK samples cemented in the working phase or prematurely in the waiting phase ($p = 0.05$), indicating no evidence of additional chemical bonding or mechanical interlock through increased wetting. However, there was a significant difference between the mean interfacial shear strengths of OPTIMA-cement and MOTIS-cement samples ($p = 0.05$), which may be related to an increased transfer of material observed on the sample surfaces post-testing. Nevertheless, the PEEK-cement shear strengths were significantly lower than those of steel-cement samples reported in the literature with similar surface roughness ($p = 0.05$) [7]. However, surface topography varies with the same R_a value (the arithmetic average of the surface texture) potentially affecting the mechanical interlock achieved [10]. Above all, the FE simulations suggest that shear stresses generated at the implant interface (~3 MPa) may exceed the reported PEEK-cement interfacial shear strength and lead to interfacial failure (Table 2).
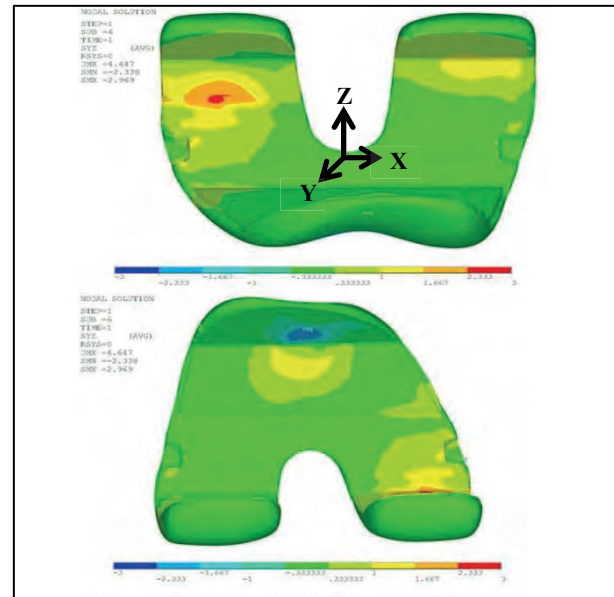

Figure 2: Posterior (top) and anterior (bottom) view of PEEK femoral component interface shear stresses. Cement thickness: 2mm. Bonded implant-cement case.

After consideration of the biomechanical environment at the knee joint, preliminary results suggest that the interfacial shear strength of the PEEK-cement construct with an interfacial roughness of 5μm may be exceeded by the interfacial shear stresses experienced at the knee joint. In addition, previous studies have reported greater metal-cement interfacial shear strengths compared to the PEEK-cement shear strength results in this study [7]. Future work will investigate the effect of surface features such as pegs and macro-textured patterns on the PEEK-cement interfacial shear strength to achieve that necessary of withstanding the forces experienced at the knee joint.

References
1. National Joint Registry for England and Wales 2010/11. *8th Annual Report*
2. G H Van Lenthe et al. 2011. *JBJS (Br)* 79B(1):117-122
3. S M Kurtz et al 2007. *Biomaterials* 28(32):4845-4869
4. J Beckmann et al. 2011. *Knee Surg Sports Trauma Arthro* 19(6):872-879
5. J Goodfellow et al. 1978. *JBJS (Br)* 60(3):358-369
6. G Lewis. 1997. *J Biomed Mate Re Part B: ApplBiomater* 28:155-182
7. J Zelle et al. 2011. *J Biomech* 44(4):780-783
8. M Vaninbroukx et al., 2009. The knee 16: 265-268.
9. D Janssen et al., 2009. *J Biomech* 41: 3158-3163.
10. B Bharat. 2000. Modern Tribology Handbook. 52-55.

PEEK Patient Specific Implants

Disegi, JA[1] and Maynard, M[1]
[1]Synthes, West Chester, PA, USA
disegi.john@synthes.com

Introduction: Synthes Craniomaxillofacial Product Development has established efficient design, production, and inspection practices for the production of PEEK patient specific implants (PSI). The implants are intended for the replacement of bony voids in the cranial and craniofacial skeleton. Solid polyetheretherketone (PEEK) polymer has been selected as the material of choice and an overview of the technology required to fabricate PEEK PSI will be presented.

Methods and Materials: Solid **e**xtruded PEEK Optima LT1® rectangular plates of various dimensions are supplied by Invibio, Thornton Cleveleys, Lancashire, UK that meet ASTM F 2026 industry standard and internal specifications. Each plate is visually inspected, assigned a unique material lot number, and quarantined. Representative samples are analyzed by FTIR for positive material identification and Rockwell R hardness measurements are performed by an independent recertification laboratory.

The surgeon sends a patient to radiology to be scanned according to a Synthes CT scanning protocol. CT scans must be less than four months old, film is not acceptable, and patient information is kept confidential. DICOM uncompressed 1 mm slice computed tomography (CT) data is received from the hospital radiology department. Validated software provides direct access to CT images and the CT data is converted to STL files. The 3D PSI model is designed, an article number assigned, and a 3D skull model is engineered. The implant and skull prototype models are shipped to the surgeon or computerized images are electronically sent to the surgeon for review. The surgeon approves the design and a purchase order is entered. The final CAD model is converted via Master Cam software for PSI manufacturing.

Cold air machining on a five axis CNC machining center is utilized in order to avoid implant contamination by machining coolant. The implant is deburred, bead blasted, laser marked, and inspected according to internal guidelines. Final inspections include PSI thickness measurement and functional check to confirm fit and symmetry when compared to the surgeon approved implant model. The implant is ultrasonically cleaned, radio frequency (RF) plasma treated, and packaged in a clean environment.

The skull model is fabricated on 3D rapid prototype equipment using a UV cured acrylic-polymer blend. The skull model is inspected for dimensional accuracy and the implant is inserted into the skull cavity to ensure proper fit. One nonsterile PSI is shipped overnight to the surgeon after manufacturing and inspection operations have been completed.

Results: An example of an anatomically correct skull model with defect created from CT data is shown in Figure 1.
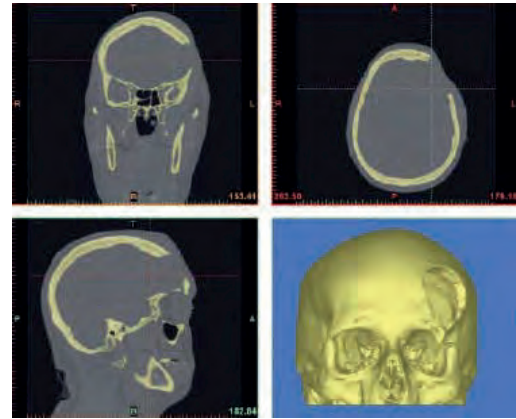

Figure 1. Anatomical Model Derived from CT Data

A single or multi-piece implant may be designed depending on the length, width and height of the implant. Multi-piece implants allow the surgeon greater flexibility when treating larger defects. An example of a multi-piece PSI is shown in Figure 2.

Figure 2. Three-Piece Craniofacial PSI

Discussion: PEEK PSI implants require minimal (if any) modification. For minor fit modifications, it is suggested that the surgeon modify the bone rather than the implant. If needed, PEEK implants can be modified with a high speed burr and rinsed in sterile saline solution away from the implant/surgical site to ensure that particulate debris does not infiltrate the surgical site after any modifications. Standard plates and self-tapping or self-drilling screws can be used to attach the PEEK implant to the patient. Screw holes, regardless of screw site and type, must be predrilled away from the surgical site. Excellent reconstructive results are achievable with PSI, including better anatomic fit, reduced operating time, and satisfying aesthetic results for the surgeon and patient because PSI are derived from the patient's own CT data.

DJ9999A

A Novel, Flexible PEEK Implant for Treatment of Vertebral Compression Fractures: From Concept to Clinic

Jeff Emery, PhD, Ryan Connolly, Tim McGrath, James Lee, and Laurent Schaller
Benvenue Medical, Santa Clara, California, USA
jemery@benvenuemedical.com

Introduction:

Vertebral compression fractures (VCFs) affect more than 700,000 people in the US alone. Such fractures may arise from daily activities in conjunction with osteoporosis, cancer, or from high-impact traumatic injury, and often involve regional loss of height of the anterior vertebral body. Acute, painful VCFs can be treated by vertebroplasty, where local injection of polymethylmethacrylate (PMMA) bone cement stabilizes the fractured cancellous bone and reduces micromotion. Balloon kyphoplasty (BKP), where the fractured cancellous bone is manipulated by balloon inflation to create cavities for facilitating cement flow, was later developed as a treatment alternative that could enhance the potential to restore some vertebral height loss and reduce the relatively high rate of cement leakage associated with vertebroplasty.

Interest for treatment of VCFs with alternative materials to bone cement is growing due to the limitations of injectable PMMA, which include excessive exothermic heat during polymerization, lack of biological healing properties, and potential for adverse clinical events due to extravasation from the vertebral body. Many injectable materials that may facilitate bone healing or remodeling, such as calcium phosphates or sulphates, may not exhibit the requisite structural properties to withstand biomechanical loading.

Treatment of VCFs using a structural implant consisting of PEEK represents a potentially viable alternative which addresses limitations of vertebroplasty and balloon kyphoplasty. We have developed a minimally invasive, radiopaque, flexible PEEK implant known as Kiva, which is designed to stabilize the fractured vertebra, reduce volume of bone cement, improve its containment, provides a mechanism for height restoration, and offers the structural support necessary for bioactive injectables. This effort describes the engineering and clinical validation to bring the design from concept to market.

Methods and Materials:

The Kiva implant is delivered by a deployment handle into the vertebral body over a nitinol guidewire via percutaneous access and attains a stacked circular configuration (Figure 1). Micromachined features communicate between the implant lumen and the inner coil diameter to allow the tubular structure to flex into the coiled shape and direct the flow of injectable materials such as bone cement toward the interior of the construct. The circumferential wedge action during deployment provides intraoperative capability to restore and maintain vertebral height.
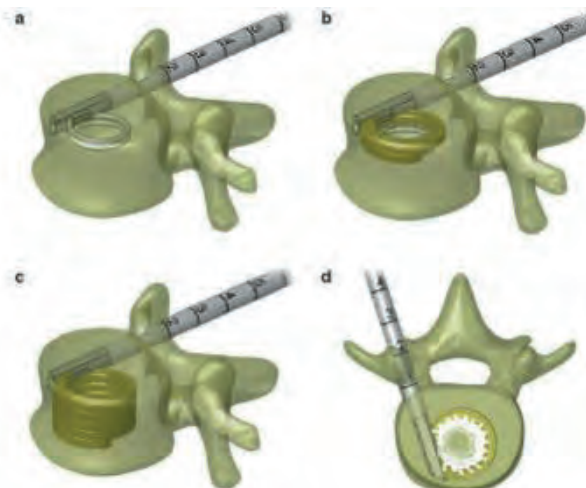

Figure 1: Deployment of the Kiva Implant

Extensive verification activity was conducted to confirm that this novel PEEK structure meets static and dynamic performance expectations. Bench testing included protocols for assessing in accordance to ASTM-F2077 for spinal implants to assess strength in static axial loading as well as dynamic loading to 5 million cycles. A cadaveric study of VCF in a three-segment vertebral model compared restoration of biomechanical properties for Kiva versus BKP in immediate and post-cyclic (50,000 cycles) conditions[1]. Additionally, restoration of vertebral mechanics after induced compression fractures were compared in Kiva with injectable PMMA versus a biphasic cement (calcium sulphate + hydroxyapatite)[2].

Initial validation efforts consisted of single-arm clinical evaluation of Kiva with PMMA for safety and efficacy in osteoporotic[3], cancer-induced[4], and traumatic[5] VCFs in outside-US (OUS) settings. Finally, Kiva is being evaluated as part of multi-center, prospective, randomized FDA-approved clinical trial for assessment of non-inferiority with respect to safety and efficacy in comparison to BKP in osteoporotic VCFs.

Results:

Biomechanical studies demonstrated that the Kiva implant without any PMMA has a static compression strength which well exceeds that of cancellous bone and meets required dynamic strength of 3kN axial loading for over 5 million cycles. Cadaveric biomechanics showed there were no significant differences between Kiva with PMMA v. BKP with respect to height restoration, height maintenance, or vertebral stiffness after initial repair or

post-fatigue testing in a three-segment VCF model. Kiva required, however, 66% less bone cement to achieve this outcome (p<0.01) and had a significantly lower rate of extravasation (p<0.05). No difference in restoration of vertebral biomechanics were seen when Kiva was injected with either PMMA or an injectable biphasic cement.

OUS clinical outcomes in VCFs across multiple centers have shown significant and durable relief of pain (up to 71% at 6 month follow-up and 66% at 12 months) as well as low extravasation rates (4.8-8%) using low volumes of PMMA. Enrollment for the Kiva v. BKP trial was recently concluded early at 300 patients due to meeting pre-defined safety and efficacy criteria. Evaluation of 1 year follow-up data is continuing.

Discussion:

By leveraging numerous material property advantages that PEEK provides such as high strength and fracture toughness, Kiva represents a minimally invasive option for treating VCFs with a biomechanically equivalent construct that uses less bone cement. Pilot clinical studies demonstrate a good safety and efficacy profile for Kiva with PMMA for relief of painful VCF resulting from osteoporosis, cancer, and trauma. The design of the Kiva may also facilitate the eventual use of alternative bioactive injectables which lack acute mechanical support.

References:

1. Wilson, D, et al. *Clin Biomech*, 2012: 27, pp. 346-53.
2. Connolly, R, et al., 19th GRIBOI Meeting, 2009.
3. Olivarez, L, et al., *SAS Journal*, 2011: 5, pp. 114-9.
4. Anselmetti, G, et al., *Intl Med Case Reports*, 2012: 5, pp. 13-17.
5. Korovessis, P, et al., 19th IMAST Meeting, 2012.

Revision and Retrieval Analysis of PEEK Rod Systems for Fusion and Posterior Dynamic Stabilization

Kurtz, Steven M.[1]; Lanman, Todd[2]; Berven, Sigurd[3]; Isaza, J[4]; Higgs, Genymphas[1]; MacDonald, Daniel[1]

[1]Drexel University and Exponent, Philadelphia, [2]University of California Los Angeles, Los Angeles, [3]University of California San Francisco, San Francisco, [4]Baton Rouge Orthopaedic Clinic, Baton Rouge
E-mail: skurtz@drexel.edu

Introduction:

Lumbar fusion the standard of care for the surgical treatment of intractable low back pain, but in the mid 2000s motion preservation was introduced as an alternative treatment paradigm to preserve the spine from adjacent segment disease (1). Artificial discs were among the first highly visible technologies proposed for motion preservation, but posterior dynamic stabilization systems were also developed as alternative to fusions. Polyaryletheretherketone (PEEK) rod systems were clinically introduced in 2006 as an alternative to metallic posterior rod fusion systems for the lumbar spine (1). Biomechanical testing suggests that PEEK rods provide equivalent stability to the instrumented spine as titanium (Ti) alloy rods, but may also increase anterior column load sharing and reduce torques at the interface between pedicle screws and bone (2,3). PEEK rods are also radiolucent and compatible with MRI (1).

In the US, PEEK rods were cleared by the Food and Drug Administration (FDA) as an adjunct to fusion (1), however surgeons have also reported applications of PEEK rods in posterior dynamic stabilization without fusion (4). In October 2009, the FDA issued 522 orders to the manufacturers of nonrigid posterior instrumentation, including PEEK rods, due to the paucity of data regarding the clinical failure modes, and revisability of these systems in fusion applications. Data regarding revision of PEEK rods in nonfusion applications is likewise unavailable.

In 2004, we started a multi-institutional retrieval program to analyze the revision of motion preserving spinal implants, including PEEK rods, and their associated explanted devices and tissues. The purpose of this study was to develop a classification system for the initial surgical indications, intention to treat, reasons for revision, and complications for the PEEK rod systems for comparison with metallic fusion rod systems. A secondary goal of this study was to establish the incidence of hardware-related complications for the revised PEEK rod systems. We sought to determine if flexible PEEK rod systems are associated with unique clinical risks or failure modes that differ from traditional Ti rods, which are considered to be comparatively "rigid" by clinicians.

Methods and Materials:

This IRB-approved, prospective clinical and retrieval study of explanted spinal devices was conducted as an ongoing collaboration between three high volume spine surgery centers and a university-based biomedical engineering retrieval center. Consent was obtained from patients to participate in this research and to donate their explanted devices to the retrieval program. 12 patients with PEEK rods and 4 patients with Ti rods were revised between 2008 and 2012. Patient history and, in the case of PEEK rods, intention to treat (fusion vs. nonfusion), was obtained from analysis of the medical records. Diagnostic imaging and the complete set of retrieved posterior instrumentation (rods, set screws, and pedicle screws) were obtained in 12/12 PEEK and 4/4 Ti cases. All of the PEEK rods were of the same design (CD Horizon Legacy, Medtronic, Memphis TN), with an elliptical cross-section, and which varied in length depending upon the number of treated levels. The designs and manufacturers of the Ti rods varied. Retrieved components were examined under optical microscopy to identify surface damage mechanisms, including plastic deformation, scratching, burnishing, pitting, and fracture.
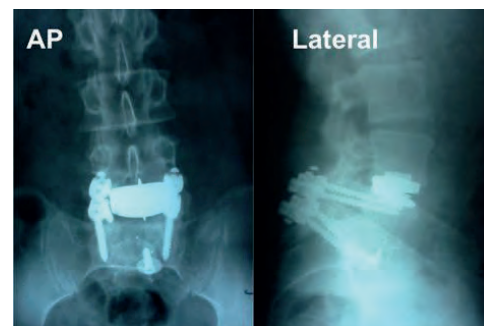

Figure 1: *Antero-posterior and lateral radiographs of a patient with PEEK rods used in conjunction with a total disc replacement.*

Results:

The intention to treat varied among the PEEK rod patients. Most of the PEEK rods in this study were from clinically failed fusions 9/12, rather than non-fusions (3/12). In 6/9 fusion cases, the PEEK rods were used as part of a salvage procedure during the revision of a previous failed fusion, and these patients generally had a longer and more complex history of low back pain and surgical intervention that the primary surgery candidates. In one case, the PEEK rods were used as part of a salvage procedure following a previous failed total disc replacement. For one of the nonfusion patients, the PEEK rods were used in a two-level construct in which only one level was fused; this patient was revised for two loose pedicle screws. In the remaining nonfusion case, the PEEK rods was used in combination with a lumbar artificial disc and were revised for screw impingement of the L4/L5 facet and pain. All of the patients in this study were revised for intractable pain, although the mechanism varied and was confirmed by intraoperative findings. The revision procedure for PEEK rods was via posterior

approach, and did not differ from the revision strategy of Ti rods.

Surgical complications in the PEEK cohort included a small dural tear in one case that was immediately repaired. There were no cases of PEEK rod fracture or pedicle screw fracture in this series. Retrieved PEEK rods exhibited scratching, as well as impressions from the set screws and the saddle of pedicle screws, similar to the retrieved Ti rods (Figure 2).
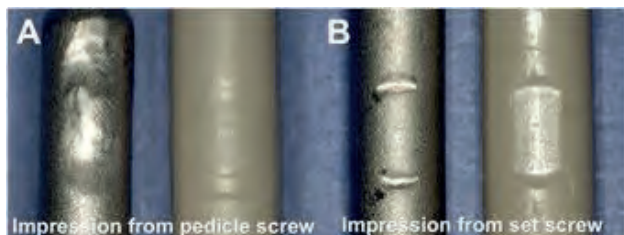

Figure 2: Typical (A) pedicle screw saddle and (B) set screw impressions in retrieved Ti rods as compared with retrieved PEEK rods.

Discussion:

The results of this study suggest that the revisability of PEEK rod systems is comparable to metallic fusion systems. Our data do not support the hypothesis that PEEK rods are associated with unique clinical risks that differ from Ti rod systems. The revision reasons for the PEEK rod systems, including disease progression and unrecognized adjacent level disease, are well documented in the literature for metallic posterior fusion systems. One concern regarding PEEK rods is their durability, which has been assessed in laboratory fatigue studies (5). During preclinical testing, fatigue fracture of PEEK rods has been shown to initiate at the rod-screw interface (5). In our examination of the retrieved rods, we documented screw impressions in both PEEK and Ti rods (Figure 2), but no evidence of fatigue cracks or fracture.

Screw loosening, while a known failure mechanism for posterior instrumented fusion, is especially a concern for nonfusion applications in which the screw interface may be loaded for a longer duration and with greater loads than in fusion applications. For example, previous retrieval studies of the Dynesys posterior dynamic stabilization system documented screw loosening as a reason for revision in 11/17 (65%) of the retrieved cases, all of which were used for nonfusion (6). In our series, screw loosening was only observed in 1/12 revisions, albeit in one of the two nonfusion applications of PEEK rods of the study. We will need additional cases to perform a quantitative comparison of the relative incidence of screw loosening among revised cases with both fusion and nonfusion applications of PEEK rods.

Like all revision retrieval studies, our research is limited to cases requiring surgical intervention and hardware removal, and thus cannot be used to establish the overall revision or complication risk for the clinical use of PEEK rod systems. Furthermore, many of our

cases were difficult salvage procedures with a history of previous spinal surgeries, which are more difficult and have generally have poorer outcomes than primary fusions. Nevertheless, the findings from this series of revisions cases are a useful complement to the data obtained in prospective clinical studies. Furthermore, the performance of PEEK rods to repair previously failed fusions may arguably provide a more challenging or worst case loading environment than primary fusion cases. Regardless, additional characterization of in vivo changes in the retrieved PEEK rods and explanted tissues is also warranted and ongoing at our institutions.

References:
1. Kurtz SM (Ed.), *PEEK Biomaterials Handbook*, 2012;
2. Turner et al., Spine, Vol. 35, 2010;
3. Gornet et al., J. Biomechanical Engineering, Vol. 133, 2011;
4. Highsmith et al., Neurosurg Focus, Vol. 22, 2007;
5. Ponnappan et al., Spine J, Vol. 9, 2009.
6. Ianuzzi et al., Spine, Vol. 35, 2010.

Characterization Of In Vivo Changes And Histological Responses Of Retrieved PEEK Rod Systems For Posterior Lumbar Stabilization And Fusion

Genymphas B. Higgs[1], Daniel M. MacDonald[1], Todd H. Lanman[2], Sigurd H. Berven[3], Jorge E. Isaza[4], Marla J. Steinbeck[1], Steven M. Kurtz*[1]

[1]Drexel University and Exponent, Philadelphia, [2]University of California Los Angeles, Los Angeles, [3]University of California San Francisco, San Francisco, [4]Baton Rouge Orthopaedic Clinic, Baton Rouge

E-mail: skurtz@drexel.edu

Introduction:

Though widely implemented to treat intractable back pain, lumbar fusion using metallic rods has been shown to generate supraphysiological stresses at adjacent vertebrae which may lead to the development of adjacent segment disease [1]. Polyaryletheretherketone (PEEK) rods have been introduced as semi-rigid alternatives to metallic rod stabilization, but little is known about the changes that occur to PEEK rods *in vivo*. This study characterizes the surface damage mechanisms, curvature variations, crystallinity changes and histological responses of retrieved PEEK rods used in posterior spinal instrumentation. We hypothesized that PEEK rods would undergo permanent deformation and crystallinity changes while maintaining histological inertness *in vivo*.

Methods and Materials:

Twelve fixation systems (23 rods) and seven periprosthetic tissue samples were collected during revision surgery. The average implantation time was 1.8±0.7 years (Range 0.8-2.8 years) and the mean patient age at implantation was 53 years (Range: 35–64 years).

Components were cleaned in a 10% bleach solution and sonicated to remove loose debris. The rod surfaces were evaluated under a stereomicroscope for the presence of 6 damage modes: burnishing, scratching, pitting, delamination, plastic deformation and abrasion. PEEK rods were also imaged with a Scanco MicroCT 80 to provide 3-dimensional reconstructions for rod curvature evaluation. Matching circles of known radii to each rod's sagittal cross-section allowed for the radius of curvature to be determined. Crystallinity changes were evaluated using specular reflectance Fourier Transform Infrared Spectroscopy (R-FTIR; ASTM F2778). Tissue samples were embedded in paraffin, sectioned, dewaxed, and stained with hemotoxylin and eoisin (H&E). Brightfield and corresponding polarized light images were taken for each sample.

Results:

All of the components in this study were revised for intractable pain. In addition to pain, the rods were revised for motor vehicle trauma (n=1), instability (n=2), pseudoarthrosis (n=2), screw loosening (n=1), pedicle screw impingment (n=1), and adjacent segment disease (n=1). Although scratching and burnishing were present to a minor extent, the predominant *in vivo* change observed was plastic deformation at the screw-rod interfaces (Fig. 1A-B). At these sites, crystallinity was found to be significantly lower than at regions of the rod without screw impressions (mean difference = 14.3%; Wilcoxon Test; Figure 2). The radius of curvature varied among the retrieved rods, averaging 119 ± 19 mm (Range: 92 – 160 mm). A correlation between radius of curvature and implantation time could not be detected (Rho = -0.28, p = 0.22; Spearman's Rank Order Correlation).
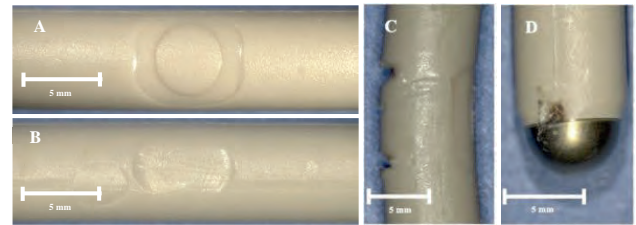

Fig. 1. Rod samples illustrating modes of wear. Plastic deformation at the convex **(A)** and concave **(B)** surfaces of Case 6 due to impressions from the pedicle screw and setscrew (respectively). **(C)** Rod exhibiting severe scratching at the screw-rod interface. **(D)** Discoloration at titanium end cap of a PEEK rod.
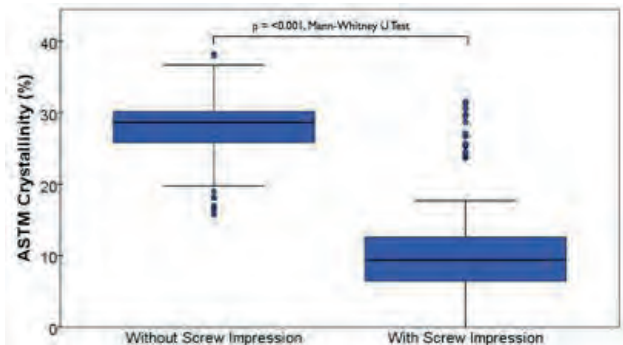

Figure 2. Regional variation of crystallinity.

For histological analysis, 3/7 patients had tissues with evidence of inflamation. Periprosthetic tissue samples of the remaining patients showed normal morphology. Using brightfield and polarized light microscopy, PEEK debris was observed in only one patient. In the case where discoloration at the titanium end caps was noted (Fig. 1D), evidence of metallosis, inflammation and tissue degeneration was seen (Figure 3B-C).
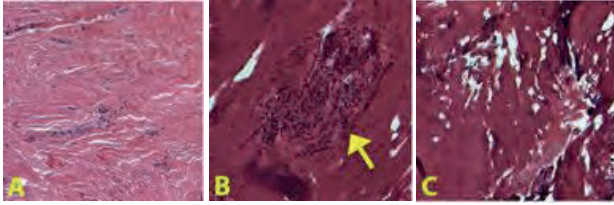
Figure 3. Representative images of periprosthetic tissue morphology. Samples of tissue **(A)** showed normal densely organized collagen and vascularized tissue. Tissue from one case showed inflammation **(B)** and degeneration **(C)**.

Discussion:

To the authors' knowledge, this study serves as the first of its kind to investigate the *in-vivo* changes to PEEK rod systems. The predominant *in vivo* change observed was plastic deformation at the screw-rod interfaces. The lower crystallinites measured at the high-stress screw-rod interface suggest mechanical disordering of the PEEK crystalline structure, consistent with the findings of Papkov et al [2]. Nevertheless, there were no instances of PEEK rod fracture in any of the cases in this study. Wear of the PEEK rods appeared to be minimal. Birefringent PEEK particles were only observed in one tissue sample. Wear products from the metal components were consistent with the inflammatory and degenerative histological observations. Long-term retrievals are needed to provide further information on the *in vivo* stability of PEEK rod systems.

References:

1   G. Cheh et al., *Spine,* 2007, **32**, 2253.
2   V. Papkov et al., *Polymer Eng. and Sci.*, 1997, **37**, 1280.

Poster Abstracts

First International
PEEK Meeting
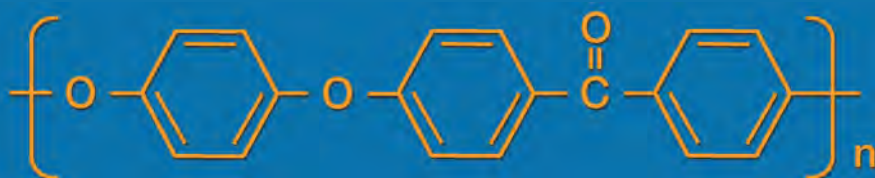
Posters

Effects of an Ellipsoidal Versus Cubic Pore Morphology on the Permeability, Mechanical Properties and Cell Infiltration of HA Reinforced PEEK Scaffolds

Conrad, TL,[1] Merrill, CH,[1] Roeder, RK[1]

[1]Department of Aerospace and Mechanical Engineering, Bioengineering Graduate Program,
University of Notre Dame, Notre Dame, IN 46556 USA

rroeder@nd.edu

Introduction: The high melting temperature of polyetheretherketone (PEEK) (~343°C) requires the use of a higher melting temperature porogen or fugitive material to prepare porous scaffolds by leaching the porogen after molding [1-3]. However, cubic (e.g., salt) porogen materials may limit pore interconnectivity due to edge-to-face and corner-to-face contacts during molding [4,5]. Limited pore interconnectivity can obstruct permeability for cell infiltration and nutrient transport. However, the effects of a cubic or spherical pore morphology on scaffold permeability have not be investigated. Therefore, the objective of this study was to investigate the effects of the porogen morphology on the permeability, mechanical properties, and *in vitro* osteoblast infiltration of bioactive hydroxyapatite (HA) whisker reinforced PEEK scaffolds.

Materials and Methods: HA whiskers (~20 x 3 μm) were prepared as described elsewhere [6]. A PEEK powder (~50 μm, LT1PF PEEK-OPTIMA, Invibio) and a NaCl porogen (Fluka) were both used as-received. Ellipsoidal NaCl crystals were prepared from as-received cubic NaCl crystals (Fig. 1) adapting methods described elsewhere [7]. Cubic and ellipsoidal NaCl crystals were both sized to 300-600 μm using a shaker sieve. PEEK scaffolds comprising 75-90% porosity, formed by either the cubic or ellipsoidal porogen, and reinforced with 20 vol% HA whiskers were prepared by compression molding a powder mixture at 250 MPa at a mold temperature of 380°C and removing the NaCl porogen in DI water for 3 d [1-3]. Scaffold permeability was measured by forced flow of DI water and Darcy's law (*n*=5/group). Scaffold mechanical properties were measured in unconfined uniaxial compression at a crosshead speed of 1 mm/min in phosphate buffered saline (PBS) at 37°C (*n*=5/group). Micro-computed tomography (Scanco μCT-80) was used to image the scaffold architecture.

Results: The permeability of HA reinforced PEEK scaffolds increased with increased porosity (*p*<0.0001, ANOVA), as expected (Fig. 2a). However, scaffolds prepared with the ellipsoidal NaCl porogen exhibited greater permeability compared to the cubic porogen (*p*<0.0005, ANOVA) (Fig. 2a). These differences suggested that scaffolds prepared with the ellipsoidal porogen possessed improved pore interconnectivity compared to the cubic porogen. Micro-CT confirmed that scaffolds prepared with the ellipsoidal porogen exhibited a similar porosity and strut morphology, but a greater pore size and strut thickness, compared to the cubic porogen, due to greater pore interconnectivity. The compressive modulus (Fig. 2b), yield strength, and yield strain of scaffolds prepared with the cubic or ellipsoidal porogen were not different (*p*>0.30, ANOVA). The compressive modulus (Fig. 2b) and yield strength of scaffolds decreased with increased porosity (*p*>0.0001, ANOVA), as expected.

Discussion: The permeability of HA whisker reinforced PEEK scaffolds was improved using an ellipsoidal NaCl porogen instead of a cubic porogen without altering the mechanical properties. In contrast, a design tradeoff exists for the benefit and detriment of increased porosity for scaffold permeability and mechanical properties, respectively. The results of this study suggest that cells will more readily infiltrate scaffolds prepared with an ellipsoidal porogen. An ongoing *in vitro* study is investigating the infiltration of primary rat osteoblasts into scaffolds prepared using either the ellipsoidal or cubic porogen for up to 2 weeks in culture and will also be presented.
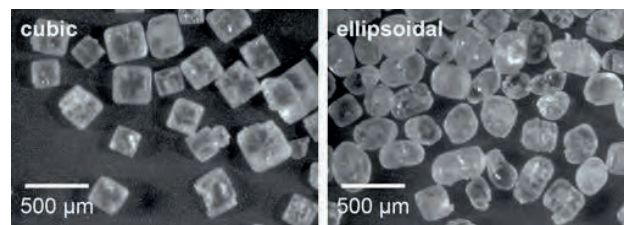
Fig. 1. Optical micrographs showing as-received cubic NaCl crystals and as-prepared ellipsoidal NaCl crystals.
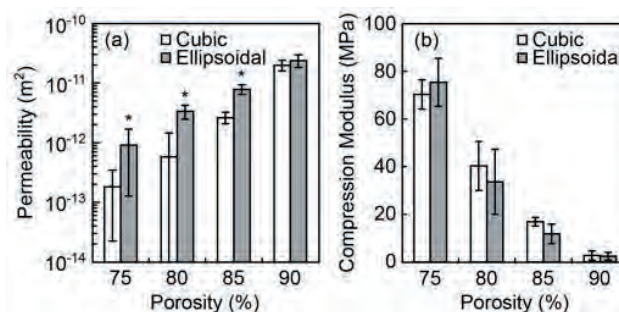
Fig. 2. (a) Effects of the porosity and porogen morphology on the (a) permeability and (b) compressive modulus of HA whisker reinforced PEEK scaffolds. Error bars show one standard deviation. *p*<0.05, Student's *t*-test cubic vs. ellipsoidal.

References: [1] Converse GL, *et al. J Mech Behav Biomed Mater* 2009;2:627. [2] Converse GL, *et al. Acta Biomaterialia*, 2010;6:856. [3] Conrad TL, *et al.*, *J Biomed Mater Res B*, submitted. [4] Gross KA, *et al. Biomaterials* 2004;25:4955. [5] Zhang J, *et al. Polymer* 2005;46:4979. [6] Roeder RK, *et al. J Am Ceram Soc* 2006;89:2096. [7] Mukhopadhyay I, *et al. Ind Eng Chem Res* 2010;49:12197.

Imparting osseo-integrating properties to the surface of PEEK implants with hydroxyapatite and titanium plasma spray coating while maintaining the substrate material's original chemical and physical properties

McCabe, A[1] Shawcross, J[1] & Armstrong, J[1]
[1]Accentus Medical plc, Oxford, UK
james.armstrong@accentus-medical.com
andy.mccabe@accentus-medical.com

Introduction: Polyaryletheretherketone (PEEK) is gaining acceptance by designers for use in medical devices. Of particular interest are its biocompatibility and mechanical properties. For example the modulus of elasticity is a close match to that of bone, enabling PEEK devices to guard against stress shielding. However PEEK surfaces are not inherently osseo-integrating, so there is a requirement for a viable method for applying coatings to enhance the biocompatibility and durability of cement-less PEEK implants, similar to that provided on metallic implants today. The series of regulatory testing to gain approval for metal and hydroxyapatite coatings on metallic implants is well documented. There is no reason why any less stringent testing should be required of PEEK devices. In addition, any processing should take into consideration, and guard against, the potential detrimental modification of the PEEK material. Designers should not be forced to take a judgement to lose substrate integrity over the benefit of an applied osseo-integrating plasma coated surface. Accentus Medical has overcome these concerns by developing a modification to their established Acusure® range of inert / reducing gas plasma spray coatings for metallic implants. The modified Acusure® technology enables the deposition of viable hydroxyapatite and titanium coatings at a low enough temperature to produce a coating that meets essential regulatory requirements and that does not impact on the structure and composition of the PEEK substrate. The effects of Acusure® lower process temperature plasma coating has been evaluated by Invibio, the major PEEK supplier, using their proprietary testing methods on PEEK-OPTIMA® material. Test results show that coating with Acusure®'s modified method with titanium, hydroxyapatite or combination of both substances does not adversely affect or degrade the substrate material. A suite of design validation testing has been conducted which demonstrates that the coatings meet the best practice guidelines and the relevant ASTM and ISO standards for metallic substrates.

Methods and Materials: The application of a thermal sprayed coating onto metallic materials relies upon the heat of the process to provide a well adhered coating. The physical and chemical properties of the coating are dependent on the process conditions. The development of a lower temperature coating process to apply calcium hydroxyapatite onto PEEK has been performed at Accentus Medical. Good understanding of plasma process technology, the properties of PEEK, and process validation methodology has been used to provide a lower temperature coating process. For HA coating, comprehensive testing has been performed of the mechanical properties (static shear, static tensile and shear fatigue), physical properties (sectioning, thickness measurements and quantitative metallography), chemical properties (Ca:P ratio, trace element analysis, solubility, dissolution, X-ray diffraction and infra red spectroscopy). In addition a suite of tests has been performed to analyse the PEEK substrate material (physically and chemically), and to specifically investigate any transfer of material between the PEEK and the coating.

Results: The chemical, physical and mechanical properties of the HA coating on PEEK demonstrate compliance with the regulatory standards. The mechanical tests are lower in strength than on metallic devices, though remain in excess of the minimum regulatory requirements for coatings on metallic devices. There is no evidence of transfer of material from PEEK to the detriment of the HA coating. Similarly the PEEK substrate has been independently tested by the PEEK manufacturer, Invibio. Results demonstrate that neither the deposition of titanium nor of hydroxyapatite have adversely affected, modified or degraded the PEEK material.

Hydroxyapatite plasma spray coating on PEEK with no adverse effects on the substrate

Discussion: A modified lower process temperature plasma spray coating has been developed and calcium hydroxyapatite successfully applied to PEEK test pieces. A series of tests have been performed to demonstrate compliance of the coatings with the regulatory requirements currently used for coatings on metallic devices. Designers do not need to take a judgment to lose substrate integrity over the benefit of an applied osseo-integrating plasma coated surface. Likewise there is no requirement for separate ASTM and ISO standards for the application of osseo-integrating surfaces onto PEEK. Regulatory dossiers, including a FDA masterfile, are being updated to include PEEK as a validated substrate for Accentus Medical's Acusure® titanium and hydroxyapatite coatings.

The Influence of different fillers on the mechanical properties of PEEK

Schwitalla, AD[1], Müller, W-D[1], Spintig, T[1]

[1]Charité University Medicine, Berlin, Germany

andreas.schwitalla@charite.de

Introduction: Since the 1990s PEEK is described as alternative implant material in the field of orthopedics and trauma in the literature. Due to its biocompatibility and elastic modulus similar to that of cortical bone, it plays an important role as viable alternative to conventional implant materials like titanium [1].

In the field of dentistry a wide range of alloplastic materials are used to replace missing teeth for example. Traditionally, metals, alloys and ceramics are used for such reconstructions. Also, titanium or titanium alloys are mostly used for dental implants [2].

Some problems associated with the use of different materials in the oral cavity could occur, such as hypersensitivity to metallic materials and conventional dental polymers such as Polymethylmethacrylate (PMMA). Additionally more and more patients desire metal free reconstructions.

Due to its mechanical properties, which can be influenced by reinforcing PEEK by different filling materials such as carbon fibers (CFR-PEEK) [3], it might be a viable biomaterial which could replace not only conventional polymers, but even conventional metals, alloys and ceramics in the field of dentistry.

The aim of this study was to evaluate the mechanical properties of different PEEK compounds.

Methods and Materials: Nine different commercial PEEK grades were available. Two unfilled (u1 and u2), two filled with ~10% TiO_2 (t1 and t2), one glass fiber reinforced (GFR-PEEK) with ~30% glass fibers (g), two samples of CFR-PEEK filled with ~30% chopped carbon fibers (cc1 and cc2) one CFR-PEEK sample filled with ~45% randomly orientated continuous carbon fibers (rc) and one CFR-PEEK sample filled with ~40% parallel orientated continuous carbon fibers (pc). The grades u1, cc1, rc and pc were medical grades for permanent implantation, whereas u2, t1 and t2 were approved for short term application up to 30 days. g and cc2 were industrial grades.

u1, u2, rc, pc and t2 were delivered as round rods with the diameters 8mm, 6mm, 5mm, 4mm, and 6mm, respectively. cc1 was delivered as a rod with a quadratic cross-section area with a length of ~30mm of each side. The grades t1, cc2 and g where delivered as quadratic plates with a length of ~10cm of each side and a height of ~1cm.

For pressure and cyclic loading tests cylindrical test specimens with the diameters 4, 5 and 6mm were manufactured with the proportion of diameter to height as 1:2 (n=5 of each diameter), whereas the samples of rc and pc had the same diameter as the original rod (n=5). For three-point bending tests small rods were produced with a height between 1-1.5mm and a width of 2-2.5mm and a length of 15mm (n=10; n=5 of rc and pc).

All tests were performed with a universal testing machine (Z010, Zwick, Ulm, Germany) and its corresponding software (TestXpert II, Zwick, Ulm, Germany).

The three-point bending tests were performed according to the test specification of DIN EN ISO 178, 02/1997 with a preload of 1 N and test speed of 1mm/min. The distance of the support span was 10mm.

The pressure tests were performed according to the test specification of ASTM D 695, 1996 with a preload of 2N and test speed of 1mm/min.

For the cyclic loading tests an individual test specification was designed, to simulate faster fatigue. The samples were loaded stepwise in a cyclic manner until the maximum force of 2000N was reached in 10 force steps, whereas each force step consisted of 100 loading cycles in a range of 200N (Fig.1). The preload was 20N and the testing speed was 1mm/min for the fiber-filled samples and 3mm/min for the others.

Additionally samples of some grades (t1, t2, cc1, rc and pc; n=5) were incubated in Ringer-solution (B. Braun Melsungen, Melsungen, Germany) at 37°C. After t=1, 7, 28 and 84 days the samples were weighed and measured again and the three test methods described above were performed afterwards (n=5 for each test method of each grade).

Statistical analyses were performed with OriginPro 7.5G SR2 (OriginLab Corporation, Northampton, MA, USA).

Results: The results of the three-point bending tests under dry conditions are listed in table 1. The results of grades with similar fillers (t1 and t2; cc1 and cc2; rc and pc) were compared and significant differences were marked.

The results of the pressure test under dry conditions are listed in table 2. The results of grades with similar fillers (u1 and u2; t1 and t2; cc1 and cc2; rc and pc) were compared and significant differences were marked. The effective maximum pressure strength of two samples of rc could not be evaluated, as they resisted the maximum force of 10000N of the testing machine.

The results of the cyclic loading tests under dry conditions are listed in table 2. The results of grades with similar fillers (u1 and u2; t1 and t2; cc1 and cc2; rc and pc) were compared and significant differences were marked. Fig.1 shows an example of a graph resulting from the cyclic loading test specification. Due to the principle of the test specification, the maximum pressure strength could not be evaluated. The limit of elastic deformation was evaluated instead, whereas of cc1 and cc2 only the samples with a diameter of 4mm could be considered to get this information, as the samples with a diameter of 5 and 6mm were not deformed within the force limit of 2000N of the test specification. Also the values for the limit of elasticity of rc and pc must be

considered as a minimum, as those specimens did not deform as well (Table 3).

To get an idea of the influence of the cyclic loading on the limit elasticity of the samples, the results were compared to the results of the pressure test (Fig.2). The results of the limit of the elastic deformation of rc and pc of the cyclic loading test cannot be compared to the results of the pressure test, as within the limitation of the test specification no deformation occurred. Of cc1 and cc2 only the samples with an diameter of 4mm could be compared as the samples with diameters of 5 and 6mm did not show deformations within the limit of the cyclic loading test specification as well. Overall the differences between the pressure and the cyclic loading test were significant. The limit of elasticity was 27.6±0.5% lower for the cyclic loading test, within a range from 20.6% (cc1) to 33.3% (u1).

The differences of the elastic modulus deriving from the pressure test to the elastic modulus from the cyclic loading test are listed in table 4.

An overview of the moduli of elasticity of the incubated samples is given in Fig.3.

Table 1: Shows the mean results of the three-point bending tests under dry conditions.

Grade	Samples [n]	Height [mm]	Width [mm]	Flexural Modulus [Gpa]	Flexural Strength [Mpa]
u1	10	1.54±0.04	2.48±0.1	2.73±0.26	182.91±12.59
u2	10	1.21±0.09	2.42±0.07	2.85±0.41	170.37±19.31
t1	10	1.18±0.11	2.41±0.1	**3.78±0.8***	206.44±37.84
t2	10	1.42±0.09	2.43±0.07	**3.14±0.3***	202.11±4.08
g	10	1.49±0.02	2.34±0.1	5.07±0.59	202.93±15.51
cc1	10	1.46±0.08	2.41±0.07	**4.09±0.8***	188.53±34.45*
cc2	10	1.51±0.02	2.35±0.05	**8.68±2.58***	319.21±46.32*
rc	5	1.26±0.16	2.35±0.2	**20.34±4.03***	532.12±164.16*
pc	5	1.32±0.16	2.37±0.14	**47.27±10.3***	1009.63±107.33*

*significant differences (p<0.05) of the particular properties (t1 vs. t2; cc1 vs. cc2; rc vs. pc)

Table 2: Shows the mean results of the pressure tests of cylindrical specimens under dry conditions.

Grade	Samples [n]	Height [mm]	Diameter [mm]	Pressure Modulus [Gpa]	Pressure Strength [Mpa]
u1	15	9.94±1.7	5.03±0.83	3.06±0.15	**136.61±1.21***
u2	15	10.01±1.68	5±0.83	3±0.28	**123.2±0.8***
t1	15	10.01±1.64	4.97±0.84	3.49±0.22	139.32±1.05
t2	15	9.95±1.71	5.05±0.81	3.47±0.62	137.31±4.84
g	15	10.01±1.65	5.01±0.86	6.71±1.48	174.65±10.32
cc1	15	9.99±1.69	5.01±0.86	**6.41±0.75***	230.50±15.08
cc2	15	9.93±1.66	5.01±0.84	**10.17±2.98***	242.22±34.49
rc	5	10.77±0.16	5.44±0.03	**37.24±5.96***	408.09±11.34*
pc	5	7.46±0.08	3.75±0.01	**106.71±14.83***	712.67±66.02*

*significant differences (p<0.05) of the particular properties (u1 vs. u2; cc1 vs. cc2; rc vs. pc)

Table 3: Shows the mean results of the cyclic loading tests of cylindrical specimens under dry conditions.

Grade	Samples [n]	Height [mm]	Diameter [mm]	Pressure Modulus [Gpa]	Limit of Elasticity [Mpa]
u1	15	9.97±1.67	5.00±0.84	**3.47±0.17***	54.18±10.93
u2	15	10.03±1.68	5.02±0.84	**2.82±0.15***	50.49±5.66
t1	15	9.93±1.71	4.99±0.84	**49.98±5.95***	50.26±5.08
t2	15	9.95±1.7	5.03±0.85	3.58±0.38	**44.66±7.05***
g	15	9.95±1.67	5.02±0.85	6.31±1.58	59.26±14.6
cc1	15	9.97±1.69	5±0.86	**10.38±1.71**	**101.37±10.25***
cc2	15	9.98±1.69	5.00±0.83	9.74±4.56	**84.15±18.45***
rc	5	10.78±0.21	5.42±0.04	52.74±11.63	86.64±1.42
pc	5	7.41±0.08	3.74±0.01	70.17±34.28	182.42±0.86

*significant differences (p<0.05) of the particular properties (u1 vs. u2; t1 vs. t2; cc1 vs. cc2)

Table 4: Shows the difference of the elastic modulus from the cyclic loading test to the elastic modulus deriving from the pressure test ((elastic modulus$_{cyclic\ loading}$)-(elastic modulus$_{pressure}$)).

u1	u2	t1	t2	g	cc1	cc2	rc	pc
13.1%*	-6.1%*	-3.7%	3.2%	-5.9%	61.8%*	-4.2%	41.6%*	-34.2%

*significant difference

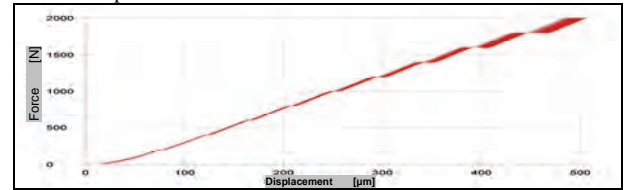Fig. 1: Shows a graph of the cyclic loading test of a cylindrical specimen of t1.

Fig.2: Shows the significant differences of the results of the limit of elasticity of the pressure test vs. cyclic loading test.
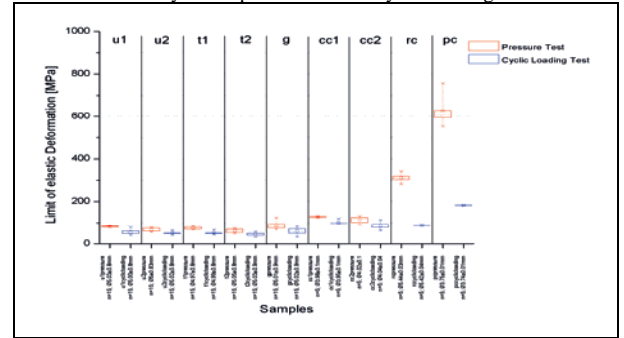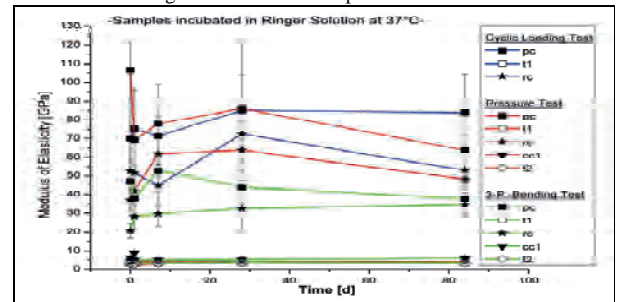

Fig.3: Results of the moduli of elasticity of the incubated samples deriving from the three test specifications.

Discussion: The results underline the assumption, that PEEK and compounded PEEK could be a viable alternative material for the field of dentistry - considering the mechanical properties. Despite the preliminary character of the present study due to the rather low number of samples available, the influence of the fillers such as the different carbon fibers on the mechanical properties of our specimens may be comparable to the data published in the literature [1]. Further investigations are necessary to underline the present results. For the applicability in dentistry further problems must be solved, e.g. the opaque color of PEEK.

References:

1. Kurtz SM, Devine JN. PEEK biomaterials in trauma, orthopedic, and spinal implants. Biomaterials. 2007 Nov;28(32):4845-69.

2. Schwitalla AD, Müller WD. PEEK dental implants: A Review of the Literature. J Oral Implantol. 2011 Sep 9.

3. Skinner HB. Composite technology for total hip arthroplasty. Clin Orthop Relat Res. 1988 Oct;(235):224-36.

Osseointegration of PEEK implants coated with nanocrystalline hydroxyapatite

Per Kjellin*[1], Martin Andersson[2], Sargon Barkarmo[3,4], Paul Handa[1],Victoria Stenport[3,4], Ryo Jimbo[5] and Ann Wennerberg [3,5].

[1]* Promimic AB, Göteborg, Sweden ; E-mail: per@promimic.se [2] Department of Chemical and Biological Engineering, Chalmers University of Technology, Sweden [3] Dept. of Biomaterials, The Sahlgrenska Academy, University of Gothenburg, Sweden [4] Dept. of Prosthodontics, Institute of Odontology, The Sahlgrenska Academy, University of Gothenburg, Sweden [5] Department of Prosthodontics, Faculty of Odontology, Malmo University, Malmö, Sweden

Introduction: PEEK is a polymeric biomaterial which is gaining popularity as an implant material because of its mechanical properties, excellent biocompability, and also due to its radiolucency. One disadvantage is that PEEK has a very slow osseointegration compared to for example titanium. We have developed a technique to modify the PEEK surface with an extremely thin (10-20 nm) layer of nanosized hydroxyapatite (HA) crystals. This surface modification preserves the underlying structure of the PEEK surface, even on the micrometer level, and also changes the surface from hydrophobic to hydrophilic. We have previously shown that it is possible to improve the osseointegration on titanium implants with nanocrystalline HA, but coating PEEK with nanosized HA is a relatively new field.

Methods and Materials:

We used a self-assembling surfactant system to create a dispersion of nanosized HA crystals. The dispersion was applied onto the PEEK implants by spin-coating, and was attached to the surface by a heat treatment at 325 °C for 5 minutes. Structural integrity of the PEEK material before and after the heat treatment was investigated with tensile testing. The resulting implant coating was evaluated with SEM and XPS. Several *in vivo* studies were performed to investigate the biological properties of the HA coating. In the first study, smooth PEEK implants were allowed to heal for 6 weeks in the tibia bone of rabbits. The bone to implant contact (BIC) and bone area were evaluated with histomorphometry. In the two subsequent studies, threaded PEEK implants were used instead of smooth. These implants were also inserted in the tibia of rabbits and examined after 3,6 and 12 weeks of healing. The integration of the implants was assessed with removal torque measurements and histomorphometry. The PEEK used in the studies was PEEK Optima from Invibio.

Results: Contact angle measurements showed that the HA coating created a hydrophilic surface, the contact angle was 80° for the untreated PEEK, and 35° for the HA coated PEEK. The tensile measurements were performed on samples which were heat treated for 10 minutes at 300 and 350 °C. The tensile measurements showed no change in the elastic modulus or peak load. From the SEM analysis, it could clearly be seen that the micro topography of the implant surface was preserved. The size of the HA crystals was measured to approximately 50-200 nm long and 5-10 nm in diameter.

The first in vivo study done on smooth cylindrical shaped implants showed higher BIC and bone area for the HA coated implants, but these differences were not statistically significant. The reason for the insignificant differences between the uncoated and coated implants was probably due to micro movement of the smooth implants during healing, the low BIC values overall support this theory. Therefore, the next *in vivo* study was performed on threaded implants, and removal torque measurements was done in addition to histomorphometry to assess the osseointegration. The HA coated threaded implants had on average a 70 % higher removal torque, with a 99 % level of significance. These large differences in removal torque were the same for the healing times 3, 6 and 12 weeks.

Discussion: Modification of PEEK implants with nanosized HA gives a hydrophilic surface. The coating method preserves the micro topography of the implant surface, and does not change the mechanical properties of PEEK. The improved osseointegration is most pronounced for implants with a good stability, such as threaded implants. For these types of implants, the osseointegration is significantly increased.

A new hip prosthesis without debris release

Adelina Borruto

University of Rome "La Sapienza", Department of Chemical Engineering and Materials,
Via Eudossiana, 18, 00184 Rome, Italy
mail:adelina.borruto@uniroma1.it

Introduction: Today, in spite of the long experience acquired in the field of total hip replacements, prosthetic systems are still far from reproducing the natural system which shows a friction coefficient between the articulation of approximately (0.005÷0.025) µ.

One of the main causes of long term failure is the amount of wear debris produced by the tribological coupling between acetabolar cup and femoral head. Therefore, in order to increase the " longevità " of total hip replacement joint, the rate of wear debris generated by the articulation surface must be reduced.

Thus, it is clear that the study of the tribosystem of coupling materials is of fundamental importance. It is necessary to state that the femoral head–acetabulum coupling, i.e. the established tribosystem once the prosthesis has been implanted, will function in a moist environment. This is a closed environment encapsulated by a membrane which is permeable to plasma, water, proteins and salts. In this system wear between the parts will occur in condition of water lubrication.

Thus, it is therefore important to study the materials in tribological coupling but it is still more important to study the mechanism that allows the formation of the supporting film between two surfaces in couplings i.e. produces an efficient lubrication condition.

This paper present an alternative bearing surface that is made of a Peek carbon fibre femoral cup and a CoCr alloy femoral head or vice versa.

In this work, which has been developed by the author for many years, a large number of tribological couplings is examined and an innovative method for an efficient lubricant condition, based on the difference of material wettability is proposed.

Furthermore the authors carried out experimental research in order to investigate the formation of debris caused by tribological coupling of three type of Peek versus cobalt chrome alloy .

This study sets new bases for the design of modern hip prosthesis without debris release .

Methods and Materials: .
In previus papers materials with different wettabilities and with two different roughness intervals, Ra (0.003-0.08) and Ra (0.08-3), were taken into consideration. The wear tests, in dry and water lubrication, have been performed with a Pin on Disk tribometer (ASTM 99G norm) with continuous drop addition system in air environment.

The wettability of each material was measured using the model of the contact angle θ. The wettability difference ($\Delta\theta$) for every tribological coupling taken into consideration, was calculated.

In this work wear and friction tests on three different types of Peek with roughness intervals Ra (µm)(0.03–0.08) have been performed in air environment:
• under dry conditions;
• with lubricants: demineralised water and human serum .
The dry wear tests were realized to know the behavior of prosthetic material in the event of accident, i.e. due to a change in the prosthesis position, other words when the prosthesis is in the absence of lubrication.

Furthermore the authors carried out experimental research in order to investigate the formation of debris caused by tribological coupling of three types of Peek versus cobalt chrome alloy.

A careful methodology of filtering under vacuum was used to extract the debris from the lubricants used in the tribological test. SEM and EDS analysis was used to characterize the debris.

Results:
From these results it is easy to note that the friction coefficient, the wear both in dry, in water and in human serum conditions, the width track, the analysis at scanning electron microscopy (SEM) and the extremely low quantity of debris produced during the tests(value less then 0.1 µm), show that they conform to the trend of the difference of wettability ($\Delta\theta$) :
The higher is the wettability difference ($\Delta\theta$) between coupling materials, the more efficient is the lubricant condition, i.e. a stable supporting meatus is formed (meatus: film of water between hydrophobic and hydrophilic surfaces).
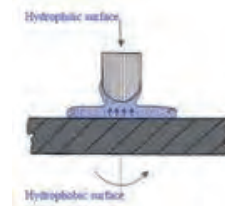
The tribological coupling peek carbon fiber-ceramic material is a classic example of not lubricated system, because formed by two hydrophobic materials.

This research, has produced two European and USA international patent.
European Patent 1438082
USA Paent 7,896,925

Effect of contact pressure on the wear of PEEK and CFR-PEEK materials against metallic counterfaces

Claire L Brockett, John Fisher, Louise M Jennings
Institute of Medical and Biological Engineering, University of Leeds, Leeds, UK
C.L.Brockett@leeds.ac.uk

Introduction:
Total joint replacement has been a successful surgical intervention for many years, with the majority of bearing joints having ultra-high molecular weight polyethylene as an articulating material. However, concerns remain regarding wear debris induced osteolysis and the longevity of TJR as patient demands change. Alternative bearing materials have been investigated, with CFR-PEEK demonstrating low wear behavior in both knee and hip replacement wear studies.

The aim of this study was to investigate the influence of contact pressure on the wear of PEEK and CFR-PEEK materials through simple configuration pin-on-plate studies.

Methods and Materials:
The wear performance of PEEK (n=4, OPTIMA, Invibio) and CFR-PEEK (n=6, MOTIS, Invibio) were investigated through pin-on-plate studies. The PEEK/CFR-PEEK materials were machined into flat-faced pins, and were articulated against polished high carbon CoCrMo plates. The pins had a counterface of 3, 5 or 8mm diameter, which under an applied load of 80N resulted in contact pressures of 11, 6 or 1.6MPa respectively. Tests were conducted in a pin-on-plate rig, which applied a unidirectional displacement to the plate, and a rotation to the pin, producing a resultant multi-directional motion. In all tests, the stroke length was 26mm and rotation was ±45°, giving a resultant average cross shear ratio of 0.18. Tests were conducted for 1Mc, gravimetric analysis of wear was completed every 0.33Mc. Tests were lubricated with 25% bovine serum supplemented with 0.03% sodium azide to retard bacterial growth. Prior to testing the pins were soaked in deionized water for a period of 10 weeks, and unloaded soak controls were used during the test to account for fluid uptake.

Results:
The wear of the PEEK material was significantly higher than the CFR-PEEK material under all contact pressure conditions. The calculated wear factors for both PEEK and CFR-PEEK materials appeared to increase with increasing contact pressure (Figure 1). It was notable that the variability within pressure conditions for the same material also increased with increasing pressure. Comparison of the mean wear factors of these materials with previously reported data for UHMWPE and moderately cross-linked UHMWPE showed CFR-PEEK had a lower wear factor than both polyethylene materials under lower contact stress conditions (Figure 2). PEEK had the highest wear factor under all test conditions.
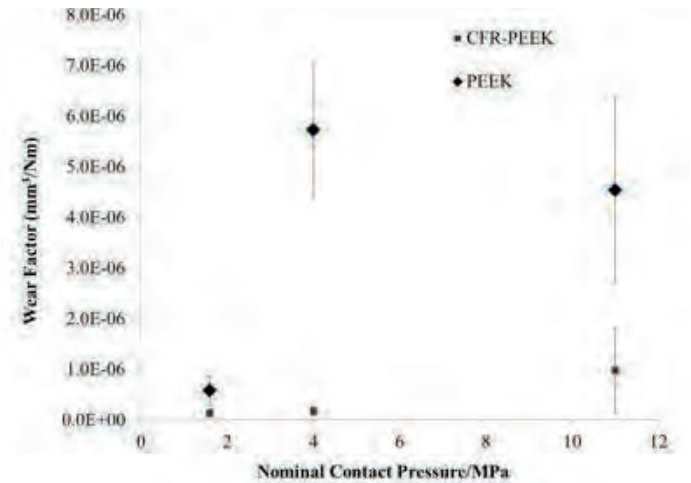

Figure 1: Effect of contact pressure on the wear factor of PEEK and CFR-PEEK materials (±95% confidence limits)
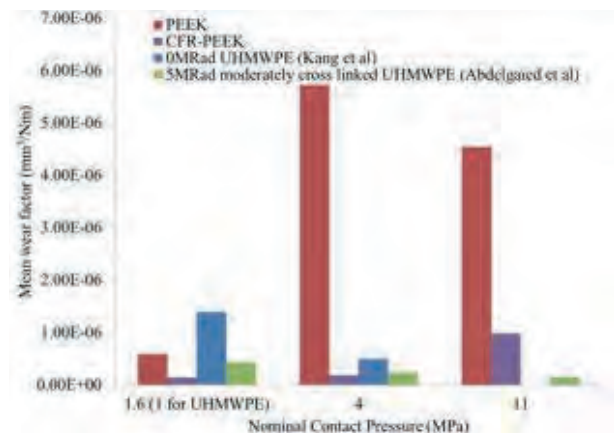

Figure 2: Comparison of wear factors from present study with previously reported studies

Discussion:
Contact pressure appears to have a significant influence on the wear of both PEEK and CFR-PEEK materials. The wear of the PEEK against a metallic counterface was higher than previously reported UHMWPE, and therefore does not indicate an advantage for application to TJR bearings such as hip or knee. The wear performance of the CFR-PEEK indicated a potential advantage compared with conventional UHMWPE, and a comparable performance with moderately cross-linked UHMWPE, suggesting it may be a suitable alternative. Further understanding of the biological response to CFR-PEEK debris is required before we can fully assess the potential clinical advantages of the material.

Characterization of Silver-PEEK Composite Biomaterials to Reduce Bacterial Adherence

Jaekel, DJ[1]; Davidson, HM[2]; Hickok, NJ[2]; Kurtz, SM[1,3]

[1]Exponent, Inc, Philadelphia PA, USA; [2]Thomas Jefferson University, Philadelphia PA, USA, [3]Drexel University Philadelphia PA, USA.

djaekel@exponent.com

Introduction: Periprosthetic infection is an infrequent yet devastating and sometimes life-threatening complication of medical device implantation [1-2]. Additionally, it is associated with increased cost, length of hospitalization, and multiple surgical interventions. While all biomaterials are prone to device-associated infection, since the early 1990s, devices comprised of polyetheretherketone (PEEK) have increasingly been used in the spine and orthopaedic device industries and, thus, their protection from infection becomes a high priority [3]. Because silver (Ag) particulates are thermally stable and have well-established antimicrobial properties [4], we examined the feasibility of creating Ag-PEEK composites with nanoAg, microAg, and Ag phosphate (Zr2K) particulates for infection control.

Methods and Materials: Three separate Ag-PEEK composites were fabricated by mixing a pellet grade of unfilled PEEK (LT1, Invibio, UK) with powder forms of a nanoAg particle (<100 nm diameter, 99.5% trace metals basis, Sigma Aldrich), a porous µAg particle (~7.5 µm diameter, Biogate HyMedic 4000, DE), and a 10% Ag-composite particle (1.3 µm diameter, Zr2k, Miliken, USA), at weight ratios of 2, 5, and 10%, respectively. The two materials were first extruded into pellets and the composites formed by injection molding the samples into tensile bars under industrially recommended settings. Unfilled PEEK (grade LT1: Invibio, UK) injection molded in the same mold was used as control samples.

All PEEK samples were sterilized prior to microbiological testing, and all studies were conducted with an osteomyelitis strain of Staphylococcus aureus (S. aureus) [5]. To assess bacterial adhesion, 6 samples of each material were incubated with an initial inoculum of 10^4 CFU/ml of S. aureus in tryptic soy broth (TSB) at 37°C for 3hr, 6hr, 24hr, and 48hrs. At each point, adherent bacteria were recovered from 4 of the samples by sonication in 0.3% Tween 20 in PBS for 5 min, plated, and quantified directly.

After testing in TSB, bacterial adhesion trials were repeated in brain heart infused media (BHI) media that ensures that differences in bacterial growth are not due to media selection. Statistical significance was evaluated using ANOVA pooled t-test (PASW Statistics version 18, IBM Corp. 2010). A p-value of less than 0.05 was used to determine significance for all tests.

Any composite groups exhibiting a significant reduction in bacterial adherence were incubated in either PBS or DI water for 25 days to measure Ag^+ elution. At regular intervals, the incubation fluid was exchanged, and Ag content was quantified with atomic absorption spectroscopy.

Ag agglomeration and deposits were investigated with light microcopy, SEM, and microCT analysis. Material density was assessed by gravimetric analysis and volume measurements from a gas pycnometer (Accupyc II 1340). Results were compared to theoretical density calculations for the composite material by the linear rule of mixtures.

Results: Incorporation of up to 5% w/w of the different Ag particles in the PEEK matrix did not cause a significant reduction in adherent bacteria (Fig 1). Repetition of the experiments in BHI media confirmed these results. When additive loading was increased to 10%, a trend towards lower surface colonization was observed, although significant reductions in bacterial counts occurred in approximately 5-6 out of 12 trials for each filler type (Fig 2A 2B) in either TSB or BHI.

For composites of all filler ratios (targets of 2, 5 and 10 w/w%), Ag particle agglomeration in masses greater than 50 µm in diameter was detected through SEM (Fig 3A), microCT (Fig. 3B), and even visually on the surface of the material. In addition, density analysis revealed an actual mass ratio of approximately 2.9-3.5% for the 5% (w/w) composites, and as low as 4.7% for the 10% (w/w) composite materials.

In Ag elution trials, nanoAg and µAg PEEK composites sustained linear and long-term release of Ag for 25 days (Fig 4); however, Zr2k-Ag composites released Ag rapidly within the first 48hrs but decreased quickly beyond 96 hours.

Discussion: Ag can be an effective bactericidal agent; however, when molded with PEEK, the anti-bacterial effects were variable and exhibited significant reduction in bacterial adhesion in 42-50% of trials. This variability was most likely caused by inconsistently low loadings and Ag particle agglomeration. Despite this, 10%Ag-PEEK displayed sustained release of Ag over 25 days at potential inhibitory concentrations for S. aureus and E. coli [6]. Future work should focus on an optimized manufacturing process for the Ag-PEEK composites to yield a uniformly dispersed material with an integrated reservoir of antibacterial agents to maintain long-term efficacy. With process optimization, the Ag content of PEEK can be tuned to achieve sustainable, bactericidal levels of Ag^+ release

References: [1] Collins et al., Euro Spine Journal 2008; [2] Calderone et al., Orthopedic Clinics of North America 1996; [3] Kurtz et al., *Biomaterials* 2007; [4] Damm et al. Journal of Biomedical Materials Research 2007; [5] Lynch et al. Annu. Rev. Med. 2008 [6] Jung et al. Appl Environ Microbiol 2008.
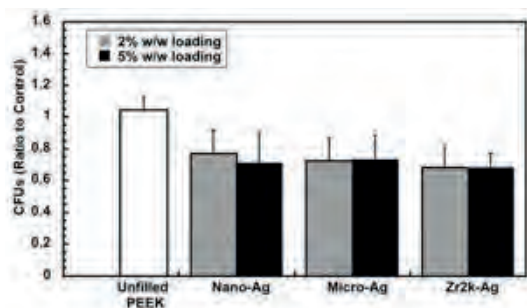
Figure 1: *48hr incubation with 2% and 5% composites exhibited no significant reduction in adherence. Results were normalized to controls after cfu were harvested from surfaces and counted*
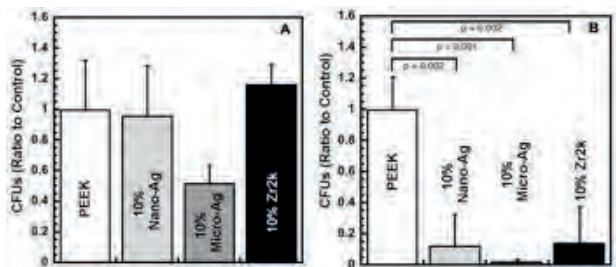

Figure 2: *48hr incubation with 10% composites show a significant reduction in adherence in trial 1 (A), but not trial 2 (B). Results were normalized to controls after cfu were harvested from surfaces and counted*
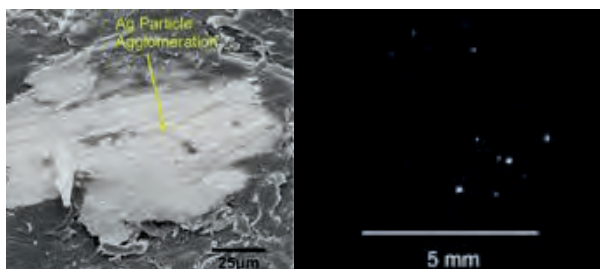

Figure 3: *Ag agglomeration can be visualized through (A) SEM imaging and (B) MicroCT on the nanoAg composites*
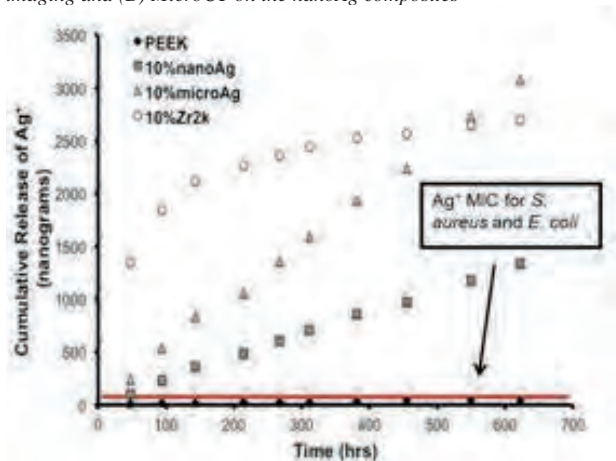
Figure 4: *Ag elution from the 10% composite materials for 25 days is displayed as cumulative mass released in PBS*

Wear factors for CFR-PEEK articulating against Biolox *delta* ceramic for increasing nominal stress

Evans A*, Horton H, Briscoe A**, Jarman-Smith M**,Simpson D***, Collins S***, Unsworth A.
School of Engineering and Computing Sciences, Durham University, UK, * Mott MacDonald, **Invibio Ltd, UK, *** Corin Ltd.
tony.unsworth@durham.ac.uk

Introduction

An interesting tribological observation when using ultra high molecular weight polyethylene (UHMWPE) sliding against stainless steel in a pin-on-plate machine is that the wear-factor reduces significantly with increased nominal stress [1]. This does not accord with the Archard wear-equation [2], but leads to interesting design issues in that less conforming contacts produce lower wear.

Recently there has been much interest shown in carbon-fibre-reinforced poly-etheretherketone (CFR-PEEK) as a biomaterial largely because the wear-rate has been shown to be only one-hundredth of that of UHMWPE in hip joint applications [3].

The current study investigated whether the wear factors for CFR-PEEK also depended on nominal stress on the contact.

Materials and Methods

A pin-on-plate machine with reciprocation and rotation was used. Pins were made from CFR-PEEK and rotated about their axes whilst the reciprocating plates were Biolox *delta* ceramic. Contact pressures ranged from 0.5 to 9.36 MPa and the pins were controlled for fluid uptake. The lubricant used was new born calf serum diluted in deionised-water to give a protein content of 18 g/l. It contained 0.2% sodium azide (NaN_3) to retard bacterial growth and 20mM of EDTA to prevent calcium deposition.

Results and discussion

Figure 1 shows the variation in wear-factor for CFR-PEEK sliding against Biolox *delta* plotted against nominal contact stress.

For contact stresses below about 5.5 MPa the wear-factor was very low and relatively constant at about 3×10^{-8} mm/Nm. This is up to 2 orders of magnitude lower than UHMWPE at these stresses and even lower than highly cross-linked polyethylene (HXLPE). However from 5.5 to 10 MPa the wear-factor increased rapidly and became erratic in its values. Indeed up to 7.5 MPa some wear results remained very low but others at a similar stress produced wear-factors which were 100 times greater than those at the lower stress and 10 times as high as UHMWPE at the same stress.

Conclusions

These results confirm the consistently low wear-rates of CFR-PEEK in situations where stresses are low to moderate such as in the hip [3] but suggest that in higher stress applications, like the knee, wear-rates may be much higher and more variable.

References

1. Vassiliou K, Unsworth A   Is the wear factor dependent on nominal contact stress in UHMWPE contacts? Proc Instn Mech Engrs **H218**,2004, 101-107.
2. Archard JF, Contact and rubbing of flat surfaces, Journal of Applied Physics, 1957,24(8) 981-988
3. Scholes SC, Inman IA, Unsworth A, Jones E, Tribological assessment of a flexible carbon-fibre-reinforced poly(ether-ether-ketone) acetabular cup articulating against an alumina femoral head. Proc. Instn Mech Engrs, Journal of Engineering in Medicine, 2008, H222, 273-283,
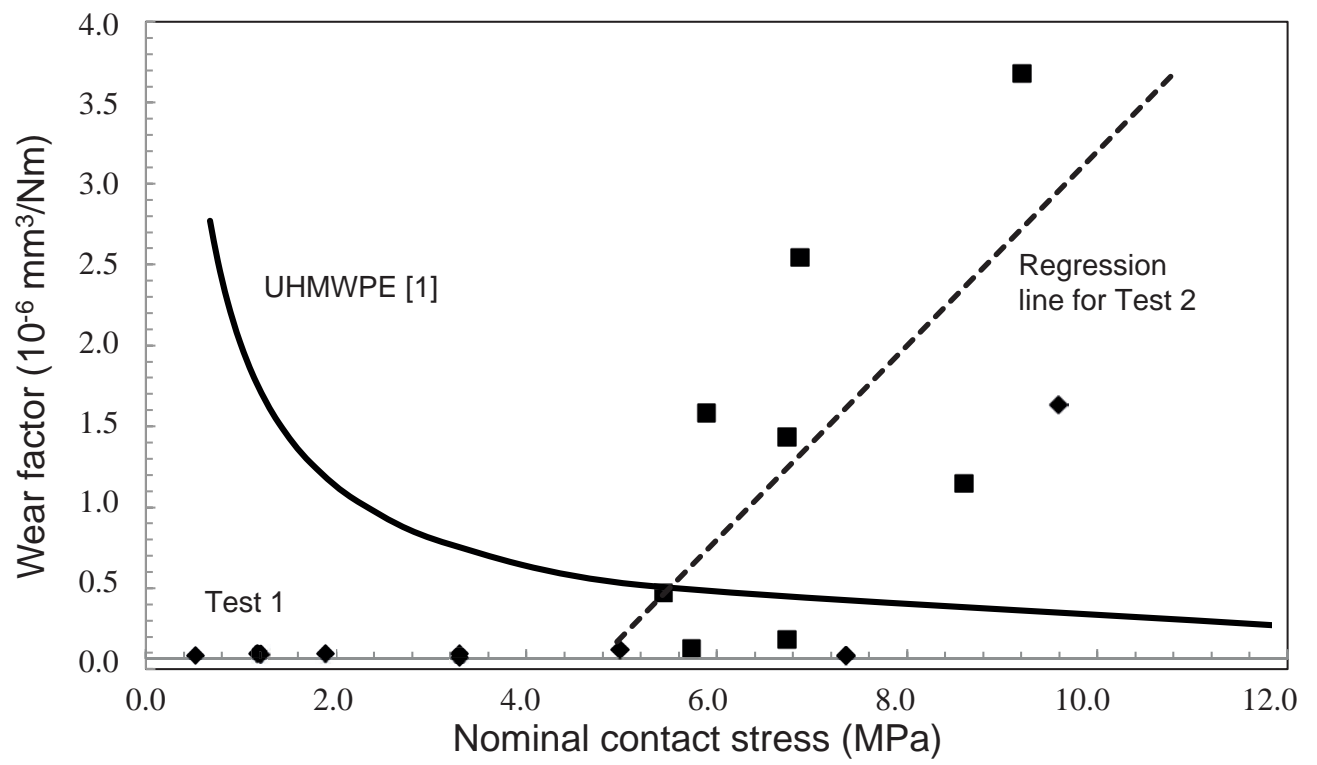
Acknowledgement

Figure 1: Wear factors for UHMWPE and CFR-PEEK.

Accelerated Neutral Atom Beam Technique Enhances Bioactivity of PEEK

Joseph Khoury, Melissa Maxwell, Raymond E Cherian, Sean R Kirkpatrick, Richard C Svrluga

Exogenesis Corp, Billerica, MA 01821

jkhoury@exogenesis.us

Introduction: Polyetheretherketone (PEEK) is continuing to gain popularity in orthopedic and spinal uses. PEEK has displaced titanium (Ti) as the predominant material in spinal applications. Ti is both biocompatible and bioactive but has a high modulus of elasticity and is difficult to image with X-rays. PEEK is biocompatible, similar in elasticity to bone, and radiolucent; however, a drawback of PEEK is it has been shown to be inert and does not integrate well with bone. Recent efforts have focused on increasing the bioactivity of PEEK by modifying the surface by adding bioactive molecules such as hydroxyapatite and calcium phosphate to improve the bone-implant interface. We have employed novel Accelerated Neutral Atom Beam (ANAB) technology to modify surfaces without adding any material onto or into the surface. ANAB employs an intense beam of cluster-like packets of accelerated un-bonded neutral argon (Ar) gas atoms. These beams are created by first producing a highly energetic Gas Cluster Ion Beam (GCIB) comprised of van der Waals bonded Ar atoms, then transferring energy to the clusters so as to cause release of most of the interatomic bonds, and finally deflecting away the remaining electrically charged cluster cores of still bonded atoms. We have shown that GCIB using argon (Ar) gas modifies a material surface to a depth less than 10nm without any subsurface damage; improving upon this, ANAB modifies material surfaces to an even shallower depth, to no more than 5nm. These modifications may lead to enhanced cell attachment and proliferation. In this study, we sought to understand the effects of ANAB treatment of PEEK surfaces in order to increase bioactivity and biointegration of implantable medical devices.

Methods and Materials: Materials used for these studies include PEEK film cut at 1cm diameter (Ø), 0.2mm thick; PEEK disks 3mm Ø, 1mm thick; Ti foil (CP1) 1cm Ø, 0.1mm thick. All materials were either left as controls or treated by ANAB using Ar gas on an Accelerated Particle Beam Alpha System (Exogenesis Corp) with a deflector to remove charged clusters. The effective dose of the Ar ANAB was 2.5×10^{17} atoms per cm^2. Atomic force microscope (AFM) measurements were performed in non-contact mode for 1µm regions (Park Systems XE-70) and R_a and R_z measurements were calculated. For proliferation studies, ANAB-treated and control PEEK film were compared to control Ti foils seeded with human osteoblasts ($2000/cm^2$) onto the surface and measured by the MTS assay at 3, 7, or 10 days and visualized by light or scanning electron microscopy (SEM). An *in vivo* study using a rat calvarial critical size defect model was done to show bone growth on the surface of ANAB-treated and control PEEK disks. Following 4 weeks after implantation into the calvarial defect, histology was performed to determine the amount of bone re-growth on the surface.

Results: AFM measurements of ANAB-treated PEEK revealed a nano-scale texturing of the surface which was not seen on controls (Figure 1). The texture is in the range of 20-50nm, however as the processing is limited to about 5nm deep, the R_a and R_z have not significantly changed. Osteoblasts growing on control Ti foils displayed significant increases from day 3 ($1,813\pm250$ cells) to day 10 ($6,880\pm420$ cells, $p<0.003$). While cells growing on control PEEK resulted in a modest increase from day 3 ($1,792\pm202$ cells) to day 10 ($2,675\pm278$ cells), ANAB treatment resulted in a significant enhancement $2,265\pm837$ cells at day 3 to $7,830\pm700$ cells at day 10, $p<0.003$ as compared to control.
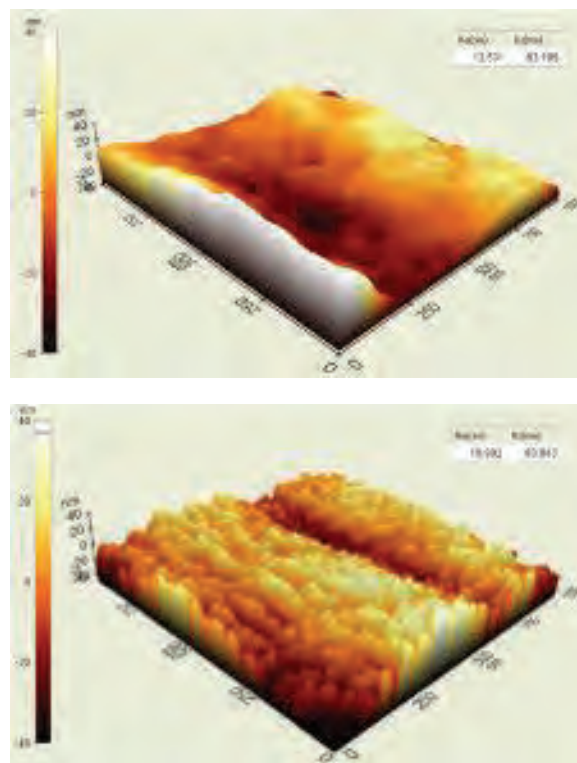

Figure 1. ANAB-treated PEEK (lower panel) results in a nano-textured surface of approximately 20-50nm as compared to controls (upper panel).

The rat calvarial defect model showed that ANAB-treated PEEK resulted in a bone ledge growing on top of the disk covering approximately 50% of the surface whereas the control PEEK resulted in only fibrous tissue with no bone growth at all. The controls displayed the start of bone resorption on the sides of the disks whereas good bone purchase is seen on the GCIB-treated disks (Figure 2).
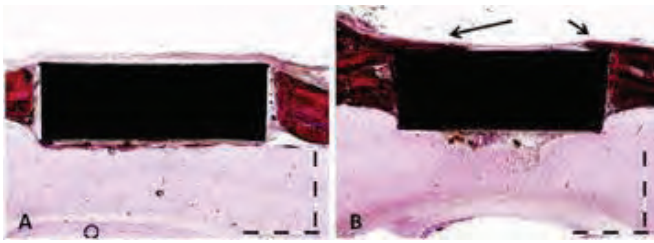
Figure 2. Rat calvarial defect model using A) control and B) ANAB-treated PEEK disks. Four weeks following implantation, control disks display fibrous tissue formation on the surface with the start of bone resorption. ANAB-treated disks display bone tissue formation (arrows) covering nearly 50% of the surface. Bar represents 1mm.

Discussion and Conclusions: ANAB treatment of PEEK results in enhanced osteoblast attachment and proliferation as evidenced by our cell proliferation study. In fact, ANAB-treated PEEK enhanced cellular attachment and proliferation greater than was seen on control Ti which is considered to be bioactive. This enhancement is due, in part, from the resulting nano-texturing on the PEEK surface. Many studies have shown the benefits of nano-texturing on various materials ranging from metals to polymers. However, due to the stability and chemical resistance of PEEK, most methods used to create the nano roughness on other materials would not work on PEEK. ANAB, which utilizes highly energetic Ar atoms, does not result in the addition of any material or any chemical changes in the surface. This enhanced surface as demonstrated in our *in vitro* results has prompted us to verify if ANAB would result in better integration between PEEK and bone. Enhanced osseointegration was demonstrated in the *in vivo* study where bone tissue formation and good bone purchase was evident only on the ANAB treated PEEK. Taken together, these data suggest that ANAB treatment of PEEK has the potential to increase bioactivity of the surface and result in enhanced bone formation and significantly decrease osseointegration time of orthopedic implants.

The Immune Response to Bacterial Contamination of Orthopaedic Implant Materials

ETJ Rochford[1,2], TF Moriarty[1], K Kluge[1], S Zeiter[1], , L O'Mahony[3], M Ziegler[3], RG Richards[1,2], AHC Poulsson[1]

[1]AO Research Institute, AO Foundation, Davos, CH. [2]IBERS, Aberystwyth University, UK, [3]Swiss Institute of Allergy and Asthma Research (SIAF), University of Zurich, CH

spoulsson@gmail.com

Introduction: The presence of any implant compromises local host immune responses and increases infection risk[1]. Previously it has been shown that implant materials can alter the immune response, which subsequently may influence infection risk[2]. In this study, a range of orthopaedic biomaterials have been examined to identify the role of material choice in the immune response to infection *in vitro*.

Methods and Materials: The following materials were used in this study to compare different surface chemistries and topographies: micro-rough titanium (TS), electropolished titanium (TE), Titanium-Aluminium-Niobium (NS), electropolished Titanium-Aluminium-Niobium (NE), stainless steel (SS)[a], injection moulded polyetheretherketone(PEEK) (PO), machined PEEK (PA) and oxygen plasma treated PO (PO30) and PA (PA30)[b] as previously described[3]. For experiments requiring adherent bacteria, approximately 2×10^5 Staphylococcus aureus JAR cm^{-2} were adhered to the materials using a bacterial adhesion chamber[3]. All experiments were performed in triplicate. The activation of complement by the materials with and without pre-adhered S. aureus JAR was assessed by exposing the samples to human serum for one hour and measured using a C3a-desArg ELISA. THP-1 monocyte cells were used to screen for NF-κB activation by the materials using the Quanti-blue assay with and without additional lipopolysaccharide (LPS) stimulation. Additionally, peripheral blood mononuclear cells (PBMC) were isolated from healthy donors and exposed to the materials, the materials and LPS or the materials pre-contaminated with S. aureus JAR for 48 hours. The PBMC were harvested for real-time PCR and samples of the cell media taken for multiplex analyte detection by Bioplex. The Bioplex screened for IL-8, IL-10, IL-12(p70), TNF-α, MIP-1α and G-CSF.
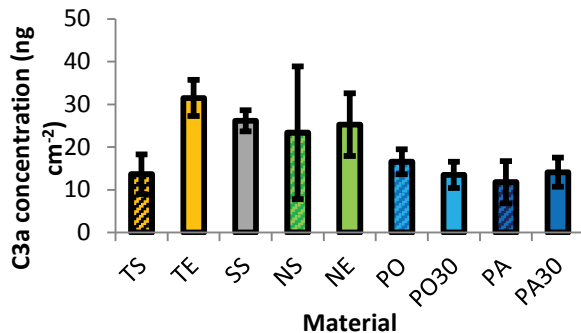

Fig.1: Complement activation by the different materials without additional stimulation (n=3, ±s.e). TS and the PEEK materials induced the lowest level of complement activation. The other metals induced an increased level of complement activation.

Results: In general, TS produced the lowest level of immune-activation as illustrated by the complement (Fig.1), NF-κB and cytokine assays in the absence and presence of bacteria. However, in the presence of additional bacterial stimulation TS gave similar results as the other metals for complement activation and NF-κB stimulation. In contrast, PEEK was generally the most immune-stimulatory of the materials; increasing complement activation, NF-κB, IL-12 and TNF-α secretion. Interestingly, oxygen plasma treatment led to increased complement activation (Fig.1), TNF-α and IL-12 production, but decreased NF-κB stimulation in the presence of bacteria and LPS. MIP-1α secretion was dependent on the material, though no clear trend for material classes could be identified (Fig.2).
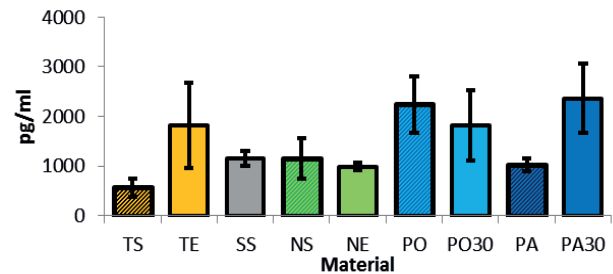

Fig.2: MIP-1α secretion by PBMCs exposed to the materials coated with S. aureus JAR (n=3, ±s.e.).

Discussion: The main differences in the immune response appear to be surface chemistry driven, particularly between TS and PEEK. TS was often the least immune-stimulatory of the materials, which may be a reflection of the biocompatibility of this material. In the presence of additional bacterial stimulation, TS gave a similar response as the other metals which may benefit removal of contaminating bacteria. In contrast, surface roughness did not have a consistent effect on the immune response. To further elucidate this and how these differences affect the immune response to bacterial contamination of an implant in a trauma wound an *in vivo* investigation is currently underway. The focus *in vivo* is on the immune response to titanium and PEEK, as these materials showed the greatest difference *in vitro*. The existing MouseFix internal fixation plate model for bone healing has been adapted to include pre-operative contamination of the implants by S. aureus bacteria. **References:** 1. Elek, S. and Conen, P. (1957) Br.J.Exp.Pathol. 38:573-586. 2. Boelens, J.J., et al. (2000) J Infect.Dis 181:1337-1349. 3. Rochford, E.T.J., et al. (2011) ESB2011.**Acknowledgements:** [a]Metal samples provided by Synthes, [b]PEEK samples provided by Invibio Biomaterial Solutions.

The Effect of Surface Roughness on the Fatigue Behavior of PEEK

N. Evans[1], D. Whittingslow[2], R. Carson[3], D. Safranski[1,4], PhD, D. McDowell[1,3], PhD, K. Gall[1,3], PhD

[1]School of Materials Science and Engineering, Georgia Institute of Technology, [2]School of Biomedical Engineering, Georgia Institute of Technology, [3]School of Mechanical Engineering, Georgia Institute of Technology, [4]MedShape Solutions, Inc., Atlanta, GA

ken.gall@mse.gatech.edu

Introduction: Polyetheretherketone (PEEK) is widely used in medical devices, especially in orthopedics. PEEK is a semi-crystalline polymer that combines chemical and hydrolytic inertness, resistance to the effects of ionizing radiation, high strength, and good tribological properties with favorable biocompatibility. Because it is a thermoplastic, it can be easily processed into complex implant shapes. PEEK can also be repeatedly sterilized using conventional steam, gamma, and ethylene oxide processes without significant deterioration. PEEK also closely matches the modulus of human bone making it ideal in various orthopedic applications. However, because PEEK is inert and non-porous, the material has relatively lower cell adhesion and lack of cellular ingrowth. Several studies are currently looking to improve the long term adhesion and function of PEEK implants by improving the osseointegration of PEEK. It has been shown that there is a correlation between average roughness of Titanium implant surfaces and bone apposition, pushout failure load, and growth factor release by osteoblasts [1-3]. Sagomonyants et. al showed that even machined versus injection molded PEEK samples showed significantly different response *in vivo* [4]. Though these relate surface roughness with improved osseointegration, it is unknown if there is a trade-off in mechanical properties, specifically fatigue. The authors seek to determine the effect of surface roughness on the fatigue life of PEEK and hypothesize that there will be a decrease in the endurance limit but that it will meet the *in vivo* demands. The fatigue behavior of PEEK is also compared to PMMA, a common clinical biomaterial.

Methods and Materials: Injection molded Zeniva® PEEK ZA-500 tensile samples were provided by Solvay Specialty Polymers. Samples were sanded in axial or transverse directions relative to the axis of loading. An electric hand sander was used to sand approximately 0.1 mm off of each side followed by a hand sand to provide uniform finish and grain orientation. 50 and 120 grit sandpaper were used to create varying levels of roughness. PMMA tensile samples were made by laser cutting samples from a PMMA sheet (McMaster-Carr).

Before performing the fatigue study, strain-to-failure tensile tests were run on the sanded and as received samples to determine the stress-strain behavior. Fatigue tests were then run on sanded samples at increasingly lower stresses below the ultimate stress of the samples to generate S-N curves and determine the endurance limits. The fatigue tests were performed in air in a servo-controlled, hydraulically actuated fatigue machine in axial stress control at a frequency of 1Hz (Satec). Tests were run until failure or runout. Runout is defined as greater than 100,000 cycles. One as-received sample was run to 1,000,000 cycles.

Results: The average ultimate tensile strength and failure strain (elongation) of the as-received and sanded samples is shown below in Table 1.

Table 1 Comparison of average ultimate tensile strength (UTS) and failure strain for the different samples

Sample	UTS (MPa)	Failure Strain (%)
As Received	97.74 ± 0.99	39.44 ± 4.08
Axial 50 Grit	99.33 ± 1.14	41.50 ± 12.46
Transverse 50 Grit	91.19 ± 1.09	23.89 ± 4.71

As shown in the table, the as-received and axially sanded 50 grit samples were not statistically different in their ultimate stress or failure strain behavior. The transversely sanded 50 grit samples did show a significant decrease in both their ultimate tensile strength and strain capacity. Note that the 120 grit sanded samples did not show any significant difference in their tensile behavior from the 50 grit sanded samples and were not tested further. Only the 50 grit sanded samples, producing the more severe sanding and therefore roughness, were tested in fatigue. Representative stress-strain curves are shown below in Figure 1.
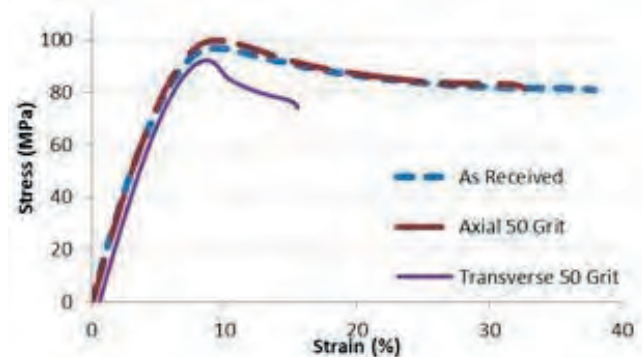

Figure 1 Representative stress-strain curves for as-received, axially sanded 50 grit, and transversely sanded 120 grit tensile samples.

After determining the tensile strength of the samples, fatigue tests were performed at increasingly lower stresses below the ultimate tensile stress. The S-N curves are shown below in Figure 2.
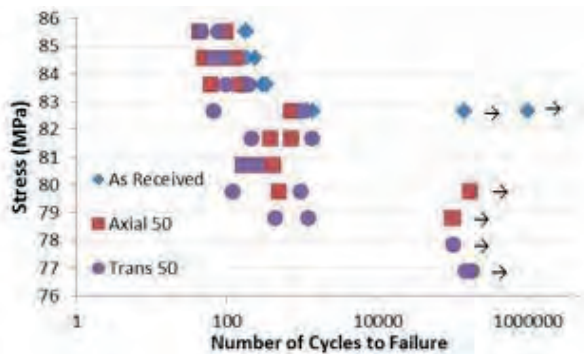
1

Figure 2 S-N plots comparing fatigue life curves of as-received, axially sanded 50 grit, and transversely sanded 120 grit tensile samples. Arrows indicate "runout".

As shown in the Figure 2, the fatigue curves for the axially and transversely sanded samples are shifted down relative to the as-received samples. The endurance limit for the as-received samples is 82.6 MPa (84.6% of UTS), 79.8 MPa (80.3% of UTS) for the axially sanded 50 grit samples, and 77.8 MPa (85% of UTS) for the transversely sanded 50 grit samples.

To compare the fatigue behavior of PEEK with another commonly used orthopedic biomaterial, we also studied the fatigue behavior of PMMA. First, strain to failure was run on PMMA tensile samples. Figure 3 below compares the stress-strain curves of PEEK and PMMA.
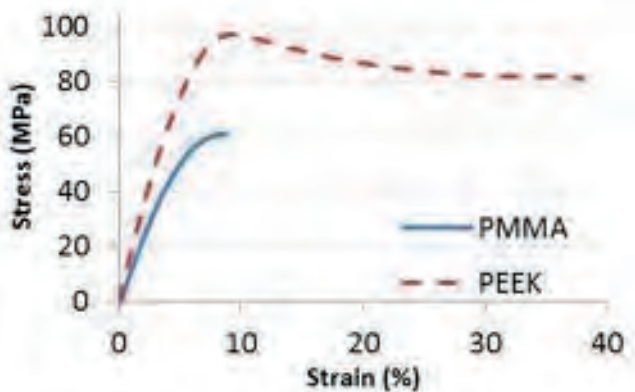
Figure 3 Representative stress-strain curves for as-received PEEK and as-received PMMA.

The average ultimate tensile strength of the PMMA is 61.08 ± 0.85 MPa with an average elongation (strain at failure) of $11.03 \pm 1.98\%$. The fatigue behavior of PMMA is shown below in Figure 4 with the as-received PEEK.
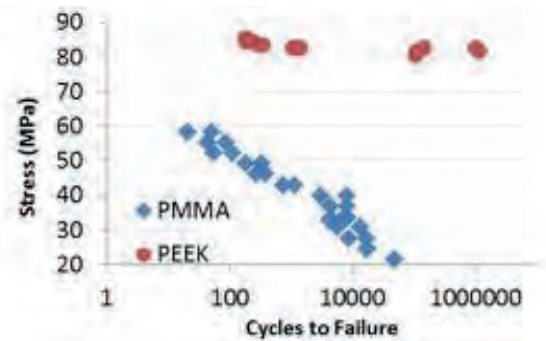

Figure 4 S-N plots comparing the fatigue life of as-received PMMA and as-received PEEK.

As shown in Figure 4, PMMA does not appear to be approaching an asymptote signaling an endurance limit but continues to show a decrease in fatigue life with increased stress.

Discussion: PEEK is widely used in orthopedic applications in which integration with the bone and surrounding tissue is advantageous if not critical. However, due to PEEK's inertness and lack of porosity, it suffers from low cell adhesion and cellular ingrowth. It has been shown in prior work that increased surface roughness leads to improved osseointegration but the effect of surface roughness on fatigue was previously unknown. Here the authors study the effects of surface roughness on the fatigue life of PEEK by sanding tensile samples and then running fatigue tests on them. It is shown that PEEK has exceptional fatigue properties, approaching an endurance limit at 85% of its ultimate strength. It was also shown that sanding does influence the fatigue life of PEEK but not detrimentally so. In both axially and transversely sanded samples, the curves are shifted down meaning that the samples fail at a lower number of cycles at the same stress compared to as-received samples. The transversely sanded 50 grit samples, serving as the "worst case", still had excellent fatigue life with an endurance limit at 77.84 MPa. PMMA has a much poorer fatigue life as there does not appear to be a distinct endurance limit but rather the decrease in stress capacity with increased number of cycles. PEEK is therefore an excellent choice for cyclic load bearing applications. The results indicate that some surface texturing may be used to increase osseointegration without a significant decrease in the fatigue life of the PEEK.

References: [1] Shalabi et al, *Journal of Dental Research*, 2006 [2] Wong et al, *Journal of Biomedical Materials Research,* 1995 [3] Kieswetter et al, *Journal of Biomedical Materials Research,* 1996 [4] Sagomonyants et al, *Biomaterials,* 2008

2

Detection of Thermally Stimulated Luminescence in PEEK

M. S. Jahan, D. Adhikari and B. M. Walters
Department of Physics, The University of Memphis, 216 Manning Hall, Memphis TN. 38152, USA
mjahan@memphis.edu

INTRODUCTION: Thermally stimulated luminescence (TSL), also known as thermoluminescence (TL), has been applied by many to understand the mechanisms for emission of light or luminescence in polymers [1]. Jahan et al. used TSL to investigate aging of orthopedic polyethylene (ultra-high molecular weight polyethylene (UHMWPE)) following gamma-sterilization in air and subsequent storage in air, liquid N_2 or saline solution [2]. TSL has been primarily attributed to recombination of trapped charges in voids and/or imperfections or radicals in a polymer matrix [3]. Thermally stimulated chemiluminescence (TSCL) can also produce luminescence when certain molecular species undergo chemical reaction (in solid state) as a result of heating. In this study, we have detected, for the first time, thermally stimulated luminescence in virgin as well as irradiated PEEK.

MATERIALS AND METHODS: 10 mil. (0.254 mm) Victrex® PEEK film was used for this study. TSL samples, each of size 2x2 mm^2 and mass 1.4-1.6 mg were placed in TSL pans (a DSC pan without top) for testing. TSL measurements were performed using a commercial dosimeter (Harshaw QS 3500) in which the heating chamber was continuously purged with dry, filtered N_2. The samples were heated from 30°C to 300°C at a rate of 1°C/s, and the resulting TSL intensity (glow curve) was recorded as a function of temperature using a WinREMS software interface. TSL glow curves were also recorded following UV- and X-irradiations of the PEEK samples. UV-irradiation was performed using a broad-band ultra-violet-visible (UV-Vis) lamp (250 Watt, Oriel® 688 10 Arc Lamp). For X-irradiation, an X-ray source (Scientific America), operating at 50 kV and 45 mA, was used. To check the effects of preheat on TSL, samples were preheated in air for 10 minutes at specific temperatures between 50°C and 340°C to check if the luminescence centre or the luminescence-producing species can be quenched or annealed.

RESULTS AND DISCUSSION: As shown in Figure 1, the glow curve of the non-irradiated (as-received) PEEK exhibits a glow peak at 150°C, and when the TSL run was repeated on the same sample without removing it from the heating compartment, the peak disappeared (pink line). This test suggests that the TSL-producing species present in the sample disappeared, recombined or converted to neutral species after producing the first glow or TSL.

When non-irradiated PEEK samples were first preheated before TSL measurements at temperatures less than 150°C, no significant changes in the glow peaks were observed (not shown in the figure). However, as the preheat temperature increased to 200°C or greater a new peak appeared at 75°C. Shown in Figure 1 (b) are the glow curves recorded following pre-

heats at 280°C (green line) and 320°C (red line). Similar, but more intense TSL was observed in UV- and X-irradiated PEEK.
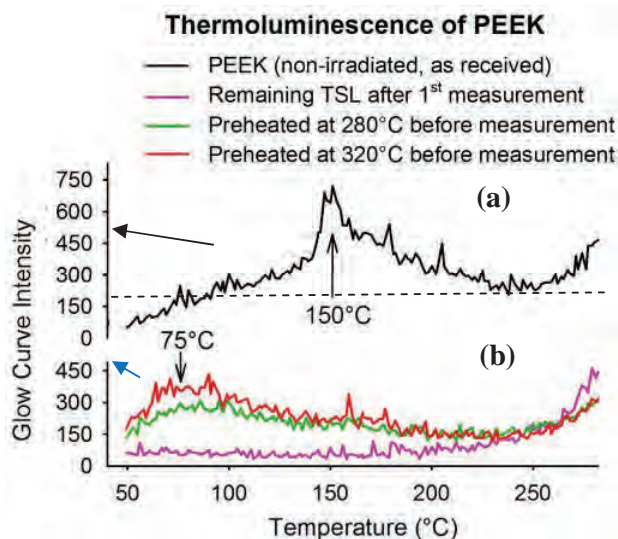

Figure 1. (a) TSL glow curve observed in PEEK before irradiation. (b) Glow curve observed (pink line) when the same sample was retested after the first TSL as in (a); glow curve for a sample preheated for 10 minutes at 280°C (green line) and 320°C (red line).
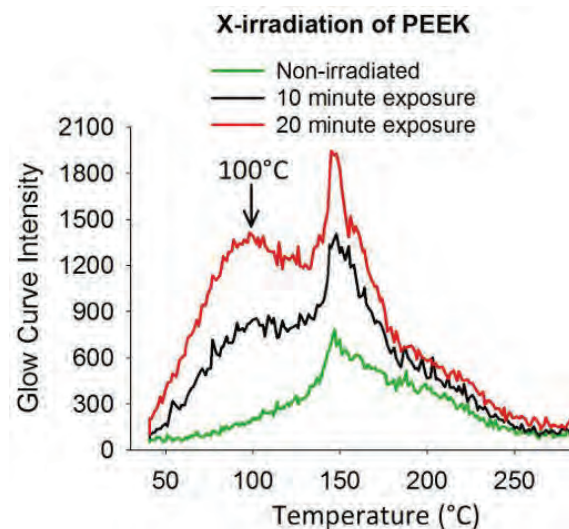

Figure 2. TSL of PEEK which was X-irradiated for 10 minutes (black line) and 20 minutes (red line), as compared to as-received PEEK (green line).

Figure 2 shows TSL glow curves recorded after X-irradiation for 10 (black) and 20 (red) min. For an illustrative purpose, the glow curve for a non-irradiated

PEEK (green) is also shown in the figure. While the 150-°C peak is present in all glow curves, a new peak near 100°C appears in the glow curves of the X-irradiated PEEK. However, the 100-°C peak was not apparent in the TSL glow curve recorded following UV irradiation (uncalibrated dose), though the 150-°C was present and the total luminescence increased as a function of UV exposure. In another study, radicals were detected in UV- or X-irradiated PEEK. Although it would be speculative at this time, the 100-°C peak could be associated with the radiation-induced PEEK radical and the 150-°C peak with the glass transition temperature (143°C [4]) of PEEK.

SUMMARY: We report, for the first time, TSL in non-irradiated (as-received), UV- and X-irradiated, and pre-heated PEEK. The TSL glow curve in non-irradiated PEEK exhibits a peak near 150°C. More intense glow is, however, observed in UV- or X-irradiated PEEK with an additional peak near 100°C. In pre-heated PEEK, heated above 200°C, weak glow with a peak near 75°C is produced. Analysis of TSL glow curves, which is in progress, is expected to shed light on thermally stimulated solid state chemistry in PEEK.

REFERENCES:
1. Partridge R. H. *The Radiation Chemistry of Macromolecules*. Vol. 1, Chap. 10. 1972.
2. Jahan *et al*. *J. Luminescence* 40/41, 242. 1988.
3. Fleming RJ, *Radiat Phys Chem* **36:**59 (1990).
4. Y. Lee and R. S. Porter, *Macromolecules* 20, 1336-1341, 1987.

Structure-Property Relationships for PEEK Powder-Reinforced UHMWPE
Kocagöz, Sevi[1]; MacDonald, Daniel[1]; Kurtz, Steven M.[1, 2]
[1]Drexel University, Implant Research Center, Philadelphia, PA
[2]Exponent, Inc. Philadelphia, PA.

Introduction: The main mechanism that leads to particulate generation and failure due to osteolysis in UHMWPE orthopedic implants is adhesive/abrasive wear of the articulating surface [1]. Cross-linking ultra-high molecular weight polyethylene UHMWPE significantly reduces wear and failure due to osteolysis; however, crosslinking by irradiation or chemical processes causes other mechanical properties (such as impact resistance) to become compromised [2]. UHMWPE matrix composites offer a good alternative to improving wear while preserving other mechanical properties such as impact resistance and tensile strength. UHMWPE fiber and matrix composite materials have commercial success in non-medical applications [3] and have been used in the past clinically for total joint replacements[4]. Candidates for reinforcing fillers include poly(ether-ether ketone) (PEEK), a biocompatible polymer already being used in a variety of biomedical applications [5]. PEEK is a thermoplastic that possesses a resonance-stabilized, aromatic structure allowing PEEK and its composites to exhibit long-term stability in vivo and not get affected by repeated exposures to steam or gamma radiation sterilization[6]. Additionally, PEEK has excellent mechanical properties[7]. In this study, we investigate the mechanical properties and fracture surface of PEEK filled UHMWPE composites and compare it to unfilled UHMWPE. Additionally, we investigate the effect of cross-linking through irradiation and the addition of vitamin-E on the mechanical properties of the materials.

Materials and Methods: A commercially relevant heat-pressure compression molding cycle [8] was used to make samples of 4 types of composites and 2 unfilled materials. 1020 and 1020E GUR resin UHMWPE and 450PF PEEK powder (Invibio) was used. The materials manufactured for this study are 1020 GUR resin UHMWPE unfilled, with 5%/w PEEK, with 15%/w PEEK and 25%/w PEEK; 1020E GUR resin UHMWPE unfilled and with 15%/w. 4 compression molded specimens (cylinders with 2.5in diameter and 1.5in height), as seen in Figure 1, were made for each material. 2 compression molded samples for each material was irradiated using E-beam 100kGy resulting in 12 different material conditions in total. Izod Impact Tests: 5 test samples of each composite as well as each control condition was machined, notched, and tested according to ASTM F648-10a. Uniaxial tensile bars (Type V ASTM 638-08) were machined from the compression-molded composites and tested in accordance with ASTM 638-08 at 10mm/min crosshead speed. At least four samples were tested for each composite as well as the samples for each control condition. Video extensometer was used for measuring the gauge length during the tensile test. Fractography was performed using Scanning Electron Microscope (Zeiss Supra 50VP) on freeze fractured and impact fractured surfaces.

Figure 1: PEEK fiber reinforced GUR1020 resin HXLPE with 5, 15 and 25%/w PEEK fibers and GUR 1020E with 15%/w.

Results: Tensile tests showed that the yield strength does not show significant variation between the different materials (minimum 15.38MPa for 1020 25%/w PEEK 0kGy, maximum 24.04MPa for 1020E Neat 100kGy) (Figure 2). The ultimate tensile strength and toughness decreases significantly with increasing filler percentage (Figures 3 and 4). The impact energy also decreases with increasing filler percentage (Figure 5). The fractography of fracture surfaces display more brittle fracture as the amount of filler in the composite is increased. The ductile rip seen in the freeze fractured and impact fractured
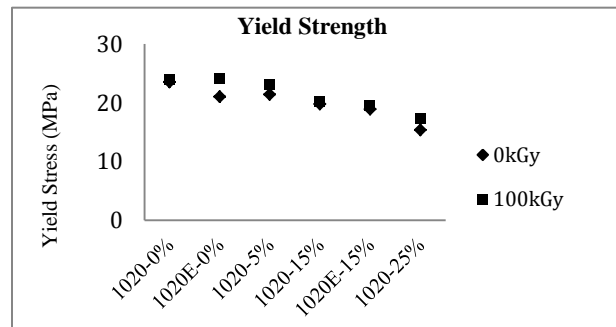

Figure 2: Plots for yield strength for 0kGy and 100kGy filled composites.
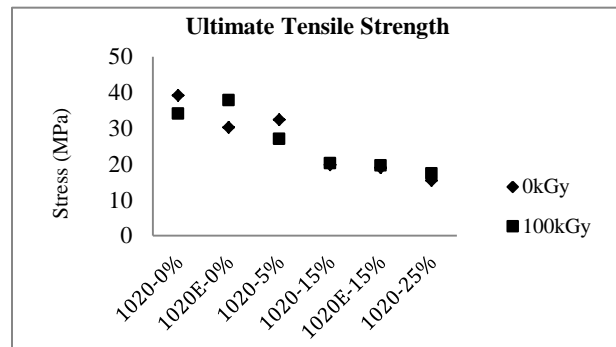

Figure 3: Plots for ultimate tensile strength for 0kGy and 100kGy filled composites. Decrease in strength is observed with increase in filler percent.

surfaces of neat 1020 and 1020E GUR resin is not seen in the composites with PEEK filling. Failure in the

composite materials is seen at the UHMWPE matrix and PEEK particle interface with mixed mode slow and fast crack growth at the matrix (Figure 5 and 6). Poor consolidation between the UHMWPE matrix and PEEK particles is seen in both 0kGy and 100kGy specimens.

Discussion: The addition of PEEK powder as a reinforcing filler did not improve the impact energy and the toughness of UHMWPE. Increasing filler amount led to a deterioration of mechanical properties and enhanced brittle behavior. Further investigation of the structure-property relationship of the matrix-filler interface will enable manufacturing composites with better consolidation and better impact resistance.
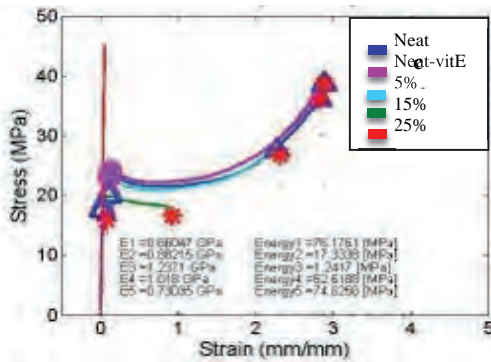
Figure 4: Tensile stress-strain curves for 100kGy samples. Pink circles: point of yielding, blue triangles: ultimate strength, red stars: fracture point. GUR 1020 neat (navy blue), GUR 1020E Neat (pink), 1020 w/ 5% PEEK (light blue), 15% (green), 25% (red).
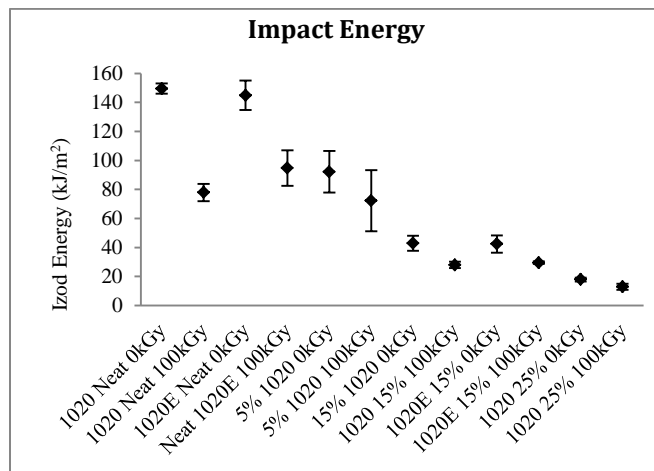

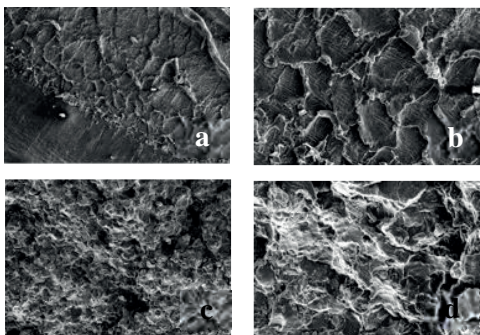Figure 5: Plot of impact energies of composites and controls.

Figure 5: 1020 Neat 0kGy a) 50x, b) 150x. Ductile fracture with polyethylene tearing. Slow crack growth in the pockets is seen as striations perpendicular to the crack growth direction. 1020-15%-0kGy c) 50x. d) 150x shows fracture around PEEK particles.
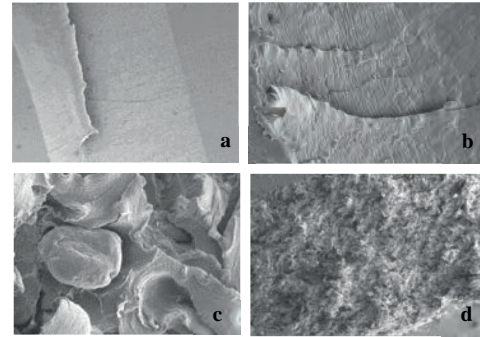

Figure 6: GUR 1020 Neat 100kGy, a) 15x. b) 500x. GUR 1020 w/ 15%/w PEEK c) 30x , d) 500x. (a) and (b) depict ductile fracture, b) displays slow crack propagation (left) before tear. c) and d) display ductile tearing of UHMWPE matrix around exposed PEEK particles.

1. Gul, R.M., et al., *Effect of consolidation on adhesive and abrasive wear of ultra high molecular weight polyethylene.* Biomaterials, 2003. **24**(19): p. 3193-9.

2. Plulee, K. and C.J. Schwartz, *Improved wear resistance of orthopaedic UHMWPE by reinforcement with zirconium particles.* Wear, 2009: p. 710–717.

3. Kurtz, S.M., *The UHMWPE Handbook: Ultra-high Molecular Weight Polyethylene in Total Joint Replacement*2004, Amsterdam: Elsevier Academic.

4. Li, S., *Ultra-High Molecular Weight Polyethylene: From Charnley to Cross-linked.* Operative Techniques in Orthopaedics, 2001. **11**(4).

5. Kurtz, S.M. and J.N. Devine, *PEEK biomaterials in trauma, orthopedic, and spinal implants.* Biomaterials, 2007. **28**(32): p. 4845-69.

6. Kurtz, S., *PEEK Biomaterials Handbook*2012: Elsevier.

7. Xiong, D., L. Xiong, and L. Liu, *Preparation and tribological properties of polyetheretherketone composites.* J Biomed Mater Res B Appl Biomater, 2010. **93**(2): p. 492-6.

8. Ramani, K. and N.C. Parasnis, *Process-Induced Effects in Compression Molding of Ultra-High Molecular Weight Polyethylene (UHMWPE).* Characterization and Properties of Ultra-High Molecular Weight Polyethylene, 1998. **ASTM STP 1307**: p. 5-23.

Evaluation of Porous PEEK and PEEK/ TCP Scaffold Candidates using Microscopy, µCT, and SEM

Sevit, AS[1]; Jaekel, DJ[2]; MacDonald, DM[1]; Day, JS[1,2]; Kurtz, SM[1,2]
[1]Drexel University, Philadelphia, USA; [2]Exponent Inc.
as3437@drexel.edu

Introduction: Macro-porous biomaterials are advantageous in orthopedic applications because they allow bone ingrowth and can become well fixed to adjacent bone. Polyetheretherketone (PEEK) is a bio-inert polymer with mechanical properties closely resembling that of bone, reducing stress shielding that is incurred with conventional metal implants. Macro-porous PEEK is thus an attractive biomaterial option for many orthopedic and spinal applications. A porous PEEK-tricalcium phosphate (TCP) composite could further promote osseointegration because of TCP's osseo-conductive properties. Comprehensive characterization of porous PEEK/ PEEK-TCP composites is necessary to optimize these biomaterials for specific orthopedic applications.

Methods/ Materials: Three different processing techniques were assessed in this study. All samples were fabricated from PEEK to produce either a porous or composite matrix. The samples were received directly from the manufacturer (Invibio Biomaterial Solutions, UK). All samples were prepared via a combination of compression molding and particulate leaching. Samples PEEK-1, PEEK-2, and PEEK-3 were all fabricated using the same-sized NaCl particles (1-1.4mm diameter). They were cold compressed for various durations (20 mins to 1hr) and all utilize varying ratios of PEEK to salt. PEEK-4 was made using smaller salt particles (.5-1mm) and was also cold compression. Samples PEEK HC-1 and PEEK HC-2 were fabricated in a similar way to the other PEEK samples, however, a hot-compression step was added which more homogeneously mixed the salt and PEEK giving the samples their white appearance. Salt was not leached out of HC1, but was leached out of HC2. Samples PEEK/TCP-1 and PEEK/TCP-2 were both fabricated using particles of TCP instead of NaCl. The TCP was not leached out of the material, leaving the TCP within the PEEK matrix. Samples are depicted in figure 1:
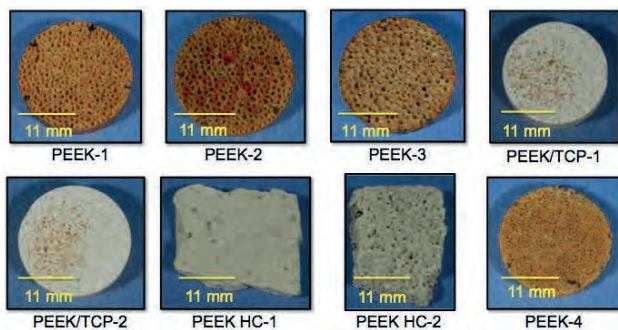

Figure 1: All samples analyzed and their compositions.

Samples were µCT scanned using a Scanco µCT 80 (.01mm voxel resolution) to analyze pore size, strut thickness, solid volume fraction, degree of anisotropy, and connectivity density. The volume of analysis had minimum dimension of 5mm in length, width and height. The surface morphology of each sample was then assessed using optical microscopy and scanning electron microscopy (SEM).

Results: µCT scans of the samples revealed the porosity of the PEEK samples (PEEK-1, PEEK-2 and PEEK-3) ranged from 83% to 88%, while the average porosity was 92% in the PEEK HC samples. The PEEK/TCP composites (PEEK/TCP-1 and PEEK/TCP-2) were not porous, showing no distinguishable empty space within the material. However, the µCT was able to distinguish between PEEK and TCP because of their varying densities. For the purposes of analysis, the PEEK phase was defined as positive space (struts) and the TCP phase was defined as negative space (pores). The percentage of TCP in both of the composites was approximately 90.5%. Sample PEEK-4 could not be analyzed using µCT. Because of a thick layer of solid polymer on the bottom of the sample, it was impossible to measure a porous region that was the minimum volume necessary for valid analysis. Pore and strut size distributions for all samples are displayed in figures 2 and 3 respectively.
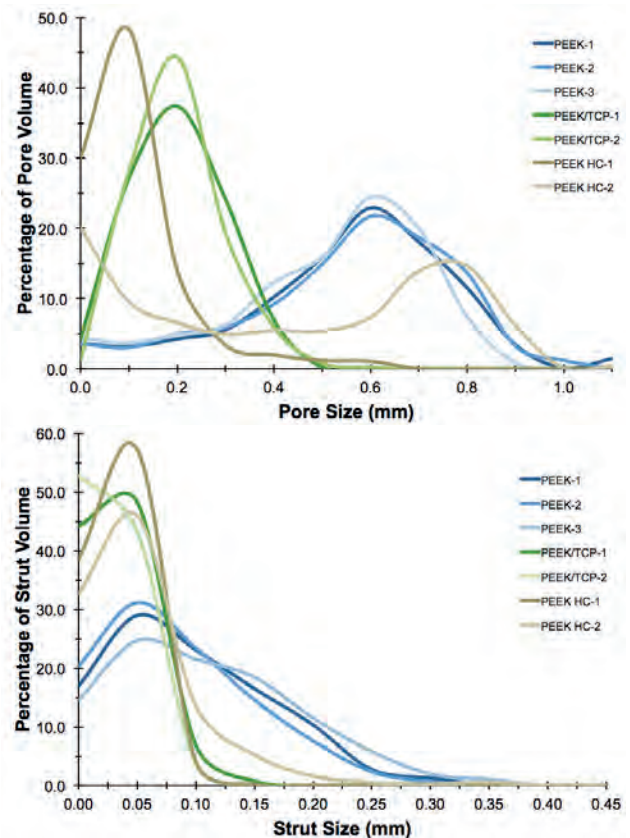
Figures 2 and 3: Pore and strut size distributions respectively.

The porous PEEK samples had a pore size distribution centered around 0.6 mm and had significantly larger pores than PEEK HC-1, and the PEEK/TCP composites. PEEK HC-2 appears to have a bimodal pore size distribution. Strut size is more widely distributed in the PEEK matrixes in contrast to the composites and TCP matrixes. The difference in average pore size between samples is best-depicted using the three-dimensional visualization shown below.
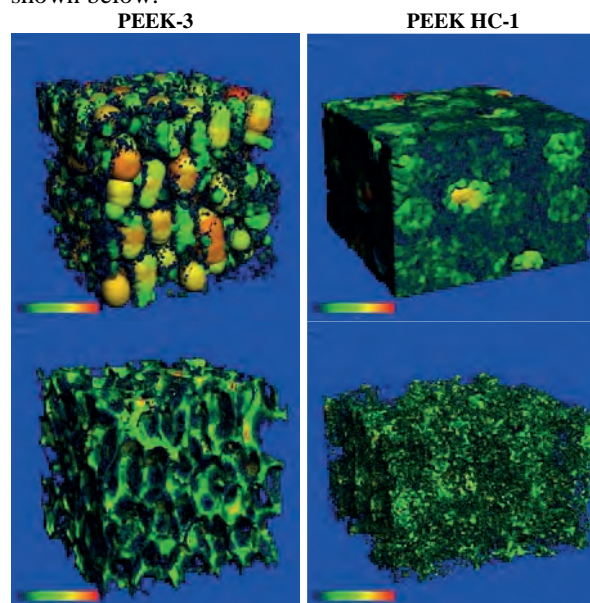
PEEK-3 **PEEK HC-1**

Figure 4: Three-dimensional pore visualization of PEEK-3 and PEEK HC-1 (top row). Three-dimensional strut visualization of the same samples (bottom row).

PEEK samples and composite samples all had a degree of anisotropy of approximately 1.5 (a degree of anisotropy of 1 corresponds to a perfectly isotropic material). The PEEK HC matrixes were more isotropic at approximately 1.1. Assessment of connectivity of the solid phase of all of the materials revealed that the PEEK HC samples were significantly more interconnected than the composite samples and the porous PEEK matrixes.

Images taken via SEM reveal the rough surface morphology of all of the samples. Commonly observed topographical features included uniaxial striations and pits, ranging in size from 5 to 100 μm. The PEEK and TCP phases of the composite scaffolds were easily identified. The TCP phase appeared to be composed of very small granules (approximately 1 μm in diameter) that were packed within the solid PEEK matrix.

In addition, SEM images were also useful in visualizing the interconnectivity of the pore structures. Some samples appeared to have highly interconnected matrixes, with multiple layers of pores visibly accessible to the surface. In contrast, other samples appeared to have more closed pore structures. Figure 5 depicts the open pore structure of PEEK-2 and the closed surface of PEEK-3.
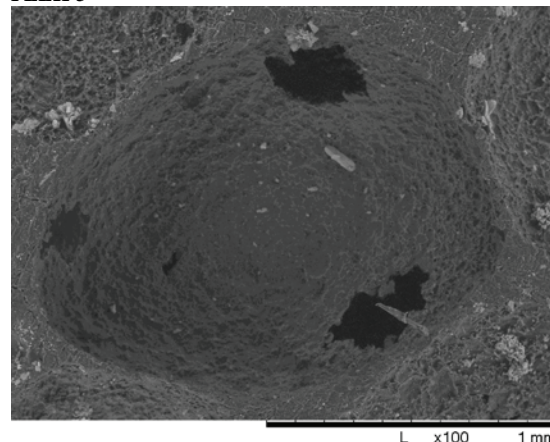
PEEK-2
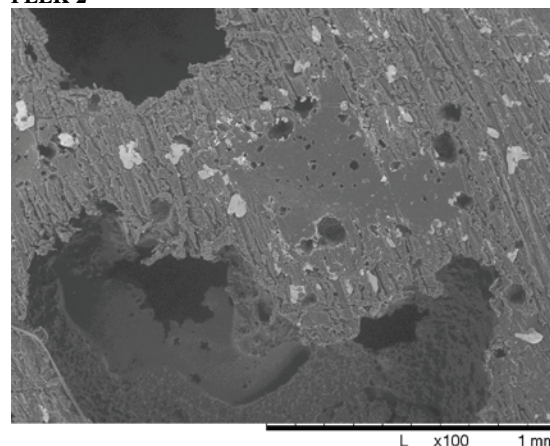
PEEK-3

Figure 5: 15kV SEM images of interconnected pore structure (PEEK-2 – Top) and closed pore structure (PEEK-3 – Bottom).

Discussion: SEM and μCT were effective in analyzing the porous PEEK samples. In selecting the optimal biomaterial to promote osseointegration, multiple criteria need to be considered. The first limiting factor is pore size: if the pores are not big enough to allow for the passage of osteocytes and neovascularization, bone ingrowth will not occur. The material must also be porous and interconnected to allow bone to grow deep into the matrix and adequately fix the implant in place.

Three of the PEEK scaffolds (PEEK-1, PEEK-2, and PEEK-3) sufficiently fulfill these criteria. All with average pore sizes of approximately 600 μm, they mimic the average pore size of trabecular bone (678 μm). The porosity of scaffolds also closely resembles that of trabecular bone (approximately 80%).

Initial assessment of these compression-molded particulate-leached scaffolds yields promising indications of their clinical relevance. More work must be done to characterize their mechanical strength, as this is an important criterion for load-bearing applications in orthopedics.

Fracture Toughness and Fatigue Crack Propagation Behavior of a Carbon Fiber-Reinforced PEEK Material

J. Bensusan and C. Rimnac
Musculoskeletal Mechanics and Materials Program
Departments of Mechanical and Aerospace Engineering and Orthopaedics,
Case Western Reserve University, Cleveland OH USA

Introduction

The fracture toughness and fatigue crack propagation behavior of neat PEEK formulations have been reasonably well-reported in the literature [1]. The reported fracture toughness, K_{IC}, for neat PEEK ranges between 2-8 $MPa(m)^{1/2}$. The fatigue crack propagation behavior of neat PEEK can be modeled using the Paris relationship and both increasing molecular weight and crystallinity improve the fatigue crack propagation resistance of the material.

Less has been reported regarding these fracture properties for PEEK carbon fiber-reinforced formulations particularly under physiologically-relevant environments for biomedical applications. The objective of this study, therefore, was to conduct fracture toughness tests and fatigue crack propagation tests of carbon fiber-reinforced PEEK under both a dry, ambient laboratory condition and in a physiologically-relevant fluid environment condition.

Materials/Methods

Carbon fiber-reinforced PEEK (Motis, InVibio, Ltd., United Kingdom) was utilized for this study.

Fracture toughness tests were conducted following ASTM E 1820 Standard Test Method for Measurement of Fracture Toughness (formerly ASTM E399). Round compact tension specimens were utilized (W = 40 mm and B = 20 mm, where W is the specimen width and B is the specimen thickness as defined in ASTM E 1820). Pre-cracking was conducted by cyclic loading. The specimens to be soaked were pre-cracked prior to soaking.

Four specimens were tested in each test group. The first group was tested in the as-received, dry condition. The second group was tested following soaking in phosphate buffered saline (PBS) for 60 days at 37 C.

All specimens were pulled to failure at a displacement rate of 1mm/sec. Dry specimens were tested in air at ambient temperature and PBS soaked specimens were tested in air at 37C. Load and displacement data were recorded. Digital photographs were taken of the fracture surface of the specimens for crack length measurements using ImageJ.

Fracture toughness, K_C, was calculated as per ASTM E 1820; strictly, the plane strain K_{IC} was not verified (because the yield stress was not available to verify all plane strain conditions had been met). The K_C mean and standard deviation (SD) of each group was determined. Statistical comparison of K_C between the two groups was done via Student's t-test (p<0.05 for significance).

Fatigue crack propagation tests were conducted on an Instron servo-hydraulic testing machine following ASTM E647 as a guide. A sinusoidal waveform of 3 Hz and R ratio of 0.1 (minimum load/maximum load) was used for loading. All specimens were fatigue pre-cracked. A traveling microscope with a resolution of 0.01mm was used to measure crack extension. Cycling was interrupted and the crack length measured for every 0.2mm of crack extension. When 0.2mm of crack extension was reached in 100 or fewer cycles, measurements were taken every 0.1mm of crack growth. Dry specimens were tested in ambient conditions with a fan directed at the specimen. PBS soaked specimens were tested in a PBS bath at 37^0C after soaking in PBS for 60 days.

Fatigue crack growth rate (da/dn), and cyclic stress intensity factor (ΔK) were calculated following ASTM 647. Linear regression of the linear portion of the log-log data was used to determine the exponent (m) and coefficient (C) of the Paris relationship (da/dn=CΔK^m). The Paris regime was defined as the range of data from a crack growth rate (da/dn) of 10^{-4} mm/cycle to 10^{-2} mm/cycle. Statistical analysis was conducted using Student's t-test to compare the mean C and m values of the Paris relationship between the two test groups (p<0.05 for significance).

Results

For fracture toughness, three dry and four PBS soaked specimens were successfully tested for fracture toughness. One specimen was lost due to testing error. K_C for the dry group was 6.78 (0.41)

$MPa(m)^{1/2}$ and for the PBS soaked group was 6.87 (0.29) $MPa(m)^{1/2}$. The fracture surface appearance of the test specimens demonstrated flat fracture; this is consistent with a plane strain fracture toughness condition. There was no significant difference between the dry and PBS soaked groups.

Four fatigue crack propagation specimens were tested in each treatment group; however, one specimen in each group was lost due to technical difficulties (**Figure 1**). Crack advance was noted to be irregular and somewhat out-of-plane in all specimens. There was a significant difference between the exponent (m) of the two test groups, but not the coefficient (C) (**Table 1**).

Discussion

In this evaluation of a carbon fiber-reinforced PEEK material, no significant difference in the fracture toughness, K_c, between testing in a dry, ambient air state and in a pre-soaked PBS condition tested at 37C was found. The flat appearance of the fracture surfaces suggests that the K_C values are likely also the plane strain fracture toughness, K_{IC}, for the two test groups. The fracture toughness of this material is at the high end of the range reported for neat PEEK [1].

There was considerable scatter in the fatigue crack propagation behavior of specimens within a test group. This is likely due to two factors: it was difficult to follow the advance of the crack tip in these tests, due to difficulty in visualizing the crack tip; and, the crack path proceeded somewhat out-of-plane in all cases, likely due to the presence of the carbon fibers. Thus, conclusions regarding similarity or differences in the fatigue crack propagation behavior between the two test groups cannot be made at this time.

Table 1. Paris regime exponent and coefficient

Test Group	Exponent, m	Coefficient, C
Dry	12.6 (2.0)	4.0×10^{-11} (4.3×10^{-11})
PBS Soaked	20.2 (2.5)	6.2×10^{-15} (1.1×10^{-14})

Figure 1. da/dn vs. ΔK for the PBS soaked and dry test groups.
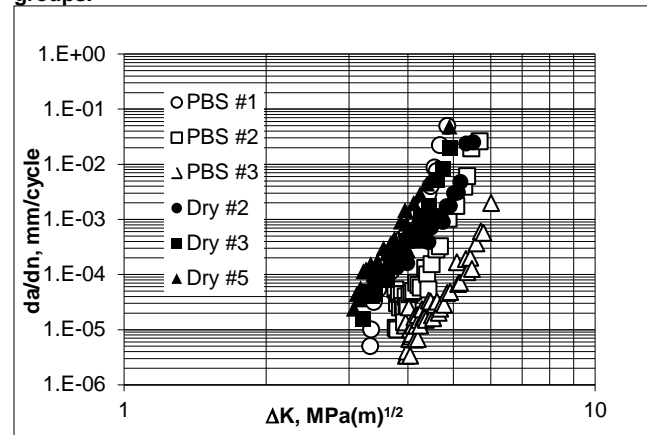
References

Acknowledgements

Macro-mechanical behaviour of CFR PEEK: a novel approach to the implant design

Regis, Marco[1,2], Fusi, Simonetta[1], Favaloro, Roberto[1], Bracco, Pierangiola[2]
[1]R&D Department, Limacorporate SpA, Villanova di San Daniele (UD), Italy
[2]Dipartimento di Chimica, Università degli Studi di Torino, Torino, Italy
pierangiola.bracco@unito.it

Introduction: Polyetheretherketone (PEEK) is one of the most promising emerging biomaterials: researchers have been evaluating its performance as a potential material for orthopaedic applications since late '80s. At present, PEEK is widely used in instrument set, spine and trauma application; on the other hand, its application in orthopaedic bearings remains limited.

Carbon fibre reinforced (CFR) PEEK has been proposed as a potential solution to extend PEEK application to structural orthopaedic components. In recent years, research has been focused on studying CFR PEEK tribological and mechanical properties [1-4], to achieve a deeper understanding of its long time performance. However, there is still debate in literature on these aspects, and thus additional studies are needed in order to assess CFR PEEK in vivo behaviour. For instance, there is still concern on wear and mechanical properties [5, 6], and further, analytical methods for PEEK biomaterials have been approached in the context of specific implants design only [7-10].

In this study, a novel approach to mechanical characterization of CFR PEEK has been proposed, in order to provide new tools to face the highlighted issues by developing a design criteria for orthopaedic components realization. Static mechanical characterization on two injection moulded CFR PEEK samples (poly acrylonitrile, PAN, and pitch based) has been conducted, and a composite material-based approach have been applied to the collected data in order to provide an appropriate design technique for the development of highly durable CFR PEEK components.

Methods and Materials: Tensile, compression and flexion tests were performed on PAN (30% wt) and pitch (30% wt) based CFR PEEK injection moulded specimens, to evaluate the elastic, compressive and shear properties of the materials, respectively. Tensile test has been performed at a strain speed of 2 mm/min, while compression and flexion test strain speeds were set at 5 mm/min. Tests were run at room temperature in air until failure or breakage of the specimens. Specimens geometries were taken from the ASTM composite material reference standards. Flat geometries and large fillets were selected, so as to ensure a constant and repeatable material flow during the injection moulding process. Three different moduli (Young, Poisson, and shear) have been calculated for both PAN and Pitch based CFR PEEK, accordingly to the obtained static mechanical test results.

In addition to the mechanical tests, sections of PEEK samples have been taken by cutting and polishing operations along the loaded axis and at their cross section, and fibre orientation was evaluated by optical microscope analysis. Polymer flow and fibre orientation were assessed by considering the fibre direction in all the examined sections, leading to the determination of the reinforcement typology.

This, together with the collected experimental data on mechanical properties, contributed to the creation of a stiffness tensor matrix for each material type, that can be proposed for a novel approach to CFR PEEK implants design.

Results: Young, Poisson and shear moduli were 21,4 GPa, 0,53 and 23,3 GPa for PAN based CFR PEEK; and 13,4 GPa, 0,28 and 14,8 GPa for pitch based CFR PEEK, respectively.

Microscope analysis revealed the formation of a well-oriented fibre surface layer during the injection moulding process for both PAN and pitch based CFR PEEK. The thickness of these areas, corresponding to the surfaces directly in contact with the mould walls, is approximately 200 μm and varies with the specimen geometry.

However, in the inner part of the specimens sections, no fibre orientation could be detected, therefore it was assumed that, globally, the composite material mechanical behaviour had to be considered as influenced by a randomized, non-oriented fibre reinforcement in two dimensions (Figure 1).

Fibre and matrix appearance is different depending upon fibre type: in pitch based CFR PEEK sections a significantly lower number of fibre breakages or voids at fibre matrix interface could be individuated in respect to PAN based CFR PEEK sections (Figure 2).

With these data, a stiffness tensor has been successfully prepared, taking into consideration the model proposed for an isotropic material with a randomized, non-oriented fibre reinforcement, for both PAN and pitch CFR PEEK (Eq.1)

Discussion: Differences in fibre reinforcement resulted in different mechanical properties, as predictable. A higher reinforcement grade was obtained for PAN based composites, as mechanical properties of pitch fibres is lower compared to PAN fibres. For different specimen geometries and carbon fibre type, the retrieved fibre orientation varied, consequently influencing the mechanical behaviour of the material. This, together with factors as fibre fragmentation, void presence, and fibre-matrix adhesion, is at the basis of the mechanical behaviour of CFR PEEK

Despite further investigation on the fibre-matrix adhesion properties is needed to provide a micro-mechanical characterization validating the prepared analytical model,

calculation of a stiffness tensor was possible, and results suggest that appropriate dimensioning studies could be set up in order to satisfy deformation and failure requirements in components design phase. With this approach, appropriate prediction of thickness and geometries for the development of new CFR PEEK orthopaedic components for joint arthroplasty can be achieved.

References:
[1] - Jones DP, Leach DC, Moore DR. Mechanical properties of poly(ether-ether-ketone) for engineering applications. Polymer 1985;26:1385–93.
[2] - Chivers RA, Moore DR. The effect of molecular weight and crystallinity on the mechanical properties of injection moulded poly(aryl-ether-ether-ketone) resin. Polymer 1994;35(1): 110–6.
[3] - Rae PJ, Brown EN, Orler EB. The mechanical properties of poly(ether-ether-ketone) (PEEK) with emphasis on the large compressive strain response. Polymer 2007;48:598–615.
[4] - Nisitani H, Noguchi H, Kim YH. Evaluation of fatigue strength of plain and notched specimens of short carbon-fibre reinforced polyetheretherketone in comparison with polyetheretherketone. Eng Fract Mech 1992;43(5):685–705.
[5] – Wang A, Lin R, Stark C, Dumbleton JH. Suitability and limitations of carbon fiber reinforced PEEK composites as bearing surfaces for total joint replacements. Wear 1999;225–229:724–7.
[6] - Flöck J, Friedrich K, Yuan Q. On the friction and wear behavior of PAN- and pitch-carbon fiber reinforced PEEK composites. Wear 1999;225–229:304–11.
[7] – Kurtz SM, Devine JN. PEEK biomaterials in trauma, orthopaedic, and spinal implants. Biomaterials 2007;28: 4845-4869.
[8] - Brown SA, Hastings RS, Mason JJ, Moet A. Characterization of short-fibre reinforced thermoplastics for fracture fixation devices. Biomaterials 1990;11(8):541–7.
[9] - Tang SM, Cheang P, AbuBakar MS, Khor KA, Liao K. Tension–tension fatigue behavior of hydroxyapatite reinforced polyetheretherketone composites. Int J Fatigue 2004;26:49–57.
[10] - Akay M, Aslan N. An estimation of fatigue life for a carbon fibre/ poly ether ether ketone hip joint prosthesis. Proc Inst Mech Eng [H] 1995;209(2):93–103.
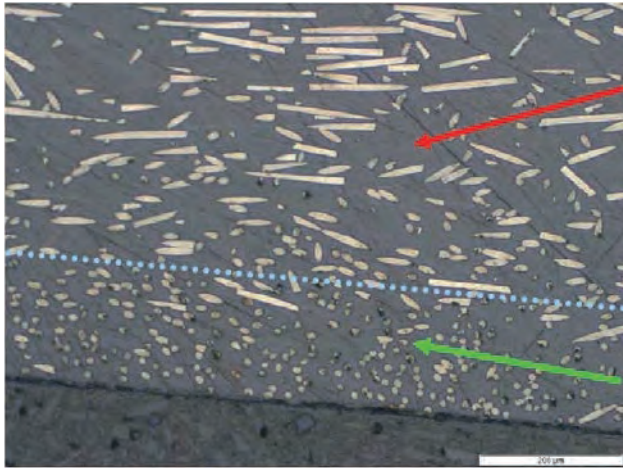
Figure 1. Randomly oriented carbon fibres in PEEK polymer matrix (red arrow), and surface layer of oriented fibres (green arrow). The blue dotted line separates the two mentioned regions.
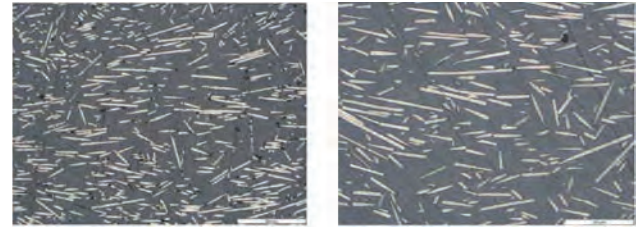

Figure 2. PAN based (left) and pitch based (right) CFR PEEK appearance.

$$
\begin{Bmatrix} N_1 \\ N_2 \\ N_{12} \\ M_1 \\ M_2 \\ M_{12} \end{Bmatrix} = \begin{Bmatrix} [E/(1-\nu^2)]h & [\nu \cdot E/(1-\nu^2)]h & 0 & 0 & 0 & 0 \\ [\nu \cdot E/(1-\nu^2)]h & [E/(1-\nu^2)]h & 0 & 0 & 0 & 0 \\ 0 & 0 & G \cdot h & 0 & 0 & 0 \\ 0 & 0 & 0 & [E/(1-\nu^2)]\dfrac{h^3}{12} & [\nu \cdot E/(1-\nu^2)]\dfrac{h^3}{12} & 0 \\ 0 & 0 & 0 & [\nu \cdot E/(1-\nu^2)]\dfrac{h^3}{12} & [E/(1-\nu^2)]\dfrac{h^3}{12} & 0 \\ 0 & 0 & 0 & 0 & 0 & G \cdot \dfrac{h^3}{12} \end{Bmatrix} \begin{Bmatrix} \varepsilon_1^0 \\ \varepsilon_2^0 \\ \gamma_{12}^0 \\ \kappa_1 \\ \kappa_2 \\ \kappa_{12} \end{Bmatrix}
$$

Eq.1. Proposed model for CFR PEEK macro-mechanical behaviour.

Comparison of BIC and BV/TV values of Titanium coated and un-coated implants in an animal model

Prof. Lauweryns, P. (MD, PhD)[1]; Schaffarczyk, D. (PhD)[2]; Willems, K. (MD)[3]

[1]Campus Sint-Josef, BE-3800 Sint-Truiden, [2]Orthobion GmbH, D-78467 Konstanz, [3]Hospital Roeselare, BE-8800 Roeselare

zyk@orthobion.com

Introduction: Polyetheretherketone (PEEK) is a non-toxic, biocompatible but inert polymer. Compared to a well accepted titanium alloys as implant, PEEK materials offer the advantage to have an elastic modulus (5GPa) closer to bone (18GPa) than titanium alloys (110GPa) and a stability to high temperature as well as to chemical and radiation damage. Despite the good mechanical properties, the adhesion of PEEK implants to bone tissue proceeds slowly due to a relatively low biocompatibility: Concerns have been raised about the inertness of PEEK and limited fixation with bone. Implant complications of PEEK cages such as subsidence and cage migration could be observed. Accordingly, increasing efforts have been directed during the past decade to improve the bone-implant interface by coating PEEK implants with a thin film titanium layer (250 nm). A thin film titanium coating with a micro-porous structure provides the implant with better cell adhesion and improved cell (on-) growth. At the same time, its mechanical properties more closely resemble those of healthy bone, and assure X-ray transparency.

Methods and Materials: In this study the titanium (Ti) thin film coating was carried out via Ti thin film vacuum deposition (TFVD), which has already been established in the company and has achieved CE market clearance. The surface of PEEK spinal cages is coated with a pure Ti-layer in order to enhance its biocompatibility and adhesion to bone tissue. The vacuum deposition method is a low-temperature coating process that forms a dense, uniform and well crystallized Ti-layer without deteriorating the characteristics of the PEEK/implants.

In this animal study the efficacy and safety was observed on Ti TFVD coated PEEK OPTIMA LT1 material and was compared to pure PEEK OPTIMA LT 1.


Pic. 1: For evaluation of the coating, sheep have been operated. They have been sacrificed after 6 weeks, 12 weeks and 26 weeks

Under general anesthesia, 2 unicortical defects have been created in both the distal lateral femur and the proximal medial tibia of left and right hind legs. This resulted in 8 defects in each sheep. Cylindrical implants, 12mm (length) x 8mm (diameter) have been placed in the defects followed by routine wound closure and postoperative care. Pain management was routinely established for 7 days post-op and as necessary based on following clinical examination. The animal study was done double blinded and comprises 3 sacrifices periods: 6weeks, 12 weeks and 26 weeks. All measurements were done by an independent company and by means of μCT. All statistical analyses have also been done blind by an independent third party reviewer.

Results: The samples of uncoated PEEK show lower bone volume and bone characterized by thinner trabeculae and more trabecular space. The samples of Ti TFVD coated PEEK show higher bone volumes and dense bone with thicker trabeculae and less trabecular space.


Control (uncoated PEEK)   **Ti TFVD coated PEEK**
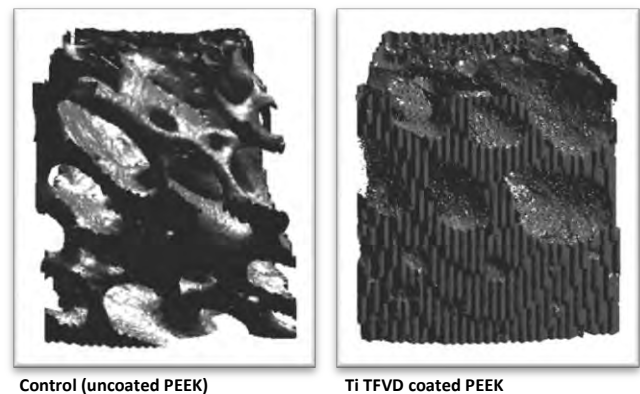
Pic. 2: Based on μCT-measurements 3D-images of the structural characteristics of the observed bone are created.

The thin film Ti coated samples show almost higher bone volume after 12 weeks compared to the pure PEEK control group. After 26 weeks the bone volume is still higher in the Ti TFVD coated group.


BV/TV (%)	6 weeks	12 weeks	26 weeks
—— Ti TFVD	21	45	47
- - - Control	37	29	40
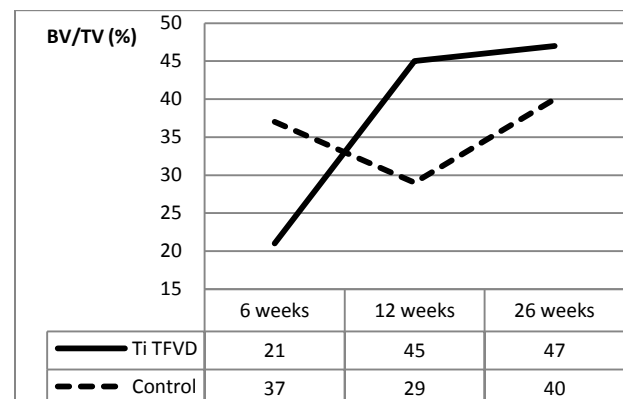
Pic. 3: Ti TFVD coated samples show higher bone volume compared to the pure PEEK control group.

Beside the BV/TV values the Bone-Implant-Contact (BIC ratio) is a crucial factor describing the performance (bioactivity) of a fusion implant. Based on the μCTs the BIC ratio can be analyzed.
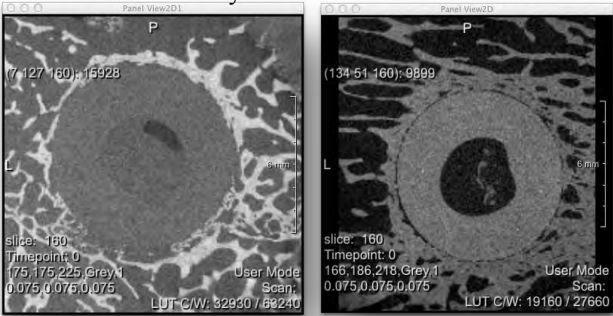
Pic. 4: Two random samples are depicted. The one on the left hand side shows a μCT of an uncoated PEEK dowel; the one on the right hand side shows a μCT of a PEEK dowel coated Ti TFVD technology.

The results of the BIC analysis showed better osseointergration of the Ti coated implants. Ti TFVD coating triggers significant more and earlier bone on-growth already after 12 weeks. The osseointegration induced by TFVD coating at this time is higher compared to the control group of uncoated PEEK samples.

BIC (%)	6 weeks	12 weeks	26 weeks
Ti TFVD	23	65	68
Control	28	42	54
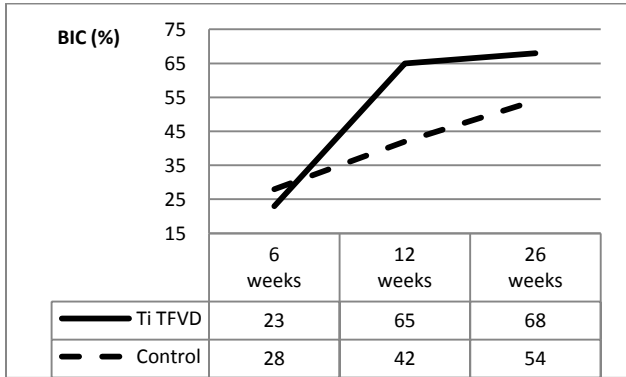
Pic. 5: Higher BIC rates indicate reduced fibrotic layers as they can be observed with pure PEEK implants.

Discussion: The results of the Ti TFVD coating obtained in this study show both good bioactivity and stability of the coating leading to a stable bone bridge and good integration of the implant.

In addition, Ti TFVD coated cages maintain the imaging capabilities of PEEK materials. Compared to Ti Plasma Spray coated cages Ti TFVD coated cages stay almost radiolucent.
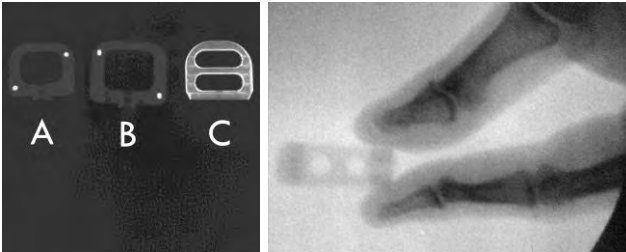

Pic. 6: The picture on the left hand side shows (A) uncoated PEEK cage, (B) Ti TFVD coated PEEK cage and (C) Ti Plasma Spray coated PEEK cage. The picture on the right hand side shows Ti TFVD coated PEEK cage.

The results obtained in this study indicate early bone formation with Ti TFVD coating which may result in lower cage migration and subsidence rates after fusion treatment of the spine as well as in less pain, a more stable bone bridge and lower non- or mal-fusion rates after spinal interbody fusion surgery. Therefore Ti thin film coated spinal implants could be a better choice for spinal fusion interventions compared to pure PEEK implants.

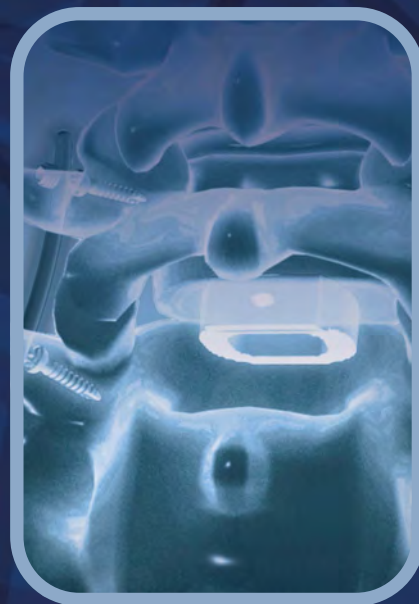# Materials.   Manufacturing.   Knowledge.

▶ Across diverse medical applications.
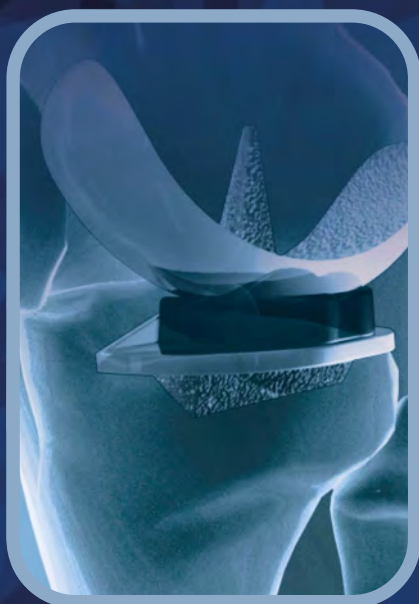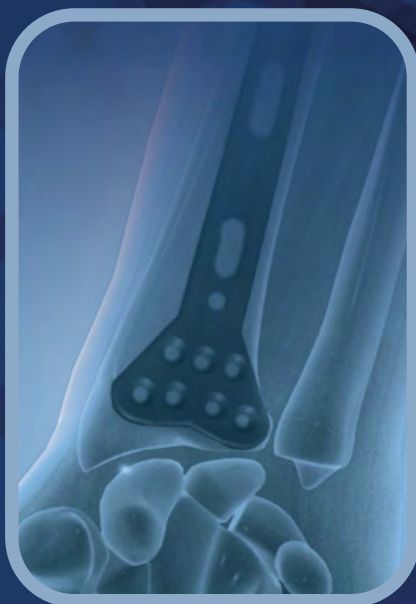
Invibio ORTHO   **Invibio TRAUMA**   **Invibio SPINE**

Realize new biomaterial innovations.

Invibio is a proven device partner and leading provider of biomaterials solutions. Our revolutionary polymer materials, unsurpassed manufacturing support and deep medical device knowledge have allowed device companies around the world to bring innovations to market for nearly 15 years.

Invibio offers unparalleled depth of knowledge and breadth of experience in the design, manufacture and commercialization of medical devices containing PEEK-based polymers. We welcome the opportunity to partner with device manufacturers to address unmet clinical needs by developing next-generation medical devices composed of PEEK-OPTIMA® polymers.

▶ **www.invibio.com**